1377

THE USE OF MOLECULAR SELF-ASSEMBLIES TO FORM COORDINATION POLYMERS WITH COPPER (II): SYNTHESIS, STRUCTURES, AND MAGNETIC PROPERTIES

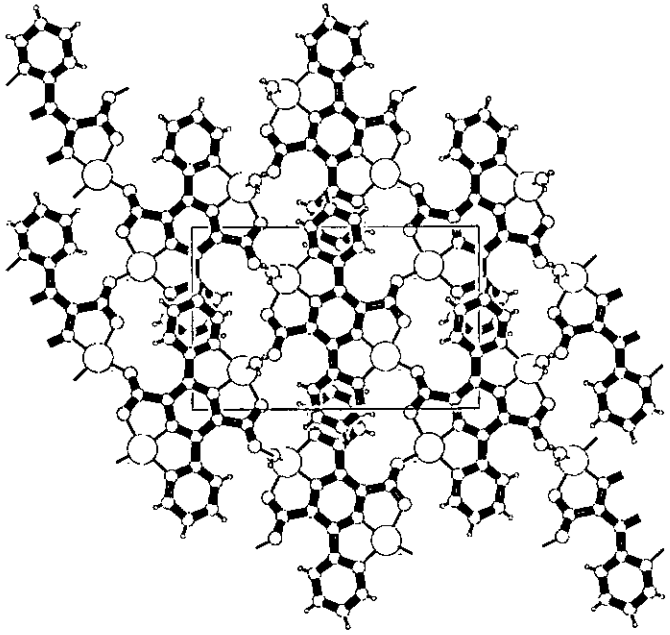

Yi Wang

Neuchâtel 1996

UNIVERSITE DE NEUCHÂTEL
FACULTE DES SCIENCES

THE USE OF MOLECULAR SELF-ASSEMBLIES TO FORM

COORDINATION POLYMERS WITH COPPER (II):

SYNTHESIS, STRUCTURES, AND MAGNETIC PROPERTIES

Thèse Presentée à la Faculté des Sciences par

Yi Wang

Chimiste diplômé de l'Ecole Polytechnique de Pékin/R. P. Chine pour l'obtention du grade de docteur ès sciences

Institut de Chimie
Université de Neuchâtel

Janvier 1996

IMPRIMATUR POUR LA THÈSE

Utilisation de l'auto-assemblage moléculaire pour la formation de polymères de coordination avec le cuivre (II) : Synthèses, structures et propriétés magnétiques

de M. Yi WANG

UNIVERSITÉ DE NEUCHÂTEL

FACULTÉ DES SCIENCES

La Faculté des sciences de l'Université de Neuchâtel sur le rapport des membres du jury,

Mme H. Stoeckli-Evans (directrice de thèse),
MM. R. Neier et A. von Zelewsky (Fribourg)

autorise l'impression de la présente thèse.

Neuchâtel, le 26 juin 1997

Le doyen:

R. Dändliker

R. Dändliker

To My Wife

To My Parents

To My Son

ACKNOWLEGMENTS

This work has been carried out from August of 1992 to January of 1996 in the Laboratory of Chemical Crystallography at the University of Neuchâtel under the direction of Professor Helen Stoeckli-Evans.

I wish to express my gratitude and my deep appreciation to Professor Helen Stoeckli-Evans for her generous support, interest, guidance, and freedom which she provided throughout this work.

I would like to extend thanks to Professor R. Neier for his kind help when I worked in his laboratory and also for co-refereeing this work.

I am much indebted to Professor A. von Zelewsky (Université de Fribourg) for co-refereeing this work.

I thank Professor K. Bernauer for his kind help during the period when I was working in his laboratory.

I am greatly indebted to Dr. C. Pasquier for her help and many interesting discussions.

I would also like to thank Professor J. Ribas, Professor A. Escuer and Professor R. Vicente (Universitat de Barcelona, Spain) for their collaboration in the magnetic measurements.

I am especially indebted to my colleague, Dr. Antonia Neels for performing X-ray diffraction analyses.

I am greatly indebted to all members of the groups of Professor Helen Stoeckli-Evans, Professor R. Neier, and Professor K. Bernauer for their friendly help in many ways and cooperation over the years.

Finally, I would like to acknowledge Professor F. Stoeckli and the Swiss National Foundation of Sciences for providing financial support for this work.

CONTENTS

ABBREVIATIONS

A	anion
L	organic ligand
M	transition metal ion
T	temperature
X	halogens (Cl^-, Br^-, I^-)
BPPZ	2,5-bis(2-pyridyl)-pyrazine
COSY	^1H-^1H correlation spectroscopy
1D	one dimensional
2D	two dimensional
DEPT	distortionless enhancement by polarization transfer
DMF	dimethylformamide
DMSO	dimethylsulfoxide
dmpz	dimethyl-pyrazine
EI-MS	electron ionisation mass spectroscopy
CI-MS	chemical ionisation mass spectroscopy
DCI-MS	direct chemical ionisation mass spectroscopy
FAB-MS	fast atom bombardment mass spectroscopy
HETCOR	Heteronuclear correlation spectroscopy
H4pztc	pyrazine-2,3,5,6-tetracarboxylic acid
H_2L^1	3, 6-dimethylpyrazine-2,5-dicarboxylic acid
Me_2L^1	Dimethyl 3, 6-dimethylpyrazine-2,5-dicarboxylate
H_2L^2	3, 6-bis(2-pyridyl)-pyrazine-2,5-dicarboxylic acid
H_2L^3	5,6-bis(2-pyridyl)-pyrazine-2,3-dicarboxylic acid
IR	infrared spectroscopy
MS	mass spectrometry
NMR	nuclear magnetic resonance
AcO	acetate

py	pyridine
pz	pyrazine
sqa	squaric acid
TAMP	2,3,5,6-Tetrakis(aminomethyl)pyrazine
THF	tetrahydrofuran
TPPZ	2,3,5,6-Tetrakis(2-pyridyl)-pyrazine
UV	ultraviolet spectroscopy
τ	index of the degree of trigonality for penta-coordination metal
λ	wave length
δ	chemical shift
χ	magnetic susceptibility
χ_m	molar magnetic susceptibility

INTRODUCTION

As molecular materials having unusual electrical, magnetic and optical properties, metal coordination polymers with one and two-dimensional structures have attracted considerable attention in recent years. An important factor has been the recognition of the significance of this new generation of materials to science and technologies for the future.

In order to obtain such polymers several strategies are possible. The development of synthetic strategies for the design of solid-state structures from soluble components is currently of intense interest. The building-block approach has been utilized for the rational assembly of inorganic and organometallic crystalline solids. The design of molecular architecture by self-assembly processes has received much attention. Metal complexes can be useful building units for the self-assembling process because they can contain a variety of structural information to guide the self-assembly reaction.

In this work we have designed and synthesized several new and novel pyrazine-based ligands in order to study the formation of coordination polymers with first row transition metals. A number of coordination polymers of copper (II) with these ligands has been prepared through a molecular self-assembly process and the structures have been crystallographically characterized. Moreover a study of the magnetic interactions, via a pathway through the pyrazine ring, has also been performed.

1.1. Supramolecular chemistry, molecular self-assembly, and coordination polymers.

In 1964 John C. Bailar, Jr. [1] proposed an analogy between organic polymers and a class of inorganic coordination complexes that he called "coordination polymers". His seminal review described and classified the synthesis and structures of inorganic chain compounds. Since that time, one-dimensional and other types of coordination polymers of metal complexes have been intensely investigated. The fundamental chemistry and physics behind these fascinating structures has stimulated interest in their possible uses as materials for new technologies.

The electrical, optical, and magnetic properties of coordination polymers are a complex function of their chemical architecture and their electronic structure. Bridging the gap between molecular characteristics and bulk properties is still one of the major challenges in science today. Supramolecular chemistry, the chemistry beyond the molecule, is the designed chemistry of the intermolecular bond. It is a highly interdisciplinary field covering the chemical, physical, and biological features of chemical species held together and organized by means of intermolecular (noncovalent) interactions [2].

Design of supramolecular systems via metal-ion-directed self-assembly or hydrogen bonding of individual components with the ultimate aim of generating new molecular materials is an area of current interest. In the structures of coordination polymers, the well-defined cooperative interactions between discrete molecules provide a continuum between chemistry and material sciences.

Molecular self-assembly is the spontaneous association of molecules under equilibrium conditions into stable, structurally well-defined aggregates joined by noncovalent bonds[3]. Molecular self-assembly is ubiquitous in biological systems and underlies the formation of a wide variety of complex biological structures. Figure 1-1 gives three biological examples of self-assembling nanoscale structures.

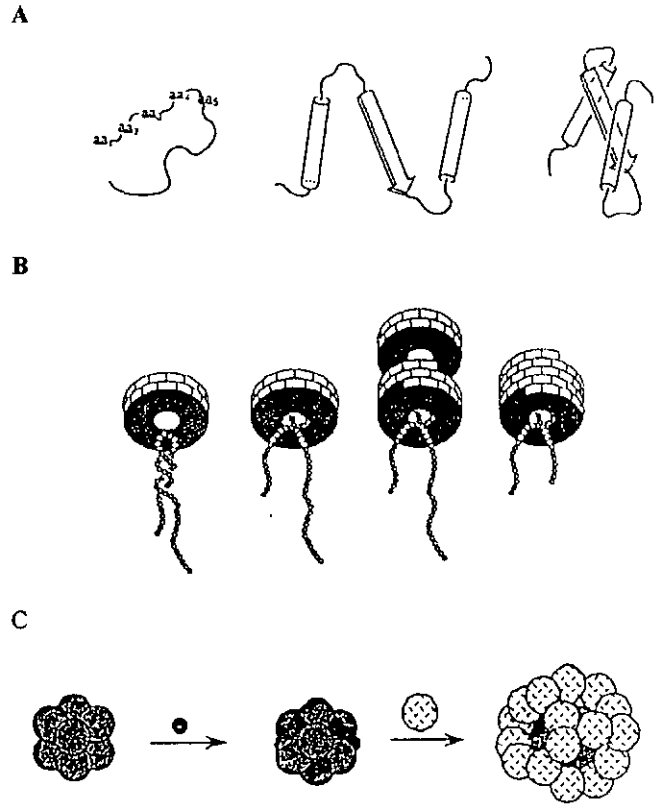

Fig. 1-1. Three biological examples of self-assembling nanoscale structures. (**A**) A schematic representation of the process of protein folding. This process is shown schematically in three stages: the unfolded primary amino acid

sequence; with the formation of structural motifs(domains); and the folding of these structures into the final protein conformation. (**B**) Self-assembly of the tobacco mosaic virus. (**C**) Formation of the pyruvate dehydrogenase complex, [see also Ref. 3].

Self-assembly is emerging as a new strategy in chemical synthesis, with the potential of generating non biological structures with dimensions of 1 to 10^2 nanometers. Self-assembly also leads to organized molecular assemblies having long-range three-dimensional order. Molecular crystals are self-organizing structures, and the interaction determining the relation between molecular structure and crystal structure are beginning to be disentangled. Fig. 1-2 represents schematically such a process in the case of two-site complementary components.

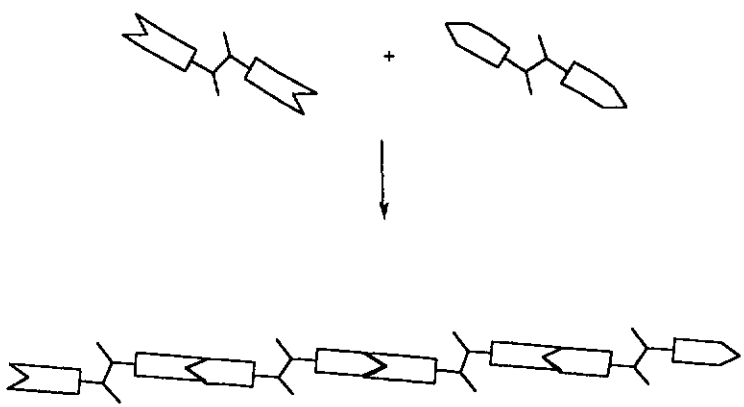

Fig. 1-2. Formation of a polymeric supramolecular species by association of two complementary components.

In a recent review, Lindsey [4] described the classification and limitation of molecular self-assembly processes. He indicated that metal coordination reactions are likely to be an example of the strict self-assembly which is defined as follows: "In this case the product forms spontaneously upon combining the component parts under the proper conditions. 'Strict' emphasizes that the assembly process is reversible and the product is stable at the thermodynamic equilibrium. The product is a direct result of the structures of the component parts. All information for assembly is contained within the subunits or precursor molecules, and neither additional factors nor energy input are required for assembly to occur." For metal chelate formation the overall equilibrium constant ($K_{M\text{-chel}}$) is the product of the stepwise formation constants (Fig. 1-3).

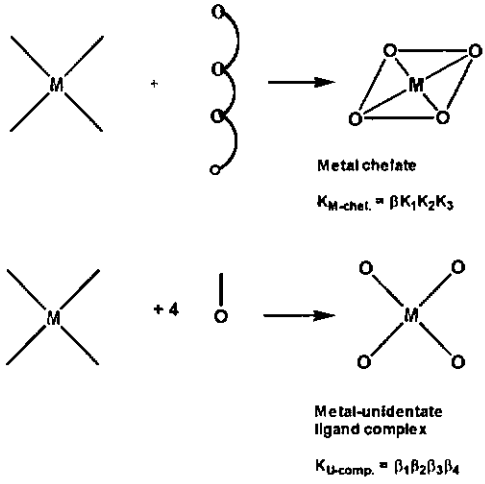

Fig. 1-3. Self-assembly of a metal chelate. The overall equilibrium constant ($K_{M\text{-chel}}$) is the product of the stepwise formation constants. where β represents the intermolecular reaction (nucleation) and K_1, K_2 and K_3 represent the

intramolecular ring closure reactions (growth) that complete the assembly. The equilibrium constant for complex formation with unidentate ligands ($K_{U\text{-comp}}$) is proportional to the product of four intermolecular reactions.

The nucleation step (β) is an intermolecular reaction while the subsequent growth steps (K_1, K_2, K_3) are intramolecular; the latter are highly favorable due to the high effective concentration of the reactive ligand and metal sites. The metal chelates provide a rich domain for studying self-assembly processes.

1.2. Choice and design of ligands

Ligands that can serve as molecular bridges between metal centers and that also contain a delocalized π system have received considerable attention in recent years. Binuclear and multinuclear metal complexes, comprising two or more metal centers bridged by multidentate ligands, can exhibit metal-metal interactions, such as energy or electron transfer, magnetic coupling, and intervalence transfer. Pyrazine and its derivatives have long been known as such ligands. During the period 1961-1963 Nyholm and his colleagues reported a series of complexes of pyrazine and its mono-, bis- and tetra-methyl substituted derivatives with first row transition metals [5-8]. They described two basic structural types based on two nickel complexes, $[Ni(2,5\text{-dmpz})Br_2]_n$ and $[Ni(2,5\text{-dmpz})Cl_2]_n$: (1) one dimensional extended chain shown in Fig. 1-4; (2) two dimensional network shown in Fig. 1-5.

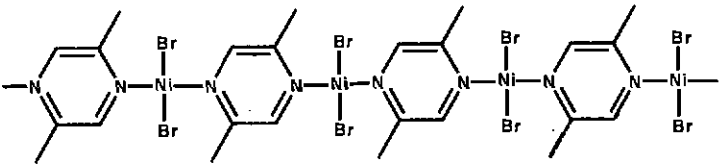

Fig. 1-4. Proposed structure shows an infinite chain for $[Ni(2,5\text{-dmpz})Br_2]_n$

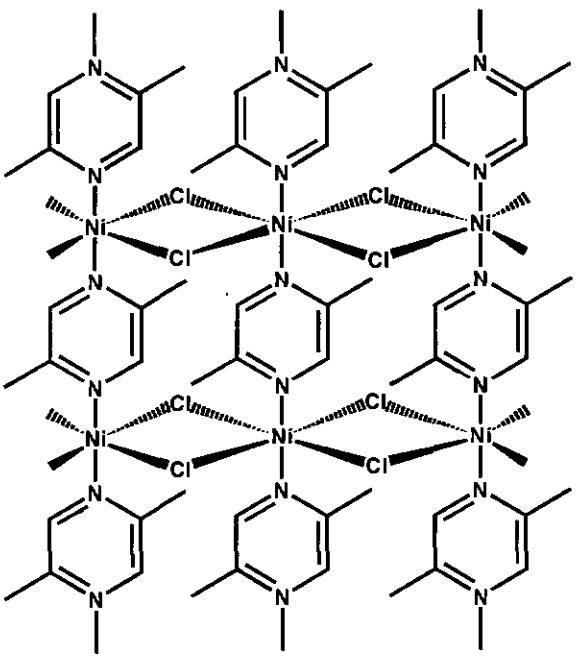

Fig. 1-5. Proposed structure with a 2D framework for $[Ni(2,5\text{-dmpz})Cl_2]_n$

Just three years later, the crystal structure of $[Ni(2,5\text{-}dmp)Br_2]_n$ was proved by Ayres et al. [9]. But the second structural type they proposed was only demonstrated in a similar compound $[Cu(pyz)Br_2]_n$ in 1989 [11]. Since that time, a number of coordination polymers with pyrazine and its alkyl derivatives as bridges has been reported [12]. Crystal structures analyses have revealed mainly one-dimensional extended chain [13] and two-dimensional square lattices [14], shown in Fig. 1-6. In addition the polymers of Cu(I) and Cd(II) with alkyl substituted pyrazines have been shown to give similar crystal structures [15, 16].

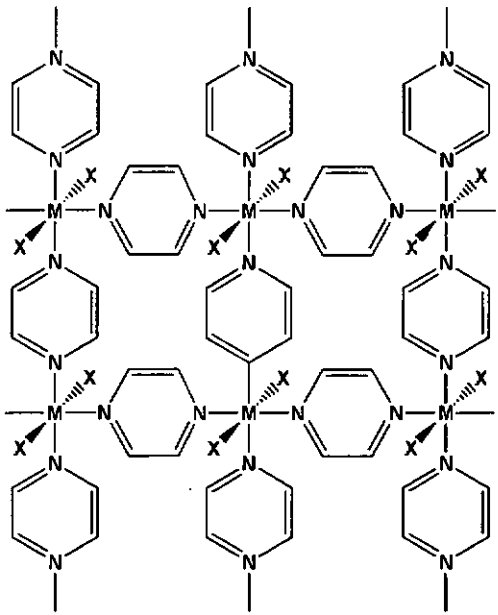

Fig. 1-6. The two-dimensional square lattices found in $[M(pyz)_2X_2]_n$, where: M = Cu(II), Fe(II), Co(II), Ni(II); X= CO_4^-, $CH_3SO_3^-$ NCO^-, halogens, etc.

In the period from 1972 to 1982, Antinelli et al. [17] prepared a series of complexes of 2,3- and 2,5-pyrazine-dicarboxylic acid with 3^d metals and most of them appear to be coordination polymers. The crystal structure of a cobalt complex of the former ligand presented an infinite chain [18]. O'Connor et al. [19,20] synthesised a copper coordination polymer using 2,3-pyrazine-dicarboxylic acid as ligand and the polymer nature of this structure was also proved by X-ray single crystal diffraction.

In the 1980s, Marty and co-workers [21-26] used tetra-substituted pyrazines as potentially bis(tridentate) chelating ligands, for example, pyrazine-2,3,5,6-tetracarboxylic acid (H_4pztc) and tetrakis(aminomethyl)-2,3,5,6-pyrazine (TAMP) shown in Figs. 1-7, with first row transition metals to prepare a number of linear coordination polymers as well as a two-dimensional polymer [27].

Another particularly interesting ligand is 2,5-bis(2-pyridyl)pyrazine (BPPZ) which has been used recently in the construction of some interesting supramolecular system with Ru [28,29]. It has also been shown to form alternating polymer chains with copper (II) with acetates as bridges [30,31]. The chains were cross-linked by copper acetate dimers to form an extensive two-dimensional polymer [32]. In addition attempts have been made to use 2,3,5,6-tetra-(2-pyridyl)pyrazine (TPPZ) as a ligand to construct polymeric structures with first row transition metals [33-35]. The ligands BPPZ and TPPZ are also shown in Fig. 1-7.

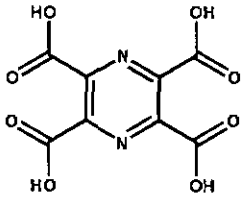

H_4pztc

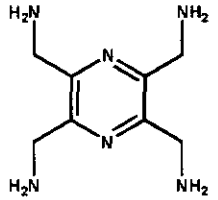

TAMP

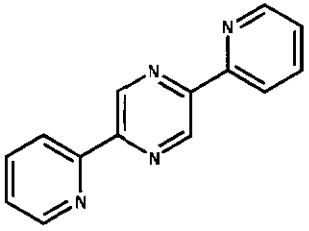

BPPZ

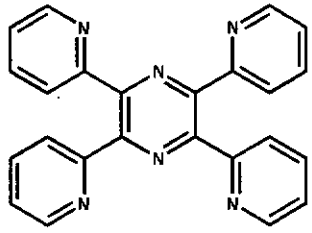

TPPZ

Fig. 1-7. Some substituted pyrazines used as ligands

In the present work the first ligand tested was 3,6-dimethyl-pyrazine-2,5-dicarboxylic acid ($\mathbf{H_2L^1}$) or its methyl ester ($\mathbf{Me_2L^1}$) shown below. They also present the possibility to form coordination polymer with 3^d metals.

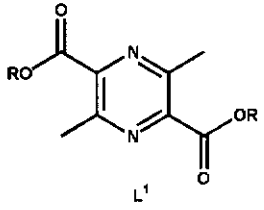

L^1

R = Me, H

The ligands shown above have been chosen for their demonstrated ability to act as bridges linking together metal centers to give a number of one and two dimensional polymer structures. The design and synthesis of polyfunctionalized ligands is still of importance in attempts to meet new requirements including infinite two- and three-dimensional coordination networks, heteropolymetallic systems, and extended chains with helical structures. Some important developments in the design of supramolecular systems incorporating metal centers have resulted from a constructive use of the conformational and bonding preferences of carefully selected organic ligands [36]. Furthermore, in order to improve the solubility of the polymers or to control the rate of the polymerization, modification of the ligands, in particular pyrazine-based ligands, is necessary.

For the reasons discussed above, preparing new pyrazine derivatives with two, three and four substituted groups to form various coordination polymers, with a diversity of structure such as helices, suitable for a wide variety of applications is of intense current interest. We now report a new strategy to synthesize symmetrically tetra-substituted pyrazines with two different kinds of functional groups. Five new ligand candidates shown in Fig. 1-8, were designed and synthesized.

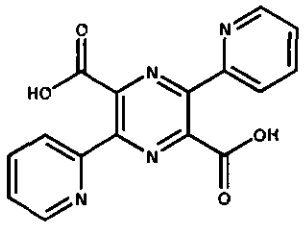

H_2L^2 (19b)

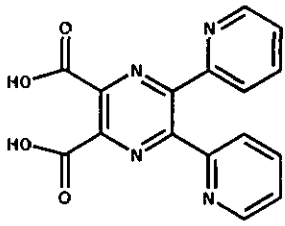

H_2L^3 (22)

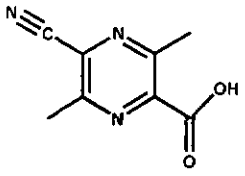

8

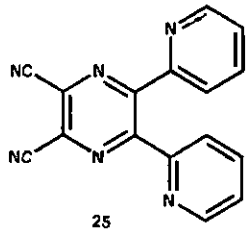

25

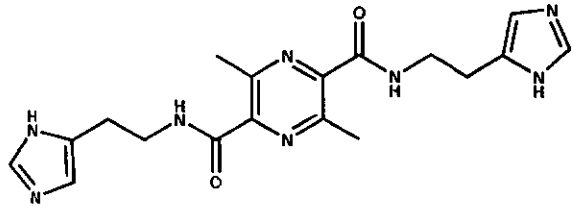

10a

Fig. 1-8. Some ligands and ligand candidates designed and synthesized in this work

Among them, H_2L^2 and H_2L^3 can not only act as ligands to form a variety of coordination polymers with copper (II), but are also capable of forming unique molecular aggregates via hydrogen bonding. The two ligands combine a bis-

bidentate BPPZ with two harder carboxylate sites. Compared with other pyrazine based ligands, H_2L^2 and H_2L^3 present a wider pH range in aqueous solution for complexation reactions and a diversity of structure in forming of polymer formation. As they are based on the more complicated reactivity and diversity of structure, we will call them "second generation" ligands.

1.3. *Molecular magnetism*

Magnetic behavior is usually detected by a substance's response - either attraction or repulsion - to a magnet. It arises from the way electron spins interact with each other. Every electron has a small magnetic moment associated with its quantum mechanical "spin". Since each orbital may have up to two electrons-one spin-up (↑) and one spin-down (↓) the spins cancel when both electrons are present. If a molecule or ion has two electrons in every orbital, it is diamagnetic and will be repelled slightly in an applied magnetic field. If a molecule has an odd number of electrons, there will be at least one unpaired electron, and the molecule will have a net spin. Such molecules or ions are sufficiently far apart so that their spin-coupling energy is small compared to the coupling-breaking thermal energy. Such spins do not couple; instead they form a very weak type of magnet called a paramagnet. When the spins are closer together, the spin-coupling energy increases and may become large enough to enable an effective parallel coupling, called ferromagnetic (↑↑), or antiparallel coupling, called antiferromagnetic (↑↓). Ferrimagnetism comes from coupling between more up-spins than down-spins, so that complete cancellation does not occur and the material as a whole has a net magnetic moment. All the four magnets are shown in Fig. 1-9.

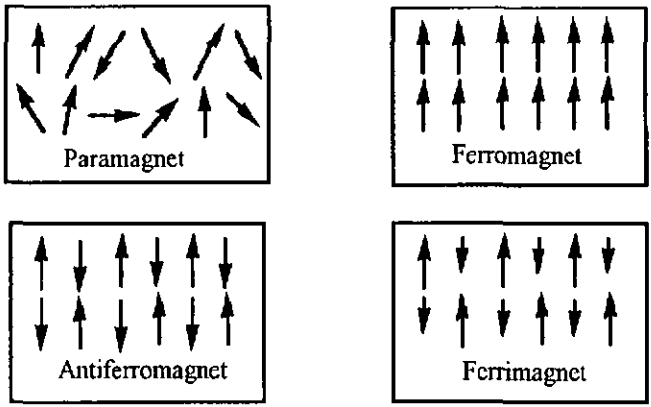

Fig. 1-9. The main types of magnets.

When the spins couple in a parallel manner, the material's response to an applied magnetic field - termed its magnetization - enhances; when their coupling is antiparallel, magnetization is suppressed. The limiting value of this response, called the saturation magnetization, comes when all spins in the material are aligned. Technologically useful ferromagnetic or ferrimagnetic behavior is not a property of a molecule or ion; like superconductivity, it is a cooperative property seen only in the solid state.

The pyrazine ring can serve as a molecular bridge between metal centers to form magnetic coupling systems. However, all pyrazine bridged polynuclear complexes reported to date show very weak antiferromagnetic coupling [37], except the latest example involving the Cu(II) complex of TPPZ [38].

The superexchange mechanism in polynuclear copper(II) complexes in which the bridging ligand is pyrazine is a controversial subject and several poorly

compatible points of view have been expressed in the past two decades. The main point of discussion concerns the type of superexchange pathway, whether π or σ. The two alternative mechanisms have MOs of adequate symmetry and energy to interact with the symmetric and antisymmetric combination of the atomic orbitals of the copper atoms that contain the unpaired electron, $dz^2_{(s)}$ and $dz^2_{(a)}$ or $dx^2\text{-}y^2_{(s)}$ and $dx^2\text{-}y^2_{(a)}$, depending on the geometry of the coordination polyhedron of the copper atom.

In 1976 Hatfield et al. [39] proposed the π pathway based on spectroscopic evidence. The superexchange pathway should occur through the π network by means of the overlap of the d_s and d_a combinations of the $d_{x^2} - y^2$ atomic orbitals with the HOMO p_s (b_{1g}) and its antisymmetric analogue p_a (b_{3u}) that give rise to the molecular orbitals Φ_s and Φ_a. A further modification was introduced in 1977 by the same author [40]. That is, the interaction of the dxy(a) orbitals with the p_a bonding MO (b_{2g}) of the pyrazine bridge. It should be noted that in this model, the antiferromagnetic character of the compounds must be weak: the b_{1g} and b_{3u} MOs have little density on the nitrogen atoms and the overlap will be very inefficient. For the interaction between the dxy(a) and the b_{2g} MOs it is assumed that only some unpaired spin density lies in the d_{xy} orbitals by mixing with the ground state $dx^2\text{-}dy^2$ orbitals.

Later Hendrickson [41] proposed that the interaction was due to overlap of the $d_{s,a}$ orbitals with the highest σ occupied MOs of the bridge, taking as reference the dinuclear copper(II) complexes [42] $[Cu_2(tren)_2(PPD)]X_4$ (X = NO_3^-, ClO_4^-, PF_6^- and PPD = *p*-phenylenediamine). Here the superexchange 2J parameters are in the range -70.2 to -39.6 cm^{-1}. The related *p*-benzidinediamine bridge, BZD, despite the large Cu-Cu separation, gives a small antiferromagnetic coupling of the same order as that observed for pyrazine bridged complexes. In

these complexes the interaction should be propergated by the highest MOs of the PPD or BZD ligands. MO calculations on PPD, BZD and pyrazine shows that these MOs are mainly a symmetric combination of nitrogen lone-pair orbitals with minor contributions of the C-ring atoms for the pyrazine and comparable C-ring contributions for PPD and BZD. The low antiferromagnetic coupling for pyrazine compounds was explained by the poor $2p_z$ contribution argument and the fact that PPD and BZD are stronger bases than pyrazine.

More recently Oshio et al. [37], after performing Extended Hückel MO calculations, suggested that even through the σ pathway the antiferromagnetic interaction should be low, as observed experimentally, owing to the small value of the J_{ab} two center Coulombic repulsion integral. The later should be low due to the long Cu-Cu distance.

In the Hatfield model (the π pathway) the dihedral angle between the coordination plane of the copper atoms and the plane of the pyrazine ring is determinant. The larger the dihedral angle the greater the orbital overlap, hence, the larger the antiferromagnetic interaction. For the σ pathway the value of this dihedral angle has no influence on the orbital overlap.

In the present work we have extensively investigated the magnetic properties of several pyrazine bridged copper(II) complexes with ligands 2 and 3, which show moderate antiferromagnetic coupling between copper ions and provide new proof to support the σ pathway.

References.

[1] Chen, C.-T.; Suslick, K. S., *Coord. Chem. Rev.*, **128**, 293-322 (1993).

[2] Lehn, J.-M., *Angew. Chem. Int. Ed. Engl.*, **29**, 1304-1319 (1990).

[3] Whitesides, G. M.; Mathias, J. P.; Seto C. T., *Science* , **254**, 1312-1319 (1991).

[4] Lindsey, J. S., *New J. Chem.*, **15**, 153-180 (1991).

[5] Lever, A. B. P., Lewis, J.; Nyholm, R. S., *Nature*, **189**, 58-59 (1961).

[6] Lever, A. B. P., Lewis, J.; Nyholm, R. S., *J. Chem. Soc.*, **1962**, 1235-1246.

[7] Lever, A. B. P., Lewis, J.; Nyholm, R. S., *J. Chem. Soc.*, **1963**, 3156-3158.

[8] Lever, A. B. P., Lewis, J.; Nyholm, R. S., *J. Chem. Soc.*, **1963**, 5042-5048.

[9] Ayres, F. D.; Pauling, P.; Robertson, G. B., *Inorg. Chem.*, **3**, 1303-1306 (1964).

[10] Valentine, J. S.; Silverstein, A. J.; Soos, Z. G., *J. Am. Chem. Soc.*, **96**, 97-103 (1974).

[11] Fetzer, T.; Lentz, A.; Debaerdemaeker, T., *Z. Naturforsch.*, **44B**, 553-556 (1989).

[12] Darriet, J.; Haddad, M. S.; Duesler, E. N.; Hendrickson, D. N., *Inorg. Chem.*, **18**, 2679-2682 (1979).

[13] Haynes, J. S.; Rettig, S. J.; Sams, J. R.; Thompson, R. C., Trotter, J., *Can. J. Chem.*, **65**, 420-426 (1987).

[14] Carreck, P. W.; Goldstein, M., McPartlin, E. M.; Unsworth, W. D., J. *Chem. Soc. Chem. Communications*, **1971** 1634-1635 .

[15] Real, J. A.; De Munno, G.; Munoz, M. C.; Julve, M., *Inorg. Chem.*, **30**, 2701-2704 (1991).

[16] Otieno, T.; Rettig, S. J.; Thompson, R. C.; Trotter, J., *Inorg. Chem.*, **32**, 1607-1611 (1993).

[17] Antinelli, J.-P.; Pâris, C. R. *Acad. Sci. Paris*, **274**, C51 (1972).

[18] Richard, P.; Tran Qui, D.; Bertaut, E. F. *Acta Cryst.*, **B29**, 1111-1115 (1973).

[19] O'Connor, C J.; Sinn, E. *Inorg. Chem.*, **20**, 545-551 (1981).

[20] O'Connor, C. J.; Klein, C. L.; Majeste, R. J.; Trefonas, L. M. *Inorg. Chem.* **21**, 64-67 (1982).

[21] Marioni, P.-A.; Stoeckli-Evans, H.; Marty, W.; Güdel, H.-U.; Williams, A. F., *Helv. Chim. Acta*, 69, 1004-1011 (1986).

[22] Marioni, P.-A., Ph.D. Thesis, Université de Neuchâtel, 1986.

[23] Ferigo, M., Ph.D. Thesis, Université de Neuchâtel, 1988.

[24] Bonhôte, P.; Ferigo, M.; Stoeckli-Evans, H.; Marty, W., *Acta Crystallogr. Section C*, **C**49, 2102-2107 (1993).

[25] Ferigo, M.; Bonhôte, P.; Marty, W., Stoeckli-Evans, H., *J. Chem. Soc. Dalton Trans.*, 1549-1554 (1994).

[26] Marioni, P.-A.; Marty, W.; Stoeckli-Evans, H.; Whitaker, C., *Inorg. Chim. Acta* , **219**, 161-168 (1994).

[27] Graf, M.; Stoeckli-Evans, H.; Whitaker, C.; Marioni, P.-A.; Marty, W. *Chimia*, **47**, 202-205 (1993).

[28] Serroni, S.; Denti, G. *Inorg. Chem.*, **31**, 4251-4255 (1992).

[29] Denti, G.; Serroni, S.; Campagna, S.; Ricevuto, V.; Juris, A.; Ciano, M.; Balzani, V. *Inorg. Chim. Acta* , **198-200**, 507-512 (1992).

[30] Neels, A.; Stoeckli-Evans, H., *Chimia* , **47**, 198-202 (1993).

[31] Neels, A.; Stoeckli-Evans, H.; Escuer, A.; Vicente, R., *Inorg. Chem.*, **34**, 1946-1949 (1995).

[32] Neels, A., Ph.D. Thesis, Université de Neuchâtel, 1995.

[33] Graf, M.; Greaves, B.; Stoeckli-Evans, H., *Inorg. Chim. Acta* , **204**, 239-246 (1993).

[34] Graf, M.; Stoeckli-Evans, H., *Acta Crystallogr. Section C*, **C50**, 1461-1464 (1994).

[35] Graf, M., Ph.D. Thesis, Université de Neuchâtel, 1995.

[36] Miller, J. S.; Epstein, A. J., *Chem. Eng. News* Oct. 2, 30-41(1995).

[37] Oshio, H.; Nagashima, U., *Inorg. Chem.*, **29**, 3321-33255(1990).

[38] Graf, M.; Stoeckli-Evans, H.; Escuer, A.; Vicente, R. *Inorg. Chim. Acta*, (1996) in press.

[39] Richardson, H. W. ; Hatfield, W. E. *J. Am. Chem. Soc.*, **98**, 835-839(1976).

[40] Richardson, H. W.; Wasson, J. R. Hatfield, J. R. *Inorg. Chem.*, **16**, 484-486(1977).

[41] Haddad, M. S.; Hendrickson, D. N.; Cannady, J. P.; Drago, R.; D. S. Bieksza, D. S. *J. Am. Chem. Soc.*, **101**, 898-906(1979).

[42] Felthouse, T. R.; Hendrickson, D. N., *Inorg. Chem.*, **17**, 2636(1978).

RESULTS

2.1. Synthesis of Ligands

2.1.1 Synthesis of Ligand 1

2.1.1.1 Synthesis of Ligand 1 and its Derivatives

The most general method for the synthesis of symmetrically substituted pyrazines, 2,5-disubstituted and 2,3,5,6-tetrasubstituted pyrazines, depends on the self-condensation of α-(primary amino)carbonyl compounds to form dihydropyrazines, which is subsequently oxidated to the pyrazines, as shown in scheme 1 [1]. In some of cases, however, α-(primary amino)carbonyl compounds are not stable but they can usually exist as the HCl salt form.

Scheme 1

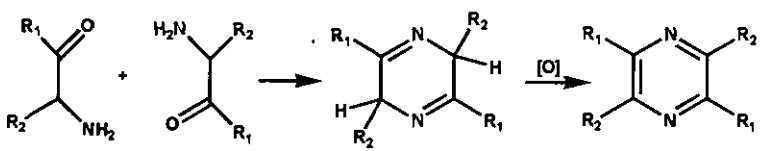

We choose 3,6-dimethylpyrazine-2,5-dicarboxylic acid alkyl esters as precursors to obtain ligand 1 (3,6-dimethylpyrazine-2,5-dicarboxylic acid). The synthesis of the 3,6-dimethylpyrazine-2,5-dicarboxylic acid alkyl esters were first described in briefly by Adkins and Reeve [2]. The key step of their method was the reduction of alkyl 2-oximinoacetoacetate to form alkyl 2-aminoacetoacetate via catalytic hydrogenation. Raney nickel was used as a catalyst to afford the product in ca. 25% yield at high pressure (100-125 atm. for initial pressure of hydrogen). Iida et al. [3] improved this

method by using supported nobel metal catalyst, Pd/C, at 18 atm in ca. 60% yield., but HCl containing solvent is involved in their reaction, which limits the application of this method. We have studied the catalytic reduction of the alkyl oximinoacetoacetate in presence of different catalysts, such as , Zn dust, Pd/C, Raney-Ni, and Rh/C in neutral solvent at low pressure (3-4 atm.). Finally compounds *3* and *4* have been synthesized by using a one-pot reaction combining catalytic reduction of alkyl 2-oximinoacetoacetate over Rh/C catalyst at low pressure (3-3.5 atm.), self-condensation, and oxidation. It is not necessary to isolate the active intermediate, alkyl 2-aminoacetoacetate, in this method. We have obtained an overall yield 55 % by this simplified one-step process. Scheme 2 presents the results of this one-pot reaction. This method will be very useful for the preparation of other symmetrically substituted pyrazine derivatives.

Scheme 2

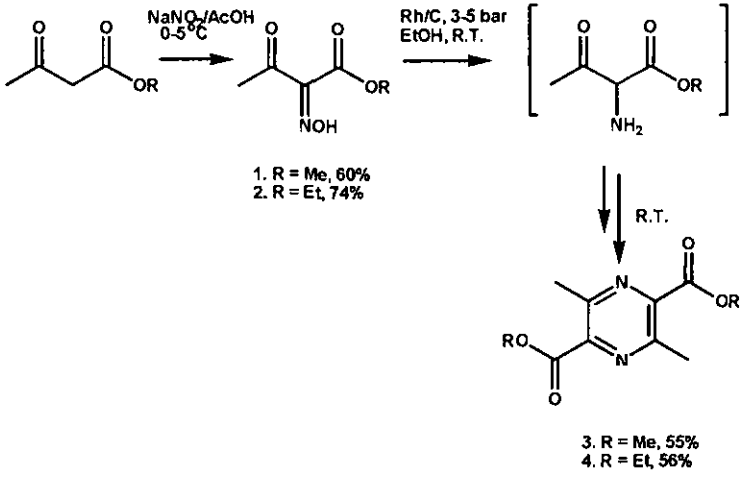

1. R = Me, 60%
2. R = Et, 74%

3. R = Me, 55%
4. R = Et, 56%

Scheme 3

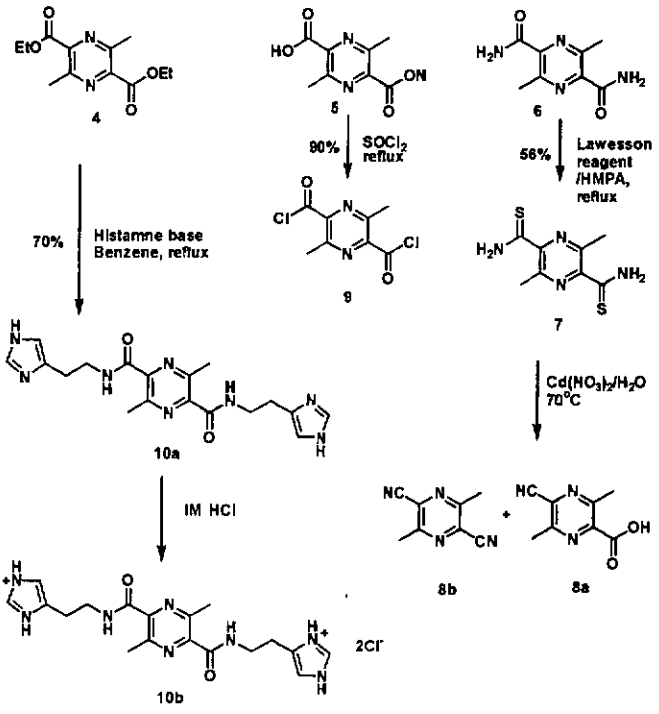

Scheme 3 presents the synthesis of some derivatives of Ligand 1. Some of them, such as compounds **8** and **10**, may be potential ligand candidates to form dinuclear and polynuclear complexes with transition metal ions.

Lawesson reagent [3] is the most efficient thiation reagent known to date, and was successfully applied in the thiation reaction of the carboxamide (**6**) to afford compound **7**. From compound **7** we can obtain an asymmetric substituted pyrazine derivative (**8a**) via a metal-catalyzed hydrolysis reaction. The detailed mechanism of this reaction remains unclear.

The peptide bonds in compound **10** have been synthesized in high yield via the ester route. This compound may be a bis-tridentate ligand. In addition 3,6-dimethyl-2,5-pyrazinedicarboxylic acid chloride (**9**) will certainly be an important starting material for preparation of other symmetrically substituted pyrazines.

2.1.1.2. Characterization of Ligand 1 and its Derivatives

All of the compounds were characterized by ^{1}H and ^{13}C NMR spectroscopy and gave satisfactory results. The mass spectra of some of the compounds has been observed with EI-MS and DCI-MS methods. The structures of ligand 1 and its most important derivatives were characterized by X-ray diffraction. Fig. 2-1 and Fig. 2-2 show the crystal structures of dimethyl and diethyl 3,6-dimethylpyrazine-2,5-dicarboxylate, **3** and **4**. The two molecules have *Ci* symmetry and the central pyrazine rings are planar. The bond distances and angles in the esters have values close to those expected for this type of compound. The pyrazine ring is not coplanar with the carboxylate substituents; the dihedral angles between the pyrazine ring and the plane of O1-C4-O2 are 12.26 (58)° for **3** and 9.15 (40)° for **4** respectively.

Fig. 2-3 presents the molecular structure of H_2L^1. The molecule also possesses *Ci* symmetry and the central pyrazine ring is planar. The protonated carboxylate group is inclined to the planar pyrazine ring by 37.50(21)°. There are two water molecules of crystallisation, which link H_2L^1 molecules to form an extensive three dimensional hydrogen-bonding network shown in Fig. 2-4 and The bond lengths, bond angles and hydrogen bonds are shown in Table 2-1.

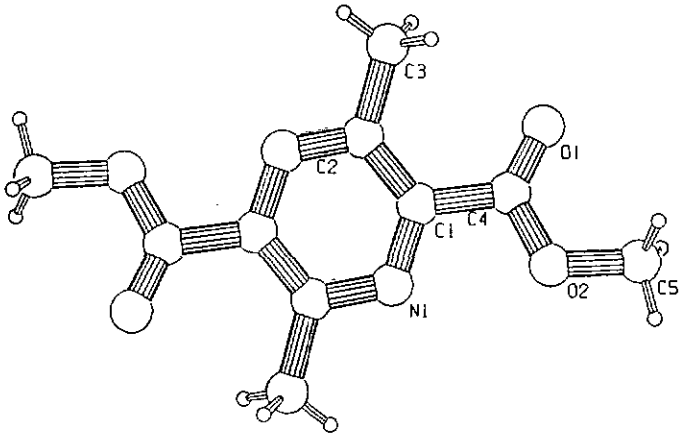

Fig. 2-1. Crystal structure of dimethyl 3, 6-dimethylpyrazine-2,5-dicarboxylate (**3**), showing the atom-numbering scheme

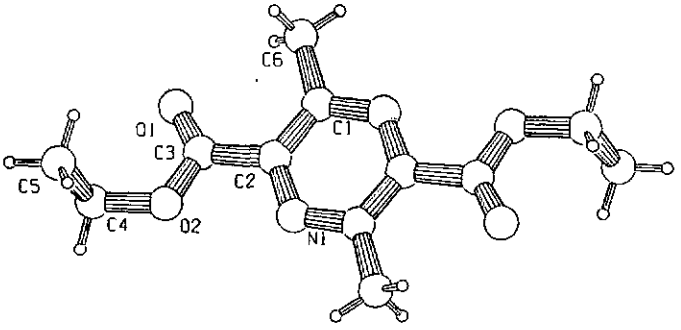

Fig. 2-2. Crystal structure of diethyl 3, 6-dimethylpyrazine-2,5-dicarboxylate (**4**), showing the atom-numbering scheme

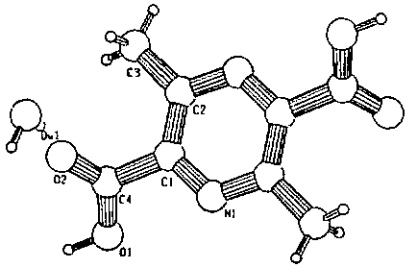

Fig. 2-3. Crystal structure of 3, 6-dimethylpyrazine-2,5-dicarboxylic acid (5), showing the atom-numbering scheme

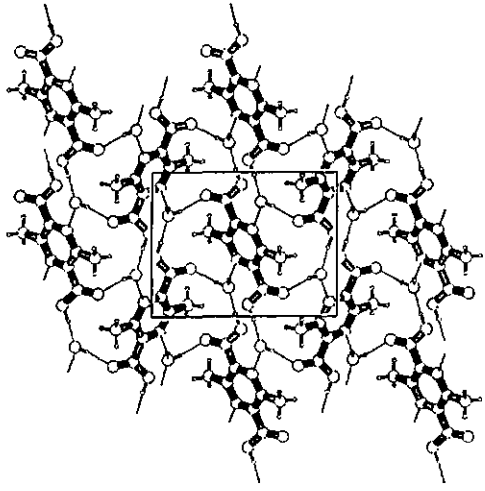

Fig. 2-4. A crystal packing diagram of compound 5, hydrogen bonds are illustrated by dotted lines

Table 2-1. Bond Lengths, Bond Angles and Hydrogen-Bonding Geometry for **5**

Bond	Lengths (Å)	Bond	Angles (°)
N1---C1	1.334(2)	C1--N1--C 2	118.9(1)
N1---C2	1.343(2)	N1—C1--C2^{i}	122.5(2)
O1—C4	1.302(2)	N1--C1--C4	115.7(1)
O2---C4	1.209(2)	C2^{i}--C1--C4	121.8(2)
C1---C2^{i}	1.398(2)	N1--C2--C1^{i}	118.6(2)
C1---C4	1.505(2)	N1—C2--C3	117.1(2)
C2---C3	1.491(3)	C1^{i}--C2--C3	124.3(2)
		O2--C4--O1	124.4(2)
		O2--C4--C1	122.8(2)
		O1--C4--C1	112.7(2)

D—H...A	D...A (Å)	D—H(Å)	H...A(Å)	D—H...A( )
O1-H1...OW1	2.547	0.944	1.607	173.22
OW1-H11...O2	2.821	0.841	1.987	171.68
OW1-H12...N1	2.913	0.849	2.079	167.09

Symmetry code: (i) -x+1, -y+2, -z

The crystal structure of compound **8a** is shown in Fig 2-5. The bond lengths and angles in the structure are normal. In the crystal the terminal hydroxyl group O2-H2 connects to O1 of an symmetry related molecule via a hydrogen bond(O2-H2...O1^{i}, O2-H2, 0.82; H2...O1, 2.13; O2...O1, 2.944 Å; O2-H2...O1, 172 °). It is of interest to study the 1H NMR spectroscopy of compound **8a**. A significant long-range H-H coupling in this molecule has been observed with ^{7}J = 0.7 Hz. Fig. 2-6. shows its ^{1}H and ^{1}H-^{1}H COSY NMR spectra. The coupling constants ^{5}J and ^{6}J for a series of 2-alkyl-3-methoxypyrazines have been reported [4,5]. The coupling constant ^{7}J, however, is observed for first time in substituted pyrazines.

A

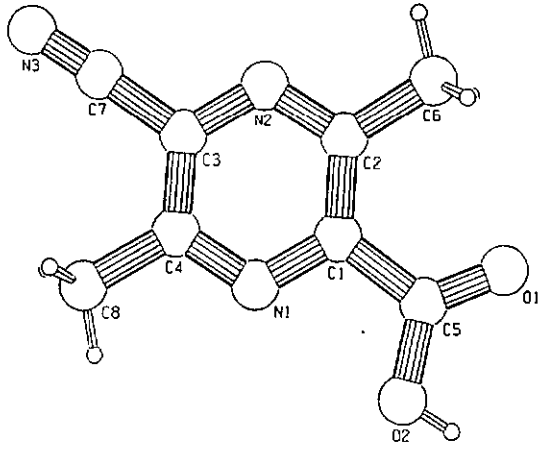

B

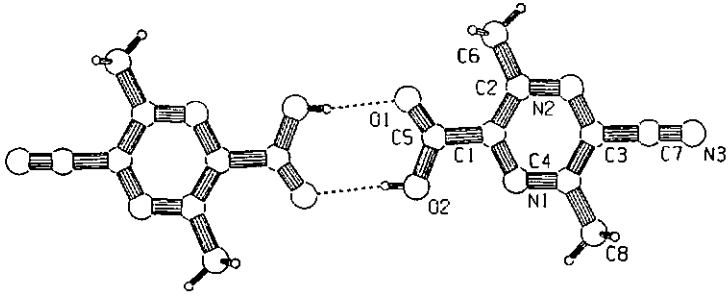

Fig. 2-5. A). Crystal structure of 5-cyano-3,6-dimethylpyrazine-2-carboxylic acid (**8a**), showing the atom-numbering scheme; B). Hydrogem bonded dimer in compound **8a** (hydrogen bonds are illustrated by dotted lines).

A

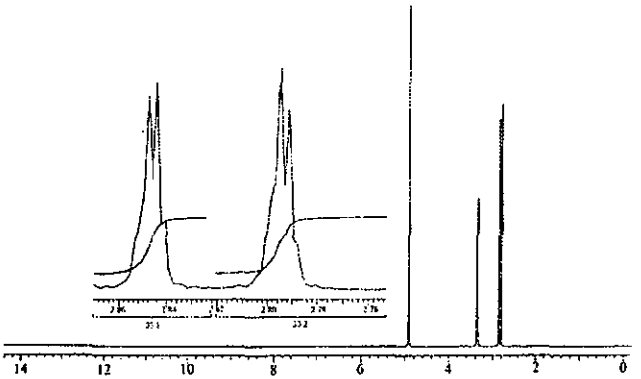

B

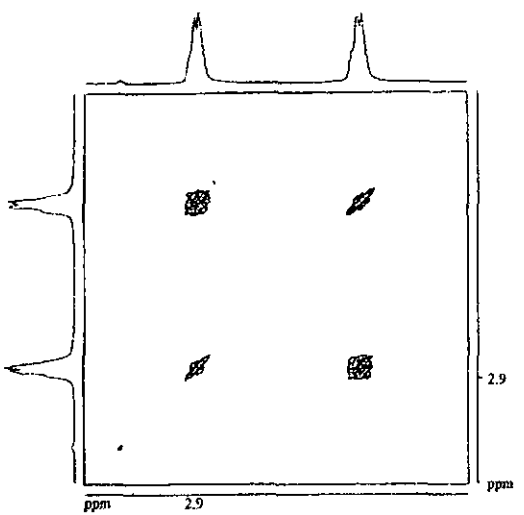

Fig. 2-6. ^{1}H NMR spectra of compound **8a**,
A). ^{1}H NMR spectrum (CD_3OD, 200 MHz);
B). ^{1}H-^{1}H COSY (CD_3OD, 200 MHz)

The structures of N,N'-Bis[2-(4-imidazolyl)ethyl]-3,6-dimethylpyrazine-2,5-dicarboxamide (**10**) and its HCl salt were charactered with IR, NMR, MS, and X-ray diffraction with atisfactory results. The crystal structure of the HCl salt (**10b**) and a packing diagram are shown in Figures 2-7 and 2-8. The molecule possesses *Ci* symmetry. The nitrogen (N3) of the imidazole moiety is protonated and the central pyrazinc ring and the imidazole rings are planar. There are two water molecules of crystallisation in the crystal. The molecules are linked by an extensive hydrogen bonding network involving the water molecule OW1, Cl^- ion, and all the N atoms of this molecule.

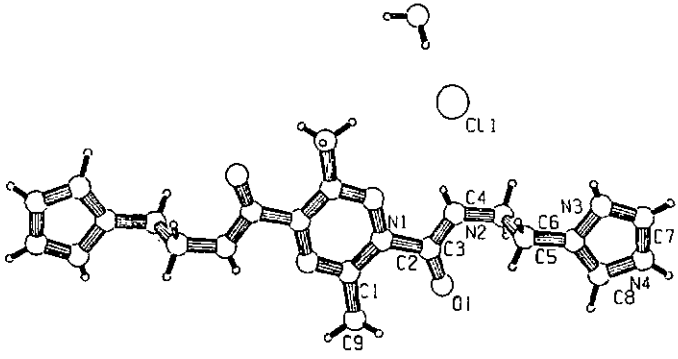

Fig. 2-7. Crystal structure of compound **10b**, showing
the atom-numbering scheme

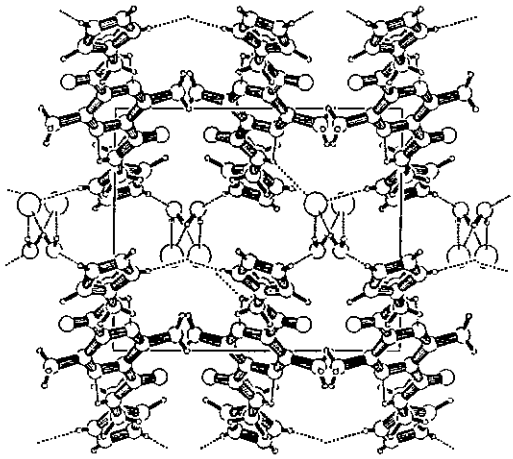

Fig. 2-8. The crystal packing diagram of compound **10b**

2.1.2. Synthesis of Ligand 2

2.1.2.1 Synthesis of Ligand 2 and Some Related Compounds

Based on the synthesis of ligand 1, 3,6-bis(2'-pyridyl)pyrazine-2,5-dicarboxylic acid (ligand 2, **19**) has been prepared by a similar method, scheme 4. Diethyl 3,6-bis(2'-pyridine)pyrazine-2,5-dicarboxylate was used as the precursor.

However, introduction of the pyridyl group raises new problems in the reduction reaction of the oximes as well as in the following reactions. Ethyl acetate was chosen as the solvent for the catalytic hydrogenation reaction. The intermediate, compound **16**, can be isolated and but still remains unstable, particularly in solution. In the following

reaction we have found that the intermediate can not carry out self-condensation in a solution of ethyl acetate. Finally chloroform was selected as the solvent for the condensation and oxidation. The overall yield is 27% for six steps. There are some by-products in the key step, condensation and oxidation reaction, which are very difficult to control. It is of interest to study these by-products in order to determine the solvent effect on the condensation and the formation mechanism of these by-products.

Scheme 4

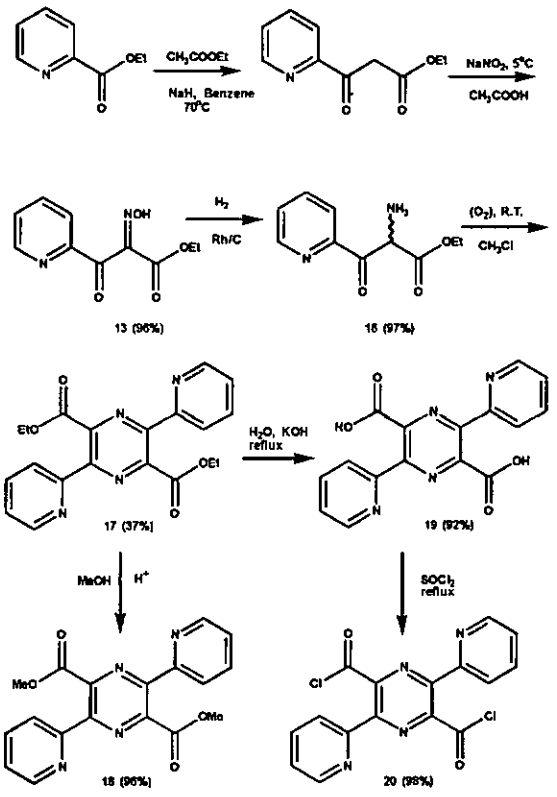

The compound **19a**, H_2L^2, is synthesized via a hydrolysis reaction of **17**. A prominent characteristic of compound **19** is its amphoteric property. This molecule presents a very complicated and a great diversity of behaviour in aqueous solution. **19b** and **19c** have been prepared in order to examine its different forms in the solid state, scheme 5. The reaction of compound **19a** with $SOCl_2$ gave the acid chloride, compound **20**. This will certainly be a very useful compound in the synthesis of new multidentate ligands.

Scheme 5

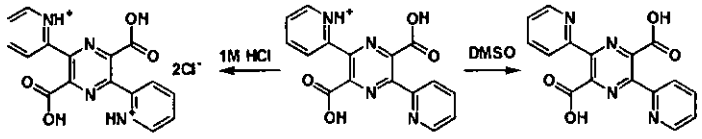

19b **19a** **19c**

In addition, in order to obtain the isomers of compounds **19**, i.e. 3,6-bis(3-pyridyl)pyrazine-2,5-dicarboxylic acid and 3,6-bis(4-pyridyl)pyrazine-2,5-dicarboxylic acid, compounds **14** and **15** have been prepared from the respective β-keto-esters. However, further attempts to synthesize the isomers were not successful. Some critical factors in the reaction of catalytic hydrogenation, self-condensation, and oxidation, such as, the stability and conformation of the intermediates and solvent effects, are still unclear.

2.1.2.2. Characterization of Ligand 2 and Some Related Compounds

All of the stable compounds were characterized by ^1H and ^{13}C NMR spectroscopy, EI-MS, DCI-MS, and FAB-MS spectrometry methods giving satisfactory results.

The X-ray crystal structures of the pyridyl oximinoacetoacetates (**13**, **14**, and **15**) are shown in Figures 2-9, 2-10, and 2-11. Selected bond distances and angles, torsion angles, and hydrogen bonds in the three compounds are compared in Table 2-2. To our knowledge no crystal structure of any compound with this structure type has been found in the Cambridge Crystal Structure Database [6]. No significant differences were found in the bond lengths, bond angles, or the conformation of the three molecules. Although, the carboxylate moiety of compound **14** presents a different orientation, this is probably due to the effect of the different substituent group, methyl rather than ethyl. The two disordered components (ester group) of compound **13** also have a slightly different orientation.

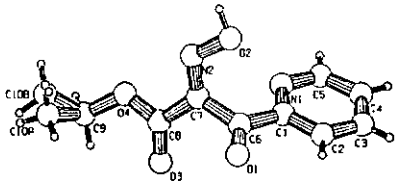

Fig. 2-9. Crystal Structure of compound **13**, Showing the atom-numbering scheme.

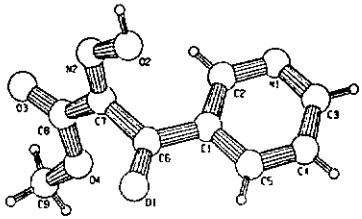

Fig. 2-10. Crystal Structure of compound **14**, Showing the atom-numbering scheme.

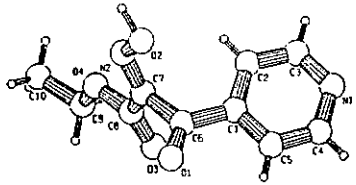

Fig. 2-11. Crystal Structure of compound **15**, Showing the atom-numbering scheme

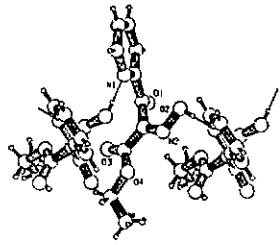

Fig. 2-12. A crystal packing diagram of compound **13**, hydrogen bonds are illustrated by dotted lines

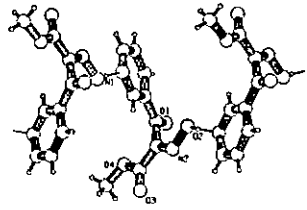

Fig. 2-13. A crystal packing diagram of compound **14**, hydrogen bonds are illustrated by dotted lines

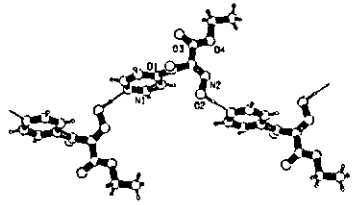

Fig. 2-14. A crystal packing diagram of compound **15**, hydrogen bonds are illustrated by dotted lines

Table 2-2. Selected distances (Å), angles (°), torsion angles(°), and hydrogen bond geometry in the compounds **13**, **14**, and **15**

Compound	**13**	**14**	**15**
C1--C6	1.489(3)	1.487(3)	1.489(3)
C6--C7	1.513(3)	1.517(3)	1.508(3)
C7--C8	1.487(3)	1.490(3)	1.490(11)
C6--O1	1.203(3)	1.207(3)	1.201(7)
C7--N2	1.279(3)	1.285(3)	1.272(7)
N2--O2	1.380(2)	1.369(3)	1.388(9)
C8--O3	1.203(3)	1.195(3)	1.201(6)
C8--O4	1.320(3)	1.320(3)	1.317(3)
O1--C6--C1	121.5(2)	121.9(2)	122.0(3)
C1--C6--C7	119.4(2)	119.2(2)	117.1(4)
N2--C7--C6	123.3(2)	122.7(2)	125.1(4)
C7--N2--O2	111.9(2)	110.8(2)	111.2(6)
N2--C7--C8	118.3(2)	116.4(2)	120.1(5)
C7--C6--O1	119.1(2)	118.9(2)	120.9(3)
C7--C8--O3	122.3(2)	125.5(3)	119.6(5)
C7--C8--O4	112.3(2)	110.5(2)	114.2(2)
C8--C7--C6	117.9(2)	120.7(2)	114.6(2)
C5--C1--C6-O1	-7.89(33)	-0.89(37)	-19.59(38)
C2--C1--C6-C7	171.22(20)	-1.73(34)	161.62(30)
O2--N2--C7--C8	176.31(17)	177.56(20)	176.37(17)
O2--N2--C7--C6	4.57(29)	3.11(31)	0.41(28)
O1--C6--C7--N2	106.21(27)	103.51(28)	-91.00(67)
C1--C6--C7-N2	-72.92(29)	-76.08(30)	90.91(64)
O1--C6--C7--C	-65.55(30)	-70.70(32)	92.85(70)
C1--C6--C7-C8	115.32(22)	109.70(27)	-85.24(67)
N2--C7--C8--O3	-172.07(22)	-0.68(44)	-172.94(21)
C6--C7--C8-O3	0.11(32)	173.89(31)	3.42(29)
N2--C7--C8--O4	7.30(29)	179.66(21)	6.16(29)
C6--C7--C8-O4	179.49(20)	-5.77(32)	-177.47(18)

Hydrogen bond: O2------H22.....N1				
	O2---N1	O2---H22	H22---N1	O2--H22--N1
13[i]	2.739	0.93	1.81	176.6
14[ii]	2.697	0.95	1.75	175.8
15[iii]	2.674	1.03	1.67	166.9

Symmetry codes: (i) -1/2 + x, 1/2 - y, z; (ii). -x, y - 1/2, 1/2 - z; (iii). 3/2 - x, 1/2 + y, -z

There is a strong intermolecular hydrogen bond, O2---H22...N1, in all three crystal structures, which links the molecules to form infinite chains. The crystal packings are shown in Figures 2-12, 2-13, and 2-14. No intramolecular hydrogen bonds were found. The structure of the three molecules in solution is very complicated, since there are at least two configurations of the oximes possible, and tautomerism is probably involved. It would be of interest to study and assign this structural problem and find the relationship between the reactivity and structure. However such a study is beyond the present work.

Compound **16** is a very active molecule and can be handled only for a short time in the solid state. The molecular ion peak has been observed by EI-MS. Some IR bands, 3296 and 2988 cm^{-1} corresponding to the amino group, have also been observed.

The X-ray crystal structure of the ethyl and methyl esters of ligand 2, compound **17** and **18**, are shown in Figures 2-15 and 2-16. Both molecules have *Ci* symmetry and similar configurations. The distances and angles in **17** and **18** are normal. The basic molecular units , the 2,5-bis(2-pyridyl)pyrazine moieties, exist in the extended form with a dihedral angle between the best plane through the pyrazine and pyridine rings of 1.5(7) and 7.6(4)°, respectively. The carboxylate ester moieties in **17** and **18** are inclined to the central pyrazine ring by 80.7(5) and 74.8(2)°, respectively.

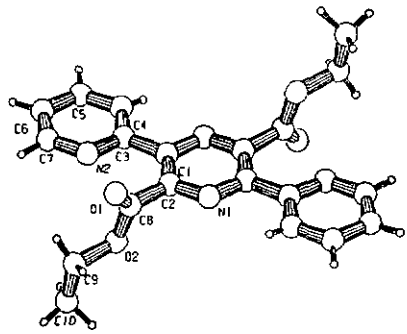

Fig. 2-15 Crystal Structure of **17**, showing the atom-numbering scheme.

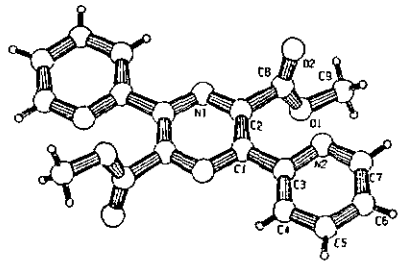

Fig. 2-16 Crystal Structure of Me_2L (**18**), showing the atom-numbering scheme.

The structure of compound **19a** was characterized by IR, NMR, and DCI-MS. The crystal structures of compound **19a**, **19b**, and **19c** have been determined by X-ray diffraction, Figs. 2-17 to 2-22. Compounds **19b** and **19c** possess crystallographic *Ci* symmetry. The selected bond distances and angles are compared in Table 2-3, which indicates that there are no obvious differences.

Table 2-3. Selected distances (Å) and angles (°) in the compounds **19a**, **19b**, and **19c**.

Compound	19a	19b	19c
O1---C10	1.211(4)	1.208(2)	1.211(3)
O2---C10	1.297(4)	1.310(2)	1.310(3)
C1---C2	1.408(4)	1.398(2)[i]	1.401(3)[ii]
C1---C5	1.487(4)	1.495(2)	1.485(3)
C1---N1	1.333(4)	1.335(2)	1.341(3)
C2---N2*	1.335(4)	1.338(2)	1.335(3)
N3**---C5	1.338(4)	1.345(2)	1.342(3)
N3**---C9	1.347(4)	1.338(2)	1.336(3)
C2---C10	1.515(4)	1.511(2)	1.506(3)
N2*-C2-C1	120.9(3)	121.2(2)[i]	122.5(2)[i]
N2*-C2-C10	115.4(3)	116.6(2)	113.5(2)
C1-C2-C10	123.5(3)	122.08(14)[i]	123.7(2)[ii]
N1-C1-C2	120.7(3)	121.21(14)[i]	119.5(2)[ii]
N1-C1-C5	117.1(3)	116.60(14)	117.2(2)
C2-C1-C5	122.2(3)	125.19(14)[i]	123.3(2)[ii]
C1-N1-C4***	118.2(3)	117.60(14)	118.0(2)
O1-C10-O2	126.4(3)	125.2(2)	125.4(2)
O1-C10-C2	120.7(3)	121.7(2)	121.0(2)
O2-C10-C2	112.8(3)	113.10(14)	113.4(2)
N3**-C5-C6	123.6(3)	119.4(2)	123.0(2)
N3**-C5-C1	115.3(3)	117.9(2)	115.9(2)
C6-C5-C1	121.0(3)	122.7(2)	121.1(2)
C5-N3**-C9	116.6(3)	122.7(2)	116.7(2)

- This atom is named as N1a in 19b and 19c;
- ** This atom is named as N2 in 19b and 19c; *** This atom is named as C1a in 19b and 19c; Symmetry codes: (i) -x+1, -y, -z; (ii) -x+2, -y-1, -z+1

Molecule **19a** in the solid state exists as an inner salt zwitterion, like an amino acid. The crystal structure of **19b** indicates that the two pyridyl groups of the molecule are protonated. Since compound **19c** was obtained from a solution of DMSO, this molecule is present as a normal organic carboxylic acid. It is very interesting to compare the conformation of the three forms of ligand 2. Although the bond lengths and angles are very similar, the conformations are different, notably the dihedral angles between the pyridine rings and the carboxylic groups and the central pyrazine ring which are given in Table 2-4. The large differences indicate that the pyridine rings and carboxylates of the molecule are very flexible and rotate about the bonds connecting them to the central pyrazine ring. In fact, this flexibility is one of the reasons responsible for the diversity of this ligand. We will discuss this relationship further in the next chapter.

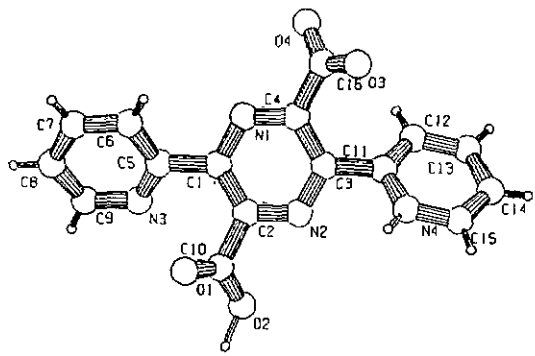

Fig. 2-17. Crystal structure of H_2L^2 (**19a**), showing the atom-numbering scheme

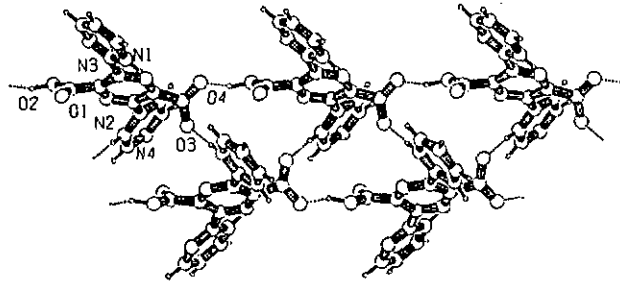

Fig. 2-18. A crystal packing diagram of compound **19a**, hydrogen bonds are illustrated by dotted lines

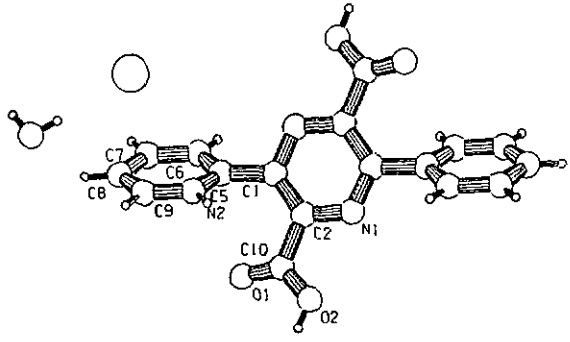

Fig. 2-19. Crystal structure of $H_2L^2.2HCl.(H_2O)_2$ (**19b**), showing the atom-numbering scheme

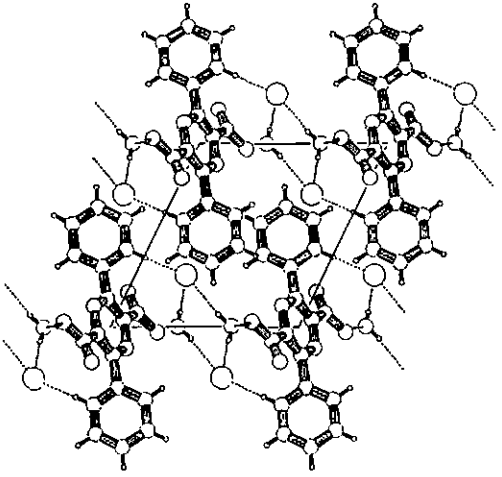

Fig. 2-20. A crystal packing diagram of compound **19b**

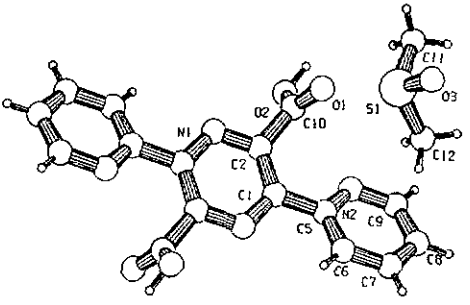

Fig. 2-21. Crystal structure of $H_2L^2 \cdot (DMSO)_2$ (**19c**), showing the atom-numbering scheme

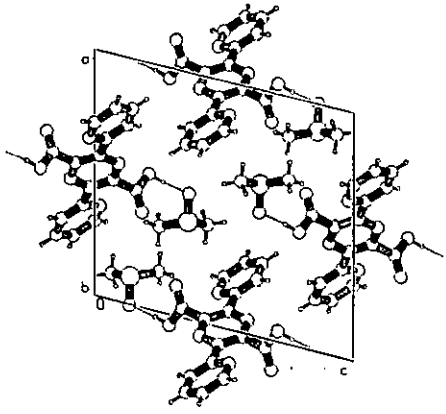

Fig. 2-22. A crystal packing diagram of compound **19c**

Table 2-4. A comparison of the dihedral angles between the pyridine rings and the carboxylate groups and the central pyrazine ring

Compound	**19a**	**19b**	**19c**
Py ^ Pyz (°)	36.8(1)	55.5(1)	23.3(1)
HPy ^ Pyz (°)	43.2(2)		
COOH ^ Pyz (°)	44.3(1)	19.8(2)	69.0(1)
COO^- ^ Pyz (°)	45.9(2)		

Molecule **19a** in the solid state forms a double-stranded molecular ribbon linked by four strong hydrogen bonds involving atom O2 of the protonated carboxylate group, atom N4 of the protonated pyridine, and atoms O3 and O4 of the deprotonated carboxylate group, see Fig. 2-18. The hydrogen bonding geometry is given in Table 2-5. We believe

that it is for this reason that compound **19a** is hardly soluble in water. In the solid state molecules **19b** are linked by an extensive hydrogen bonding network involving the Cl^- ion, the water molecule of crystallisation, OW1, atom O2 of the protonated carboxylate group, and atom N2 of the protonated pyridine, Fig. 2-20. There is only one strong hydrogen bond between atom O2 of the protonated carboxylate group and atom O3 of the included DMSO molecule, Fig. 2-22.

Table 2-5. The hydrogen-bonding geometry in **19a**, **19b** and **19c**.

Compound	H-Bond	D.....A (Å)	D------H (Å)	H.....A (Å)	D---H...A (°)
19a	O2--H2...O4 [i]	2.534	1.13	1.45	159.0
19a	N4--H4...O3[ii]	2.665	0.91	1.76	171.2
19b	OW1--H1..Cl1	3.145	0.82	2.33	171.4
19b	O2--H1...OW1	2.559	0.84	1.72	171.9
19b	N2--H2...Cl1	3.022	0.92	2.11	175.4
19b	OW1--H2..Cl1	3.147	0.81	2.34	173.6
19c	O2--H2...O3	2.611	0.93	1.68	173.8

Symmetry codes: (i) x -1+y z; (ii) 1-x -0.5+y 0.5-z

2.1.3. Synthesis of Ligand 3

2.1.3.1 Synthesis of Ligand 3 and its Derivatives

Using $KMnO_4$ as oxidising agent to react with the quinoxalines in neutral or basic media is the common method [1] for the synthesis of 5,6-disubstituted-pyrazine 2,3-dicarboxylic acid. Some successful reactions are shown in scheme 6.

Scheme 6

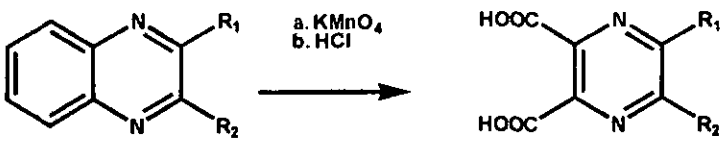

$R_1 = R_2 = H$
$R_1 = R_2 = Me$
$R_1 = R_2 = Ph$
$R_1 = R_2 = Cl$
$R_1 = Me, R_2 = H$

In order to synthesize ligand 3 (compound **22**) some precursors such as compounds **21** and **25** were considered. Scheme 7 presents the results of the synthesis of ligand 3 and its derivatives. The oxidation reaction is carried out in water. Compound **23** can be obtained by the reaction of **22** with thionyl chloride instead of acetic anhydride. Compound **24** was prepared as a potential ligand to construct supramolecular systems. Scheme 8 shows another synthetic strategy for ligand 3. However the preliminary results were unsatisfactory. Compound **25** has been obtained as a by-product in about 30% yield. This molecule may also be a potential ligand candidate in coordination chemistry.

Scheme 7

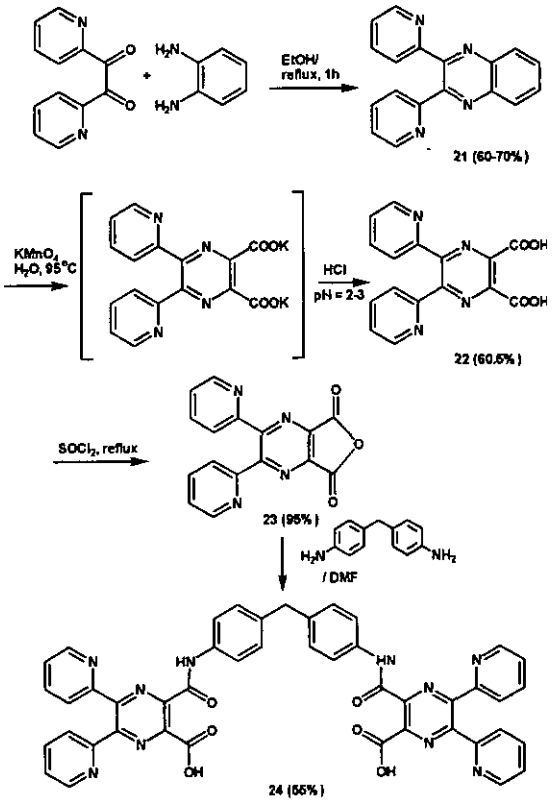

Scheme 8

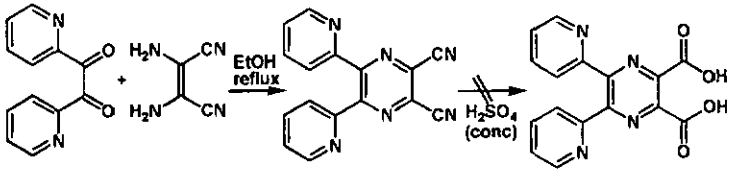

2.1.3.2. Characterization of Ligand 3 and its Derivatives

The structure of compound **22** was characterized by IR, NMR, and DCI-MS. The crystal structure of **22** has been determined by X-ray diffraction, Fig. 2-23. This molecule exists as an inner salt zwitterion like compound **19a**. There is a very strong intramolecular hydrogen bond between the atom N3 of the protonated pyridine and the atom N4 of the adjacent pyridine ring, which makes the central pyrazine ring and two substituted pyridine rings almost coplanar, Table 2-7. On the other hand this hydrogen bonding results in the central pyrazine ring being slightly twisted. This type of hydrogen bond has been reported previously in a substituted quinoxalines [7]. The selected bond distances and angles are given in Table 2-6. As a result of the hydrogen bonding, two unusual large exocyclic angles, C3--C4--C5 131.1(3)° and C4--C3--C10 131.1(3)°, have been found.

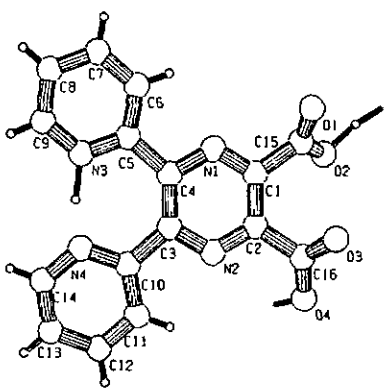

Fig. 2-23. Crystal structure of H_2L^3 (**22**), showing the atom-numbering scheme

Table 2-6. Selected distances(Å) and Angles (°) for **22**

Bond	Length (Å)	Bond	Angle (°)
N1---C1	1.325(4)	C1--N1--C4	120.2(3)
N1---C4	1.351(3)	C2--N2--C3	120.5(3)
N2---C2	1.327(3)	N1--C1--C2	120.7(3)
N2---C3	1.350(4)	N1--C1--C15	115.3(3)
C1---C2	1.397(4)	C2--C1--C15	123.9(3)
C3---C4	1.412(4)	N2--C2--C1	119.8(3)
C1---C15	1.511(4)	N2--C2--C16	117.4(3)
C2---C16	1.517(4)	C1--C2--C16	122.8(3)
C3---C10	1.503(4)	N2--C3--C4	119.3(3)
C4---C5	1.502(4)	N2--C3--C10	109.6(2)
O1---C15	1.213(4)	C4--C3--C10	131.0(3)
O2---C15	1.300(4)	N1--C4--C3	119.1(3)
O3---C16	1.233(3)	N1--C4--C5	109.8(3)
O4---C16	1.264(3)	C3--C4--C5	131.1(3)
		N3--C5--C4	120.1(3)
		N4--C10--C3	120.0(3)
		O1--C15--O2	126.7(3)
		O1--C15--C1	121.9(3)
		O2--C16--C1	111.3(3)
		O3--C16--O4	125.7(3)
		O4--C16--C2	117.8(3)
		O3--C16--C2	116.5(3)

Fig. 2-24a presents the molecular packing in the crystal. Each molecule in the crystal is involved in two strong hydrogen bonds to two neighbouring molecules to form a double-stranded molecular ribbon with a unique hollow cavity, shown in Fig. 2-24b. The hydrogen bonding geometry is given in Table 2-7.

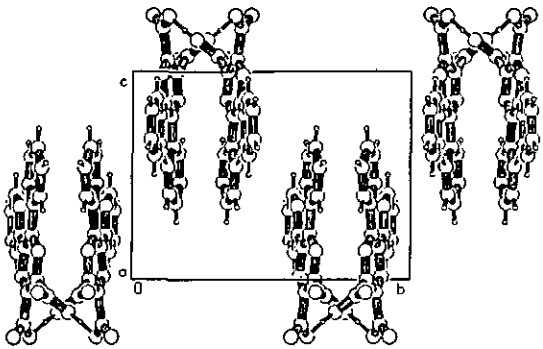

Fis. 2-24a. A crystal packing diagram of compound **22**, hydrogen bonds are illustrated by dottede lines.

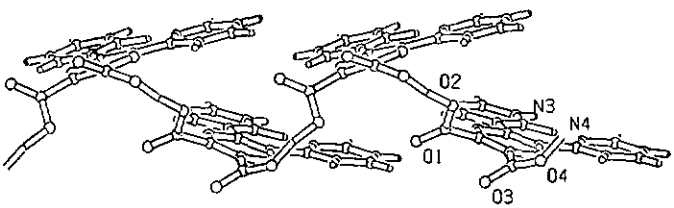

Fig. 2-24b. The intermolecular hydrogen-bonding of compound **22**, Hydrogen bonds O2-HO2....O4^{i}.

Table 2-7. The dihedral angles between the pyridine rings and the carboxylate groups and the central pyrazine ring and the hydrogen-bonding geometry for compound **22**.

	HPy ^ Pyz	Py ^ Pyz	COOH ^ Pyz	COO^- ^ Pyz
Dihedral Angle (°)	4.38(.09)	7.93(.08)	58.33(.21)	38.00(.11)
	Hydrogen	Bonding	Geometry	
H-bond	D.....A (Å)	D------H (Å)	H.....A (Å)	D---H...A (°)
O2--H2O..O4^{i}	2.475	1.207	1.285	166.7
N3--H3N..N4	2.530	1.234	1.313	166.9

Symmetry code (i): 0.5+x 1.5-y z.

Compound **24** was characterized and investigated by IR, ^{1}H and ^{13}C NMR, and FAB-MS. The preliminary results reveal a very complicated chemistry of this molecule in aqueous solution.

Compound **25** was completely characterized by IR, ^{1}H and ^{13}C NMR, EI-MS, and X-ray crystal structure analysis, with satisfactory results. A PLATON drawing of the two independent molecules is shown in Fig. 2-25. No obvious difference in the conformation has been found between the two molecules.

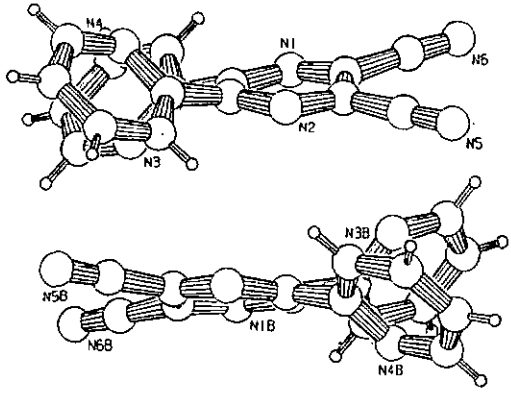

Fig. 2-25. Crystal structure of compound **25**,

2.1.4. Synthesis of the Oxazolines

The chiral pyridine having two oxazoline rings, and their complexes, have been recently designed and synthesized as auxiliaries for enantiotopic-differentiative reactions [8, 9]. In order to prepare coordination polymers containing a chiral centre, bis-bidentate ligands includes two chiral oxazoline rings introduced at the 3,6-positions of a 2,5-dimethylpyrazine skeleton, compound **26** and **28**, were rcpared. The chirality of the oxazoline rings is derived from commercially available optically active β-amino alcohols, e.g. **26** from (R)-2-amino-1-butanol and **28** from (R)-phenylglycinol. Compound **27** was

also synthesized from a non-optically active β-amino alcohol, 2,2-dimethyl-2-amino ethanol. The results are shown in Scheme 9.

Scheme 9

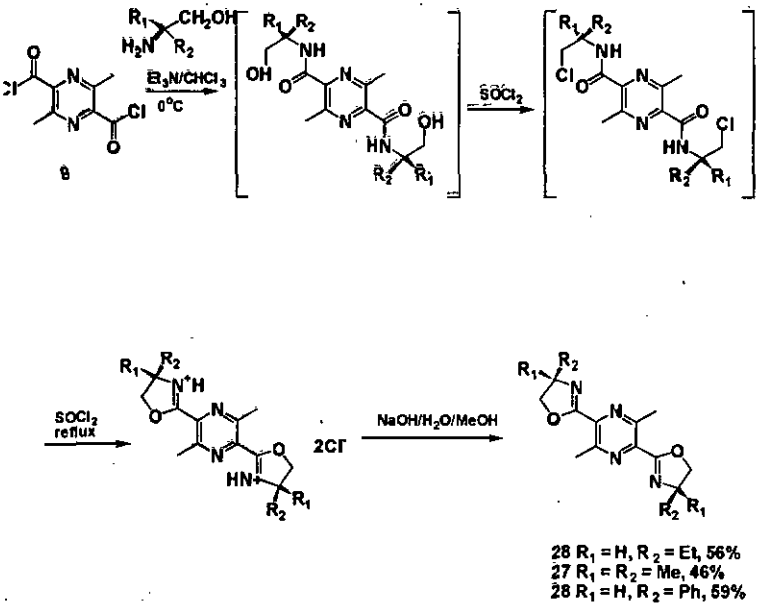

Compounds **26-28** were characterized by IR, ^{1}H and ^{13}C NMR, and EI-MS (HR-MS for **26-27**) with satisfactory results. No X-ray quality crystals were obtained for these three compounds.

2.2. Copper(II) Complexes with Ligands L^1, L^2 and L^3

2.2.1. Synthesis and Structure of Cu(II) Complexes of Ligand 1

The mononuclear complex $[Cu(Me_2L^1)_2(H_2O)_2]$ (29) was synthesized via a hydrolysis reaction of $Cu(ClO_4)_2.6H_2O$ and Me_2L^1 in 2:1 molar ratio in water, scheme 10. In fact, this compound was usually obtained irrespective of the Cu^{II}/Me_2L^1 ratio used. It is of interest to note that the coordinated ligand exists in an asymmetric form, even if there are a number of excess Cu^{II} ions in solution.

Scheme 10

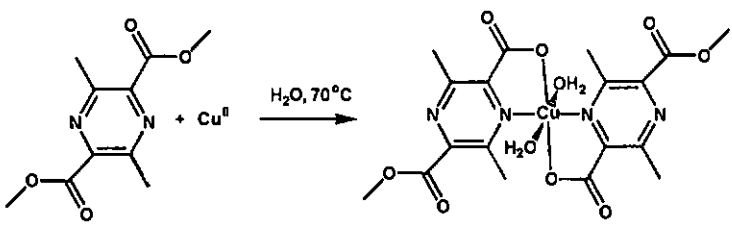

29

The structure of this complex was characterized by X-ray diffraction, Fig. 2-26, and IR spectroscopy. The Cu atom lies on an inversion center which imposes N1---Cu1---N1^i, O3---Cu1---O3^i, and Ow1---Cu---Ow1^i (i: -x, -y, -z) angles of 180°. The two MeL^1 ligands bound to the Cu atom are *trans* with respect to each other, with Cu1---N1 and Cu1---O3 distances of 2.135(4) and 1.895(4) Å, respectively, and angles O3--Cu--N1 80.6(2) °, O3--Cu--Ow1 91.6(2) °, N1--Cu--O3^i 99.4(2)°, and N1--Cu--Ow1 91.8(2) °. The Cu---N and Cu---O distances and angles are almost identical to those found in the structure of the coordination polymer $\{Mg(H_2O)_6[Cu(pztc)\cdot 2H_2O]\cdot 2H_2O\}_\infty$ [10].

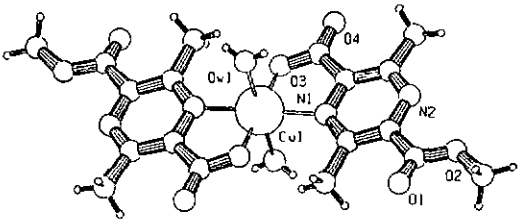

Fig. 2-26. Crystal structure of $[Cu(MeL^1)_2(H_2O)_2]$ **(29)**, showing the atom-numbering scheme

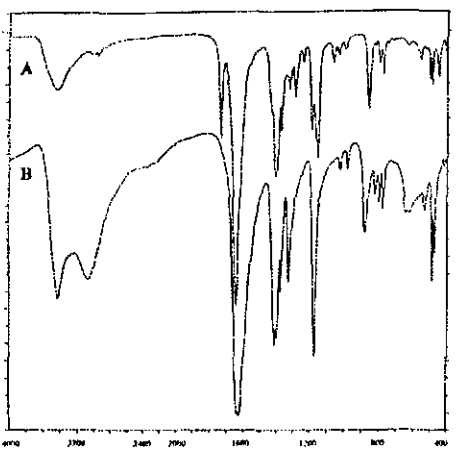

Fig. 2-27. A comparison of IR spectra,
A. $[Cu(MeL^1)_2(H_2O)_2]$ **(29)**; B. $[Cu(L^1)(H_2O)_2](H_2O)_{0.5}$ **(30)**

The coordination of the copper atom is square planar with the Cu atom lying in the best-plane through atoms N1, O3, $N1^i$, and $O3^i$ with atoms Ow1 and $Ow1^i$ occupying

position ± 2.470(4) Å from the square plane. The non-coordinated carboxylate groups, involving O1 and O2, are inclined by 17.7(7)° to the best plane through the pyrazine ring. The coordinated water molecules and non-coordinated O atoms of the carboxylate groups are involved in relatively weak hydrogen bonds of the type Ow---H.....O.

The reaction of $CuCl_2 \cdot 2H_2O$ with 3,6-dimethylpyrazine-2,5-dicarboxylic acid, H_2L^1, directly in water, gave a pale green precipitate. The elemental analysis and a comparison of its IR spectra, to that of complex **29**, Fig. 2-27, showed that it may be a uniform chain polymer, with unit formula $[Cu(L^1)(H_2O)_2] \cdot (H_2O)_{0.5}$ (**30**), Scheme 11. Table 2-8 presents the selected IR bands of complexes **29** and **30**.

Scheme 11

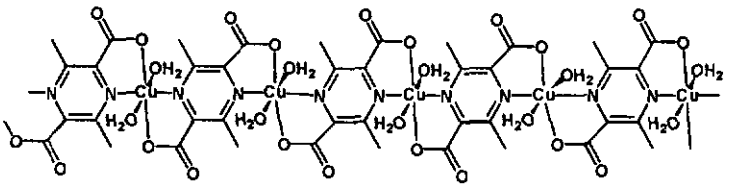

$[Cu(L^1)(H_2O)_2] \cdot (H_2O)_{0.5}$ (**30**)

Table 2-8. Selected IR bands for **29** and **30**

Complex	$\nu_{sym\ (OH)}$ cm^{-1}	$\nu_{asym(COO)}$ cm^{-1}	$\nu_{sym(COO)}$ cm^{-1}
29	3449	1647, 1737	1414
30	3427, 3072	1625	1415

The magnetic behaviour of the complex **30** has also been investigated. Fig. 2-28 shows plots of the molar magnetic susceptibility χ_m *vs* T in the range 4.2 and 300 K.

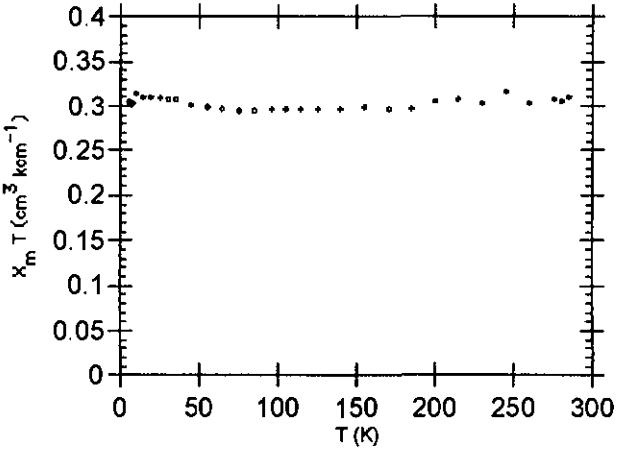

Fig. 2-28 . The molar susceptibility ($\chi_m T/T$) for $[Cu(L^1)(H_2O)_2]\cdot(H_2O)_{0.5}$ (**30**)

No coupling was observed in the magnetic measurement of complex **30** and the $\chi_m T$ value at room temperature is approximately 0.32 slightly less than normal value 0.39 cm^3Kmol^{-1} from the *Curie* law (1), where $S_i = 1/2$:

$$\chi_m T = (N\beta^2/3k)2g_i^2S_i(S_i + 1) \qquad (1)$$

2.2.2. Synthesis, Structures, and Magnetic Properties of Cu(II) Complexes of Ligand 2

The reaction of ligand 2 with first-row transition metals in water can afford a number of complexes. So far five types of the complexes or polymers have been obtained, shown in Fig. 2-29, (A). a mononuclear complex (M^{II} = Ni^{II} and Co^{II}) [11], (B). a dinuclear complex , (C). coordination polymers with a uniform chain structure, (D). coordination polymers with an alternating chain structure, and (E). a two dimensional coordination polymer. The mononuclear copper(II) complex (A) was not found irrespective of the

Cu^{II}/H_2L^2 ratio used. Scheme 12 presents the different Cu(II) complexes prepared with ligand 2 in this work.

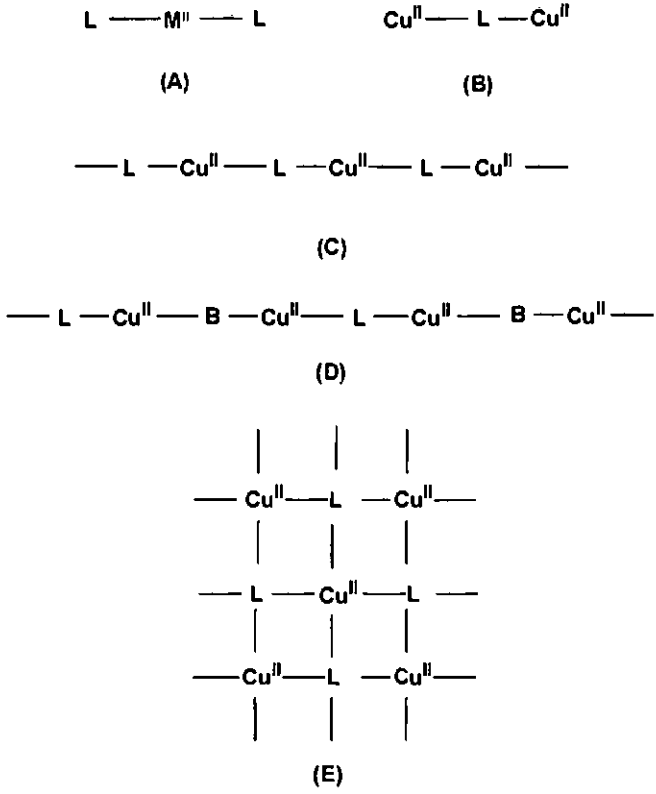

Fig. 2-29. The main types of the complexes of ligand 2.
Note: L could be any form of the ligand; B represents a bridging ligand, i.e. acetate, Cl^-, water and squarate.

Scheme 12

Uniform Polymer Chain

$\{[Cu(HL^2)(H_2O)](ClO_4)(H_2O)\}_n$ (**32**)

$\{[Cu(HL^2)(H_2O)](NO_3)\}_n$ (**33**)

$\{[Cu(HL^2)(H_2O)](C_4HO4)(H_2O)_2\}_n$ (**34**)

$\{[Cu(L^2)](H_2O)_{6.5}\}_n$ (**35**)

Alernating Polymer Chains

$\{[Cu_2(L^2)(CH_3COO)_2](H_2O)_3\}_n$ (**36**)

$\{[Cu_2(L^2)(L^{2*})(H_2O)_2](H_2O)_8\}_n$ (**37**)

$\{[Cu_2(L^2)(H_2O)_5](SO_4)(H_2O)_3\}_n$ (**38**)

$\{[Cu_2(L^2)Cl_2(H_2O)](H_2O)\}_n$ (**39**)

$\{[Cu_2(L^2)(C_4O_4)(H_2O)_2](H_2O)_{1.5}\}_n$ (**40**)

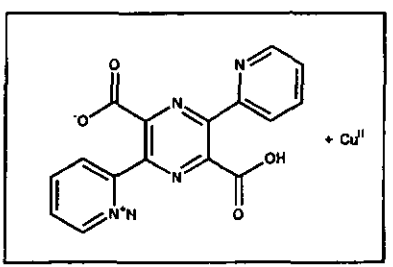

Dinuclear Complex

$[Cu_2(L^2)(H_2O)_4](ClO_4)_2(H_2O)_{3.75}$ (**31**)

Two Dimensional Polymer

$\{[Cu_2(L^2)(H_2O)_2](NO_3)_2\}_n$ (**41**)

2.2.2.1. Dinuclear Complex $[Cu_2(L^2)(H_2O)_4](ClO_4)_2(H_2O)_{3.75}$ (31)

Complex $[Cu_2(L^2)(H_2O)_4](ClO_4)_2(H_2O)_{3.75}$ (**31**) was obtained by the reaction of $Cu(ClO_4)_2.6H_2O$ with H_2L^2 in the molar ratio 4:1. This complex was also prepared by

the hydrolysis reaction of Et_2L^2 with $Cu(ClO_4)_2.6H_2O$. Dark green block-like crystals were obtained whose structure analysis showed it to be a dinuclear complex with the ligand coordinated in a bis-tridentate manner, Fig. 2-30a and Fig.2-30b. It is of interest to note that there are two independent molecules, A and B, in the unit cell with coordinated water molecules *cis*-- in A and *trans*-- in B. Selected bond distances and angles for the two independent molecules are given in Table 2-9.

Table 2-9. Selected bond distances (Å) and angles (°) in **31**

Bond Distance	Molecule A	Molecule B	Bond Angles	Molecule A	Molecule B
Cu1---N1	1.938(7)	1.936(8)	N1--Cu1--Ow1	162.8(3)	160.9(4)
Cu1---Ow1	1.946(7)	1.967(7)	N1--Cu1--O1	81.3(3)	81.9(3)
Cu1---O1	1.980(7)	1.976(7)	O1--Cu1--Ow1	97.7(3)	96.6(3)
Cu1---N3	2.001(8)	1.993(8)	N1--Cu1--N3	80.0(3)	80.0(3)
Cu1---Ow2	2.200(9)	2.188(10)	N3--Cu1--N3	99.1(3)	99.7(3)
Cu2---N2	1.951(7)	1.935(8)	O1--Cu1--N3	161.0(3)	161.8(3)
Cu2---O3	1.978(7)	1.952(7)	N1--Cu1--Ow2	105.5(3)	108.0(4)
Cu2---Ow3	1.987(7)	1.953(7)	Ow1—Cu1--Ow2	91.7(4)	91.0(4)
Cu2---N4	1.998(8)	1.993(9)	O1--Cu1--Ow2	92.8(3)	95.6(4)
Cu2---Ow4	2.172(9)	2.226(9)	N3--Cu1--Ow2	95.6(3)	92.0(4)
			N2—Cu2--O3	80.5(3)	81.6(3)
			N2--Cu2--Ow3	154.9(4)	162.8(3)
			O3--Cu2--Ow3	98.5(3)	99.3(3)
			N2--Cu2--N4	80.4(3)	80.5(3)
			O3--Cu2--N4	160.9(3)	162.0(3)
			N4--Cu2--Ow3	98.2(3)	98.2(3)
			N2--Cu2--Ow4	119.0(3)	105.4(4)
			O3--Cu2--Ow4	94.6(4)	94.2(3)
			Ow3--Cu2--Ow4	86.1(4)	91.7(4)
			N4—Cu2--Ow4	95.6(4)	89.4(4)

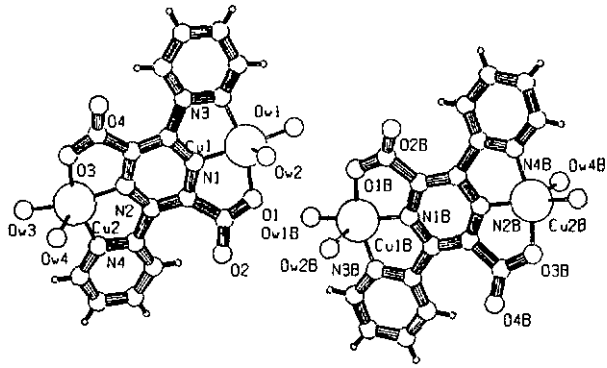

Fig. 2-30a. Crystal structure of the two independent molecules of $[Cu_2(L^2)_2(H_2O)_4](ClO_4)_2(H_2O)_{3.75}$ (**31**), showing the atom-numbering scheme.

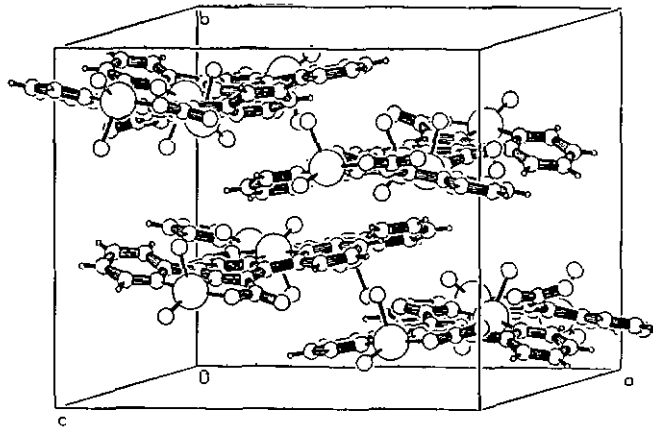

Fig. 2-30b. A crystal packing diagram of complex **31**, the anions and the water molecules of crystallization have been omitted for clarity.

The pyrazine rings are twisted by 8.4(4)° and 5.6(7)° (defined by the dihedral angle between the planes made up of atoms N1, C1, C4 and N2, C2, C3) for molecule A and B, respcctively. Pyridine rings I and IB (Py I: N3, C7-C11; Py IB: N3B, C7B-C11B), coordinated to atom Cu1 and Cu1B, are inclined to the center pyrazine ring by 11.4(2)° and 9.6(2)°, while rings II and IIB (Py II: N4, C12-C16; Py IIB: N4B, C12B-C16B), coordinated to Cu2 and Cu2B, are inclined by 16.1(2)° and 17.6(3)°. The carboxylate groups I and IB (plane I: C5, O1, O2; plane IB: C5B, O1B, O2B), coordinated to atom Cu1 and Cu1B, are inclined to the center pyrazine ring by 18.4(5)° and 15.2(5)°, while carboxylates II and IIB (plane I: C6, O3, O4; plane IB: C6B, O3B, O4B), coordinated to Cu2 and Cu2B, are inclined by 12.0(9)° and 17.0 (9)°. The ligands are twisted as seen by the dihedral angles, 26.9(3) and 24.6(3)°, between opposite pyridine rings for molecules A and B, respectively. The coordination of Cu1, Cu1B and Cu2B are described as perfectly square pyramidal with τ values of 0.03, 0.02 and 0.01, respectively ($\tau = 0$ for SP, $\tau = 1$ for TBP, according to the definition of Addison et al [12], also represented below).

$$\tau = | \beta - \alpha | / 60 \qquad (2)$$

β is the largerof the basal angles and α is the second larger of the basal angles of the square pyramidal geometry.

The coordination of atom Cu2 is described as slightly distorted square pyramidal with a τ value of 0.1. The average Cu-N(pyrazine) distance of 1.940(8) Å is shorter than the standard average value 2.024 Å [13]. The average Cu-N(pyridine) distance is 1.996(9) Å, is close to the average value reported [14, 15] for the Cu dinuclear complexes formed with BPPZ and TPPZ. The average Cu-O (carboxylate) distance is 1.972(7) Å, which is close to the usual carboxyl oxygen to copper distance of 1.94 Å. The average

Cu-O(water) distance is 1.963 (7) for the O atoms of water in the square plane and 2.197(10) Å for the axial O atoms, respectively. The Cu1 to Cu2 distances are 6.508(8) and 6.488(8) Å for molecules A and B, respectively. As a result of comparing the two molecules it appears that molecule B, with the *trans* conformation of the axial water molecules, should be more stable than the *cis*- conformation of A.

2.2.2.2. Uniform Polymer Chains 32, 33, 34, and 35

We have obtained three compounds with a uniform chain structure, **32**, **33** and **34** by reacting aqueous solutions of different Cu(II) salts with ligand 2, scheme 13.

Scheme 13

$$H_2L^2 + 2\,Cu(ClO_4)_2\cdot 6H_2O \xrightarrow[H_2O]{R.\,T.} \{[Cu(HL^2)(H_2O)](ClO_4)(H_2O)\}_n \quad (32)$$

$$H_2L^2 + 2Cu(NO_3)_2\cdot 3H_2O \xrightarrow[H_2O]{R.\,T.} \{[Cu(HL^2)(H_2O)](NO_3)\}_n \quad (33)$$

$$H_2L^2 + 2Cu(ClO_4)_2\cdot 6H_2O + C_4H_2O_4 \xrightarrow[H_2O]{R.\,T.} \{[Cu(HL^2)(H_2O)](C_4HO_4)((H_2O)_2\}_n \quad (34)$$

$C_4H_2O_4$ = squaric acid

a) Synthesis and Structures of Complexes 32, 33 and 34

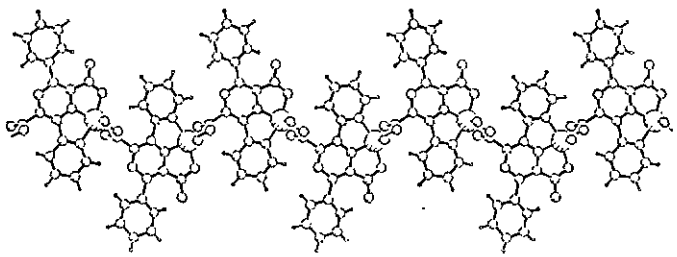

Figure 2-31. A uniform chain representation found in the structure of complex **33**

Fig. 2-31 presents the general structural feature of this type of polymer found also in complex **34**. The ligand is coordinated in an asymmetric manner, combining a tridentate and a monodentate coordination with a protonated pyridine. The crystal structures of complexes **32** to **34** are given in Figures 2-32, 2-33 and 2-34. Selected bond lengths and angles for the three complexes are give in Table 2-10. In Table 2-11 dihedral angles between the pyrazine ring and the pyridine rings and the carboxylate groups are compared for complexes **32** to **34**.

The copper atoms have a slightly distorted square pyramidal coordination, but with different τ values given in Table 2-10, and a coordinated water molecule occupies the axial position of the square pyramidal geometry in all three compounds.

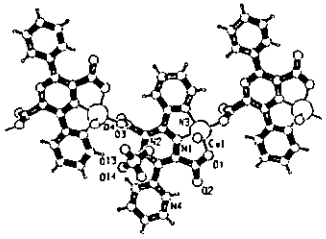

A

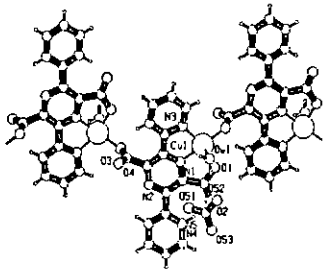

B

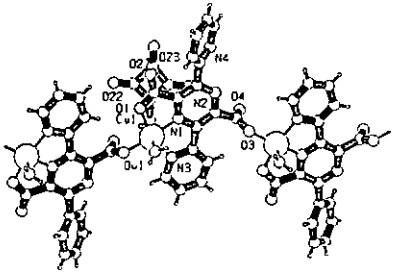

C

Fig. 2-32. Crystal structures and the atom numbering schemes for

A). Complex **32**; B). Complex **33**; C). Complex **34**,

The intramolecular hydrogen bonds involve atoms O2 and N4H in complexes **32** and **33**

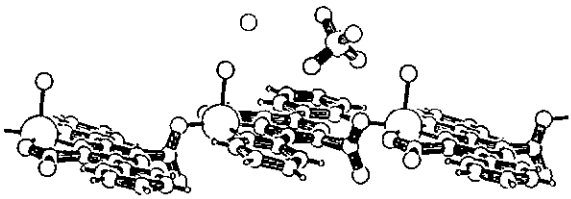

A

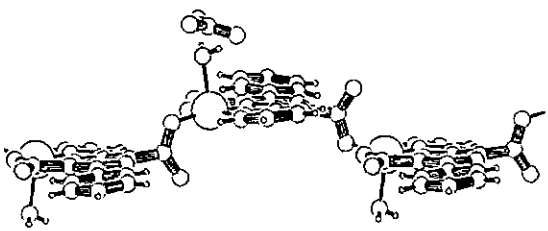

B

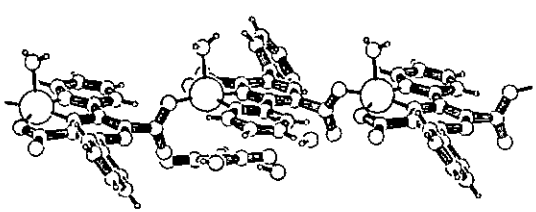

C

Fig. 2-33. A conformational comparison

A). Complex **32**; B). Complex **33**; C). Complex **34**

A

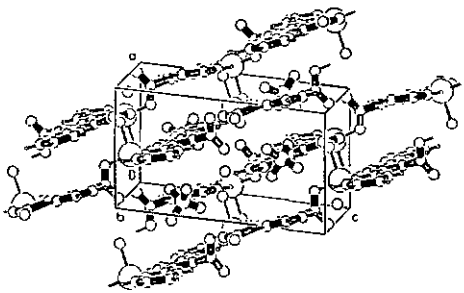

B

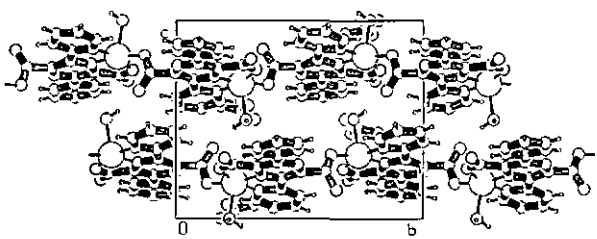

C

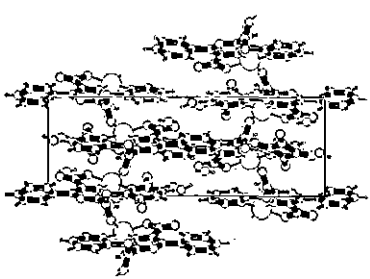

Fig 2-34. Crystal packing diagrams: A). Complex **32**; B). Complex **33**; C). Complex **34**.

As seen from the figures and Table 2-11 the ligand, although coordinated in a similar mode, presents two different conformations in the complexes **32** to **34**. An intramolecular hydrogen bond between the N atom of the protoned pyridine and the O atom of the adjacent carboxylate, see Table 2-12, is involved in the first conformation. This results in the three rings and a carboxylate of the ligand being almost coplanar. The second carboxylate is almost perpendicular to this plane. The ligand is extremely twisted in the second conformation, found in the complex **34**, with a dihedral angle of 43.9 (2)° between the protonated pyridine ring and the coordinated pyridine ring.

From Fig. 2-33 it can be seen that there are two different chain compositions in the three polymers. The first is composed of subunits related by a mirror (enantiomers), which leads to a step-like type chain for complexes **32** and **34**. The second is composed of the same conformational (all *R* or all *S*) subunits related by a 2-fold screw axis, which leads to a helical chain for complex **33**.

In Table 2-10 a comparison is made of similar Cu-N and Cu-O bond distances and the bond angles in complexes **32-34**. It can be seen that the Cu-Npz (Pyrazine) distances, Cu1-N1, are similar in **33** and **34** and longer than found in complexe **31**, 1.937 Å. An extremely short Cu-Npz distance 1.905(14) Å was observed in complex **32**. The Cu to Npy (pyridine) and O(carboxylates and water) distances are also similar and close to the distances found in **31** except for the unusually short Cu-O distance, 1.892(11) Å, in **32**. However, a similar distance, 1.901(1) Å has been observed in complex $\{Mg(H_2O)_6[Cu(pztc)\cdot 2H_2O]\cdot 2H_2O\}_n$ [10]. The intramolecular Cu....Cu distances are 7.604(19), 7.495(4) and 7.726(7) Å for **32**, **33** and **34**, respectively. In general the bond angles involving the Cu atoms are similar in the three polymers.

Table 2-10. Selected bond lengths (Å) and angles (°) for **32**, **33** and **34**

	Complex **32**	Complex **33**	Complex **34**
Cu1---O3	1.892(11)	1.940(3)	1.947(5)
Cu1---N1	1.905(14)	1.949(3)	1.945(6)
Cu1---O1	1.987(12)	1.958(3)	2.003(5)
Cu1---N3	2.01(2)	2.000(4)	2.031(6)
Cu1---Ow1	2.221(12)	2.231(4)	2.181(7)
O3--Cu1--N1	170.9(5)	168.1(2)	168.9(2)
O3--Cu1--O1	97.9(5)	94.41(14)	97.3(2)
N1--Cu1--O1	81.8(5)	80.46(14)	80.7(2)
O3--Cu1--N3	98.7(6)	103.1(2)	100.7(3)
N1--Cu1--N3	80.1(6)	80.2(2)	79.0(3)
O1--Cu1--N3	160.0(5)	159.3(2)	157.5(2)
O3--Cu1--Ow1	92.4(5)	93.9(2)	89.2(3)
N1--Cu1--Ow1	96.7(5)	97.1(2)	101.8(3)
O1--Cu1--Ow1	95.4(5)	93.5(2)	93.9(3)
N3--Cu1--Ow1	94.9(5)	96.1(2)	99.5(3)
τ value	0.18	0.15	0.19

Table 2-11. Dihedral angles (°) between the pyrazine ring (Pz) and the pyridine rings HPy and Py, and carboxylates planes A and B

Angles	Complex **32**	Complex **33**	Complex **34**
C' ^ C''	0.1(14)	3.1(4)	2.7(10)
HPy ^ Pz	2.3(4)	6.2(1)	42.5(11)
Py ^ Pz	4.6(4)	7.6(2)	1.1(9)
HPy ^ Py	6.1(4)	13.3(2)	43.9(2)
A ^ Pz	9.1(22)	5.0(6)	0.8(9)
B ^ Pz	80.1(9)	86.4(2)	78.7(10)
plane C' = N1, C1, C4; plane C'' = N2, C2, C3 plane A = C15, O1, O2; plane B = C16, O3, O4			

The presence of the different anions and the coordinated water molecules, as well as the water molecules of crystallization, plays an important role in crystal cohesion. The

stronger hydrogen bonds are given in Table 2-12. In **32** and **33** parallel polymer chains are linked by a two dimensional hydrogen bonding network involving the coordinated water molecules and the anions, as well water molecule of crystallization for **32**. The most interesting hydrogen bonding network is found in complex **34**. The chains are linked by a three-dimensional hydrogen bonding network involving all four O-atoms of the squarate anion, two water molecules of crystallization, the axial coordinated water molecule, and N-atom of the protonated pyridine, and the two carbonyl O-atoms of the carboxylate groups.

Table 2-12 Hydrogen bonding in complexes **32**, **33** and **34**

Complex	Hydrogen bond	D...A (Å)	D--H (Å)	H...A (Å)	D-H..A(°)
32*	N4--H4....O2	2.527	0.86	1.70	162
	Ow1....Ow2	2.764	------	------	------
	Ow2....O2	2.783	------	------	------
	average e. s. ds.	0.018	0.02	0.02	0.6
33	N4--H4....O2	2.537	0.90	1.66	165.3
	Ow1--H1A...O52	2.753	0.85	1.93	163.3
	Ow1--H1B....O4^{i}	2.762	0.79	2.03	153.0
	e. s. ds. rang	0.006	0.01	0.01	0.3
34	Ow1--H1w1....O24	2.780	0.68	2.11	169
	Ow1--H2w1....O22	2.740	0.84	1.97	154
	Ow2--H2w2....O24	2.803	0.77	2.08	157
	Ow3--H1w3....O2^{ii}	2.673	0.84	1.90	151
	N4--H4....Ow2^{iii}	2.662	0.86	1.82	168
	Ow3-H2w3..O23^{iv}	2.784	0.93	1.85	176
	O21--H21....O4^{v}	2.591	0.62	1.97	175
	e. s. ds. rang	0.010-0.012	0.08-0.13	0.01-0.13	8-14

Symmetry code: (i) x, 1/2-y, z - 1/2; (ii) 1/2 + x, 1/2 - y, z
(iii) 1/2 - x, 1/2 + y, 1/2 + z; (iv) 1/2 - x, 1/2 + y, z - 1/2
v) x, y -1, z
* Because of limited reflections, H-atoms could not be located.

b). Magnetic Measurements

The molar χT product *vs* T of **33** is given in Figure 2- 35. The $\chi_m T$ value decreases when the temperature is lowered. Below 25K $\chi_m T$ decreases abruptly reaching a value of 0.14 cm^3 K mol^{-1} at 4 K.

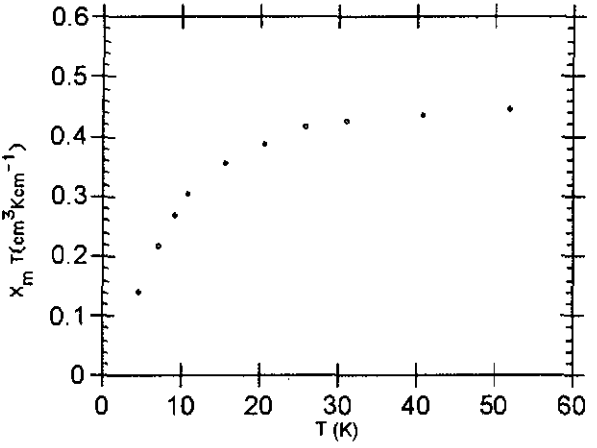

Fig. 2-35. The molar susceptibility ($\chi_m T/T$) for $\{[Cu(HL^2)(H_2O)](NO_3)\}_n$ **(33)**

The molar susceptibility, χ_m *vs* T plot for complex **33** is shown in Fig. 2-36. The χ_m value increases as the temperature decreases, reaching a maximum at ca. 7 K with a χ_m value of 3.15 x 10^{-2} cm^3mol^{-1}. The position of the maximum indicates moderate *antiferromagnetic coupling between the copper(II) ions through the ligand bridges.*

The experimental susceptibility data for **33** was fitted to the theoretical expression as a uniform chain in the rang 4 to 60 K. The expression used was formula (3) [16]

$$\chi = \frac{Ng^2\beta^2}{kT} \quad \frac{0.25 + 0.074975x + 0.075235x^2}{1.0 + 0.993\,1x + 0.172135x^2 + 0.757825x^3} \qquad (3)$$

with $x = |J| / kT$

The best fitting parameters obtained are J = -6.5 cm^{-1} and g = 2.32, also see Fig. 2-36. This is very a rare phenomenon in such a system with large Cu···Cu separation, 7.495(4) Å.

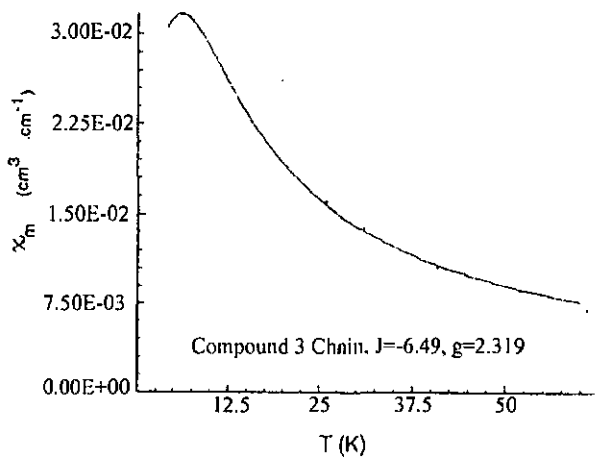

Fig. 2-36. Temperature dependence of χ_m for complex **33**, experimental (x) and theoretical (—)

The molar $\chi_m T$ product *vs* T of **34** is given in Figure 2- 37. No coupling, however, has been observed in the magnetic measurement of complex **34** and the $\chi_m T$ value at room temperature is approximately 0.51, more than normal value 0.39 cm^3Kmol^{-1}.

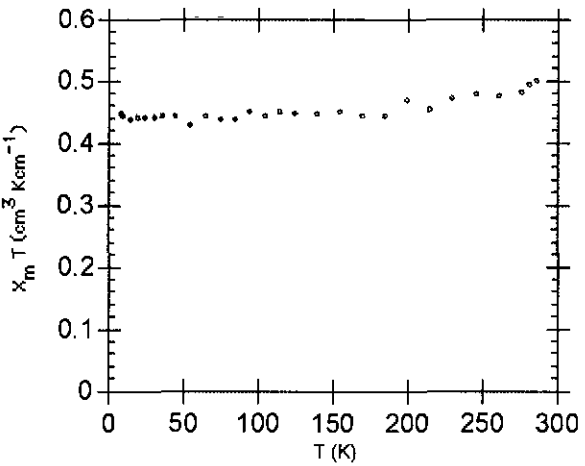

Fig. 2-37 . The molar susceptibility ($\chi_m T/T$) for $\{[Cu(HL^2)(H_2O)](C_4HO_4)(H_2O)_2\}_n$ (**34**)

The polycrystalline ESR spectra of complexes **33** and **34** were recorded at room temperature, see Fig. 2-38, they are almost axial with $g_{\parallel} = 2.28$; $g_{\perp} = 2.07$ for **33** and $g_{\parallel} = 2.25$, $g_{\perp} = 2.07$ for **34** as expected for a square-pyramidal coordination[17]. No resolved hyperfine structure for the copper ions was observed.

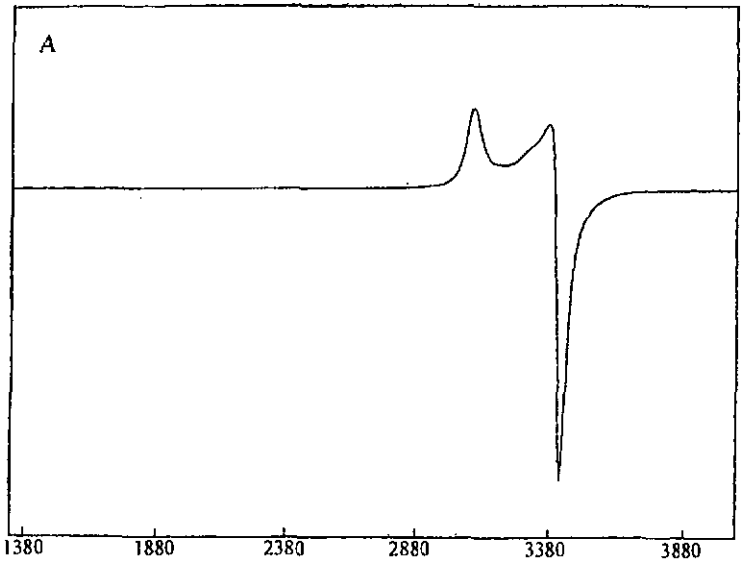

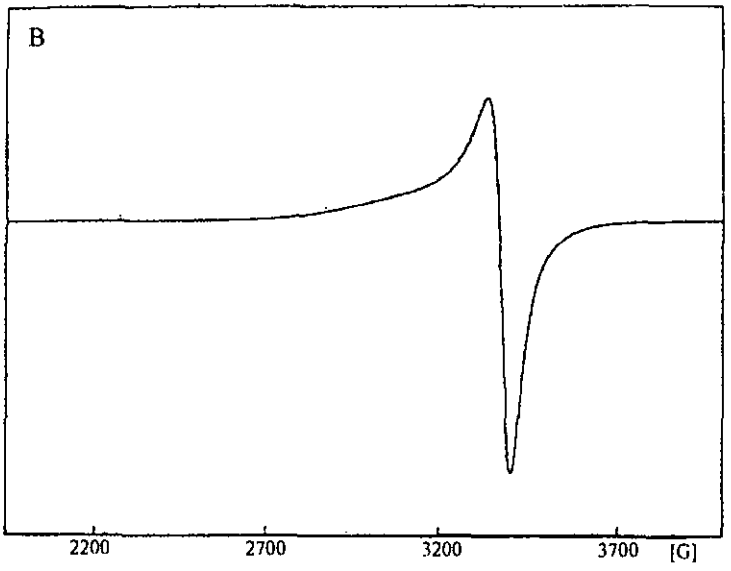

Fig. 2-38. ESR powder spectra (X-band at 298 K): A) **33**; B) **34**

c). Complex $\{[Cu(L^2)(H_2O)_2]\ (H_2O)_{4.5}\}_n$ (35)

Finally Complex **35** was obtained as a pale green cottonwool-like solid by reacting an aqueous solution of Cu(II) salts with ligand 2 in a 1:1 molar ratio. The elemental analysis and IR spectrum indicate that there is no anion in this complex and it may be a uniform chain with unit molecular formula $[Cu(L^2)(H_2O)_2](H_2O)_{4.5}$. The initial magnetic measurement shows no coupling between copper(II) ions. The proposed structure is given in Fig. 2-40. This complex is a very important intermediate. It occurred frequently in the initial stages of the formation of many of the complexes formed with ligand 2.

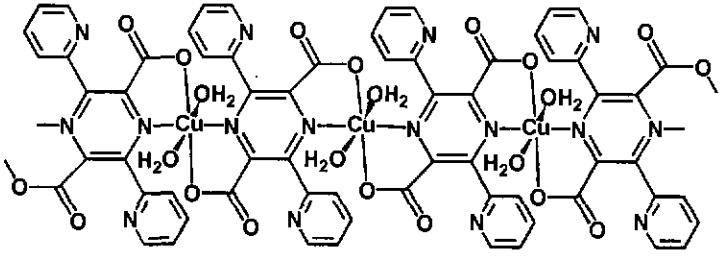

Fig. 2-39. A proposed structure for complex **35**

The molar $\chi_m T$ product *vs* T of **35** is given in Figure 2- 40. No coupling, however, has been observed in the magnetic measurement of complex **35** and the $\chi_m T$ value at room temperature is approximately 0.56, more than normal value 0.39 cm^3Kmol^{-1} .

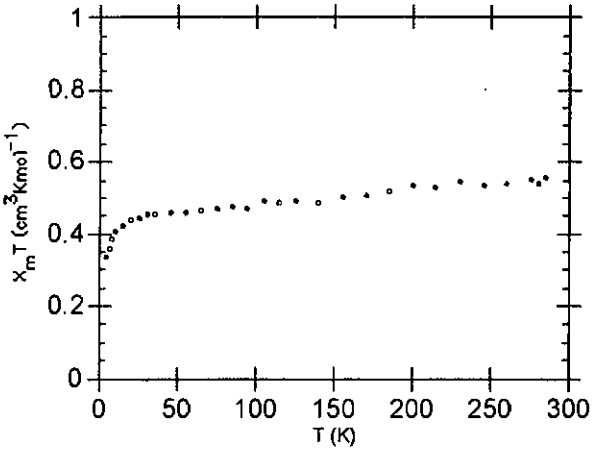

Fig. 2-40. The molar susceptibility ($\chi_m T/T$) for $\{[Cu(L^2)(H_2O)_2]\ (H_2O)_{4.5}\}_n$ **(35)**

2.2.2.3. Alternating Polymer Chains 36, 37, 38, 39, and 40

Five copper complexes with an alternating chain structure, **36** to **40**, were obtained by reacting aqueous solutions of different Cu(II) salts with ligand **2**, scheme 14.

Scheme 14

$H_2L^2 + 2Cu(ClO_4)_2{\cdot}6H_2O \xrightarrow[AcOH/AcOK]{R.\ T.\ H_2O} \{[Cu(L^2)(AcO)_2](H_2O)_3\}_n$ **(36)**

$H_2L^2 + 2CuSO_4{\cdot}5H_2O \xrightarrow[H_2O]{R.\ T.} 1/2\{[Cu(L^2)(L^{2*})(H_2O)_2](HO_2)_8\}_n$ **(37)**

$H_2L^2 + 2CuSO_4{\cdot}5H_2O \xrightarrow[H_2O]{R.\ T.} \{[Cu(L^2)(H_2O)_5](SO_4)((H_2O)_3\}_n$ **(38)**

$H_2L^2 + 2CuCl_2{\cdot}2H_2O \xrightarrow[H_2O]{R.\ T.} \{[Cu(L^2)Cl_2(H_2O)](H_2O)\}_n$ **(39)**

$H_2L^2 + 2Cu(ClO_4)_2{\cdot}6H_2O + C_4H_2O_4 \xrightarrow[H_2O/EtOH]{R.\ T.} \{[Cu(L^2)(C_4O_4)(H_2O)_2](C_4HO_4)((H_2O)_{1.5}\}_n$ **(40)**

$C_4H_2O_4$ = squaric acid

Note: L^{2*} represents ligand 2 coordinated in a bis-bidentate manner with two free carboxylate groups.

In the complexes **36-38** the ligand chelates the copper atom in a bis-tridentate manner to form symmetrical binuclear units, $[Cu_2(L^2)]$. Furthermore, these binuclear units were linked by the bridging ligands, such as acetate groups, chlorine ions, water molecules, squarate anions, and even a second ligand in complex **37**, to construct an alternating polymer chain.

a). $\{[Cu_2(L^2)(AcO)_2](H_2O)_3\}_n$ (36)

Figures 2-41 shows the crystal structure of complex $\{[Cu_2(L^2)(AcO)_2](H_2O)_3\}_n$ (**36**). Selected bond distances and angles are given in Table 2-13.

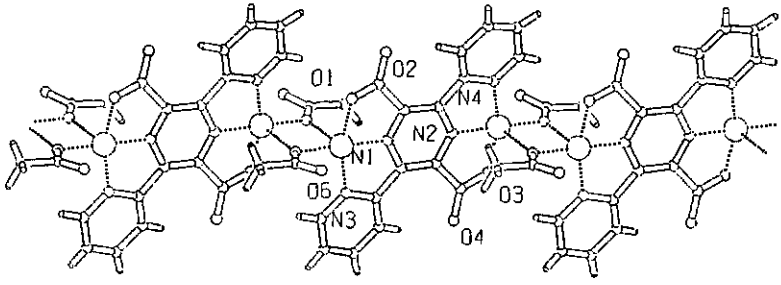

Fig. 2-41. Crystal structure of $\{[Cu_2(L^2)(CH_3COO)_2](H_2O)_3\}_n$ (**36**), showing the atom-numbering scheme

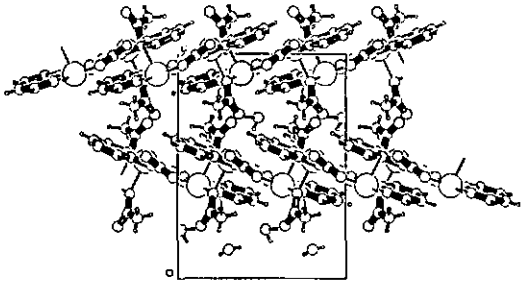

Fig. 2-42. A crystal packing diagram of complex **36**.

Table 2-13. Selected Bond distances and angles in **36**

Bond	Distance (Å)	Bond	Distance (Å)
Cu1---O5	1.918(4)	Cu2---O7	1.919(4)
Cu1---N1	1.944(5)	Cu2---N2	1.944(5)
Cu1—O1	1.966(4)	Cu2—O3	1.952(4)
Cu1---N3	1.988(5)	Cu2---N4	1.996(5)
Cu1---O7^{i}	2.396(4)	Cu2---N5^{ii}	2.378(5)
Bond	**Angle (°)**	**Bond**	**Angle (°)**
O5--Cu1--N1	179.5(2)	O7--Cu2--N2	178.6(2)
O5--Cu1--O1	97.6(2)	O7--Cu--O3	96.5(2)
N1--Cu1--O1	82.1(2)	N2--Cu2--O3	82.1(2)
O5--Cu1--N3	99.9(2)	O7--Cu2--N4	100.8(2)
N1--Cu1--N3	80.4(2)	N2--Cu2--N4	80.5(2)
O1--Cu1--N3	162.2(2)	O3--Cu2--N4	162.5(2)
O5--Cu1-O7^{i}	80.4(2)	O7--Cu2--O5^{ii}	80.9(2)
N1--Cu1--O7^{i}	99.8(2)	N2--Cu2--O5^{ii}	99.2(2)
O1--Cu1--O7^{i}	89.9(2)	O3--Cu2--O5^{ii}	91.8(2)
N3--Cu1--O7^{i}	96.4(2)	N4--Cu2--O5^{ii}	93.1(2)
Cu1--O5--Cu2^{i}	99.7(2)	Cu2--O7--Cu1^{ii}	99.0(2)

Symmetry code: (i). x - 1/2, y + 1/2, z; (ii). x + 1/2, y - 1/2, z

In complex **36**, the binuclear units with a *trans* conformation, like molecule B in **31**, were linked by two acetate groups coordinating in the following mode:

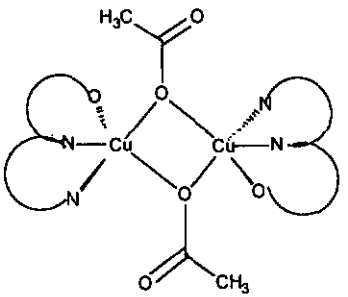

In fact the O atoms of the acetate groups were coordinated to two Cu atoms in an asymmetrical manner, for example the Cu1---O5 and Cu2---O5^{ii} distances are 1.918(4) and 2.378(5) Å, respectively. The average Cu---Npz distance of 1.944(5) Å is slightly longer than the same distances in **31** (for molecule B 1.936(8) Å). The Cu---Npy distances are comparable, the average distance is 1.992(5) Å in **36** compared to 1.993(9) Å in **31**. The Cu1---Cu2a bridging distance is 3.297 Å. The Cu1---Cu2 cross-linking distance is 6.490 Å. In **36** the Cu atoms are pentacoordinate and the geometry of the Cu atoms are highly distorted square-pyramidal with τ values of 0.29 for Cu1 and 0.27 for Cu2. The ligand is slightly twisted in **36** and the pyrazine-pyridine and pyrazine-carboxylate dihedral angles are given in Table 2-14.

Table 2-14. Dihedral angles (°) between the pyrazine ring (Pz) and the pyridine rings, Py1 and Py2, and the carboxylates planes, A and B, in **36**

C' ^ C"	Py1 ^ Pz	Py2 ^ Pz	Py1 ^ Py2	A ^ Pz	B ^ Pz
1.4(1.3)	10.5(0.9)	13.4(0.9)	6.4(0.5)	20.4(0.7)	16.1(0.7)
plane C' = N1, C1, C4; plane C" = N2, C2, C3; ring Py1 = N3, C7 - C11; ring Pz = N1, N2, C1-C4; ring Py2 = N4, C12 - C16; plane A = O1, O2, C5; plane B = O3, O4, C6					

The presence of the acetates and the water molecules of crystallization, plays an important role in crystal cohesion. The stronger hydrogen bonds are given in Table 2-15. In **36** parallel polymer chains are linked by a three dimensional hydrogen bonding network involving the coordinated acetate groups, the water molecule of crystallization and the two carbonyl O-atoms of the carboxylate groups.

Table 2-15. Hydrogen bonding in **36**

Hydrogen bond	D...A (Å)	D--H (Å)	H...A (Å)	D-H..A(°)
Ow1--H11A...O2^{i}	2.859	0.82	2.06	164
Ow1--H11B...Ow2^{ii}	3.016	0.93	2.13	160
Ow2--H22A...O4^{iii}	2.864	0.88	2.01	163
Ow2--H22B...Ow3^{iv}	2.745	0.69	2.10	156
Ow3--H33A...O6	2.734	1.00	1.74	169
Ow3--H33B...O8^{v}	2.757	1.26	1.63	145
average e. s. ds.	0.009	0.10	0.10	8

symmetry code: (i). 1 + x, -y, 1/2 + z; (ii). 1/2 + x, -1/2 + y, z
(iii). -1/2 + x, 1/2 + y, z; (iv). x, 1 + y, z; (v). x, -y, 1/2 + z

The molar $\chi_m T$ product *vs* T of **36** is given in Figure 2-42. The $\chi_m T$ value decreases when the temperature is lowered. Below 20 K $\chi_m T$ decreases abruptly reaching a value of 1.16 x 10^{-3} cm^3 K mol^{-1} at 2 K.

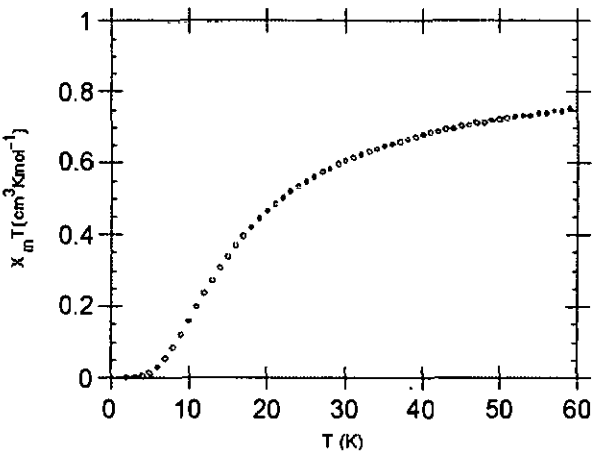

Fig. 2-43. The molar susceptibility ($\chi_m T/T$) for $\{[Cu_2(L^2)(CH_3COO)_2](H_2O)_3\}_n$ (**36**)

The χ_m value increases when the temperature decreases, reaching a maximum at ca 20 K with χ_m value of 2.37 x 10^{-2} cm^3mol^{-1}, Fig. 2-43. Below this temperature the curve decreases abruptly. Although the acetate bridging Cu---Cu distance is shorter, 3.297 Å, than the Cu1---Cu2 cross-linking distance (6.490 Å), the asymmetrical coordination of the acetate and the bridging Cu--O--Cu angle, ca 99 °, indicate a weak or negligible exchange pathway. Therefore the position of the maxima indicates moderate antiferromagnetic coupling between the copper (II) ions through the pyrazine bridges.

The experimental susceptibility data for **36** were fitted to the theoretical expression as a copper (II) dinuclear complex in the range 2 to 60 K, also see Fig. 2-43. The expression used was formula (4) [18].

$$\chi = \frac{2Ng^2\beta^2}{kT\,[3 + \exp(-J/kT)]}\,(1 - \rho) + \frac{Ng^2\beta^2}{2kT}\,\rho \qquad (4)$$

ρ is the molar fraction of noncoupled species

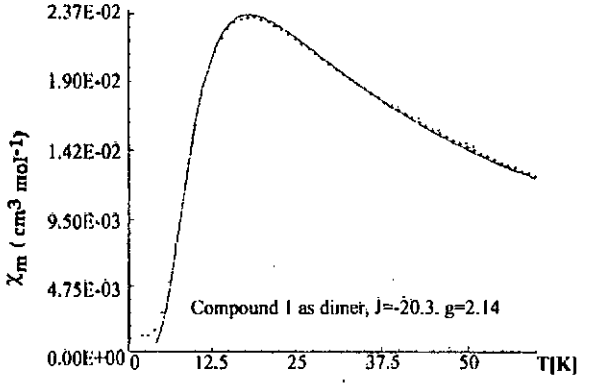

Fig. 2-44. Temperature dependence of χ_m for $\{[Cu_2(L^2)(CH_3COO)_2](H_2O)_3\}_n$ (**36**), experimental (+) and theoretical (—)

The best fitting parameters obtained are J = -20.3 cm^{-1}, g = 2.14.

The polycrystalline ESR spectra of complex **36** was recorded at room temperature, see Fig. 2-45, it is axially distorted with $g_{\parallel} = 2.25$; $g_{\perp} = 2.06$ as expected for a square-pyramidal coordination. No resolved hyperfine structure for copper ions was observed.

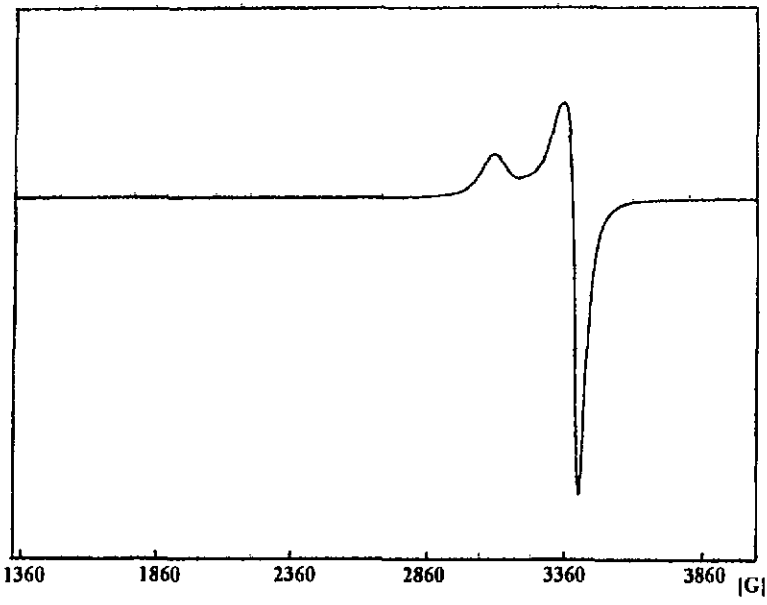

Fig. 2-45. ESR powder spectra (X-band at 298 K) for $\{[Cu_2(L^2)(CH_3COO)_2](H_2O)_3\}_n$ **(36)**

b). $\{[Cu_2(L^2)(L^{2*})(H_2O)_2](H_2O)_8\}_n$ (37)

Perhaps the most interesting alternating chain structure is found in complex **37**. Here there are two different coordinating forms of ligand 2. The first form of the ligand is coordinated in a bis-tridentate manner to form symmetrical $[Cu_2(L^2)]$ binuclear units. For the second form the two COO^- substituents do not coordinate, and the ligand (L^{2*}) acts as a bis-bidentate bridging ligand to link two binuclear units, so forming an alternating polymer chain. Figures 2-46 and 2-47 show the crystal structure and the crystal packing of complex $\{[Cu_2(L^2)(L^{2*})(H_2O)_2](H_2O)_8\}_n$ **(37)**. Selected bond distances and angles are given in Table 2-16.

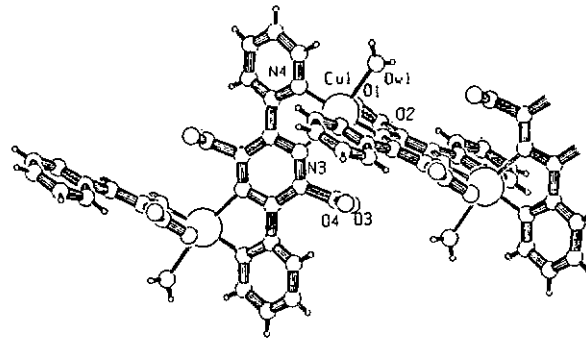

Fig. 2-46. Crystal structure of $\{[Cu_2(L^2)(L^{2*})(H_2O)_2](H_2O)_8\}_n$ (**37**), showing the atom-numbering scheme.

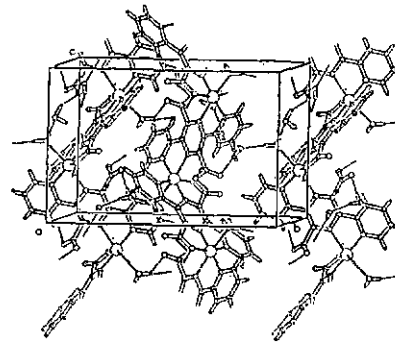

Fig. 2-47. A crystal packing diagram of complex **37**.

Table 2-16. Selected Bond distances and angles in **37**

Bond	Distance (Å)	Bond	Distance (Å)
Cu1---O1	1.971(6)	Cu1---N1	1.973(6)
Cu1---N2	1.977(6)	Cu1---N4	2.005(6)
Cu1---N3	2.348(6)	Cu1---Ow1	2.574(6)
Bond	**Angle (°)**	**Bond**	**Angle (°)**
O1--Cu1--N1	81.1(2)	O1--Cu1--N2	161.4(2)
N1--Cu1--N2	80.4(2)	O1--Cu1--N4	95.7(2)
N1--Cu1--N4	175.1(3)	N2--Cu1--N4	102.6(3)
O1--Cu1--N3	90.7(2)	N1--Cu1--N3	108.3(2)
N2--Cu1--N3	96.8(2)	N4--Cu1--N3	75.3(2)
Ow1--Cu1--O1	89.3(3)	Ow1--Cu1--N1	82.2(3)
Ow1--Cu1--N2	81.7(3)	Ow1--Cu1--N3	169.3(3)
Ow1--Cu1--N4	94.1(3)		

It is of interest to note that the Cu atoms are hexacoordinate in **37** s a square-bipyramid. The Cu---Npz distance of 1.973(6) Å in the binuclear units is slightly longer than the same distances in **31** and **36**. The Cu---Npz distance of 2.348(6) Å concerning L^{2*} is much longer than the same distance in all of the Cu complexes with ligand 2 in this work, as well as other Cu(II) complexes with pyrazine-based ligands studied so far. The Npy---Cu distances of 1.977(6) Å for L^2 and 2.005(6) Å for L^{2*} are close to the average value of the same distances in **31** to **34** and **36**. In fact the Npz atom for L^{2*} and the coordinated water molecule occupy axial positions of the pseudo-octahedron and the coordinated Npz, Npy, O atoms of L^2, and Npy of L^{2*} are located in the basal plane with the Cu atom. The Cu1---Cu1a distance, across -L^2, is 6.555 Å. The Cu1---Cu1b distance, across-L^{2*}, is 7.413 Å.

In Table 2-17 a comparison is made of the conformation of L^2 and L^{2*} in **37**. The bridging ligand L^{2*} is highly twisted compared to L^2 as the dihedral angle between opposite pyridine rings is 40.1(0.7)° and the uncoordinated carboxylates are almost perpendicular to the central pyrazine plane with a dihedral angle of 83.9(0.4)°.

Table 2-17. Dihedral angles (°) between the pyrazine ring (Pz) and the pyridine rings Py1 and Py2, carboxylates planes A and B in **37**

L	C' ^ C"	Py1 ^ Pz	Py2 ^ Pz	Py1 ^ Py2	A ^ Pz	B ^ Pz
L^2	0(1.7)	6.5(1.3)	6.5(1.3)	13.0(1.3)	18.1(1.4)	18.1(1.4)
L^{2*}	0 (0.8)	20.7(0.7)	20.7(0.7)	40.1 (0.7)	83.9(0.4)	83.9(0.4)

(L^2). plane C' = N1, C1, C2; plane C" = $N1^i$, $C1^i$, $C2^i$; ring Py1 = N2, C4 - C8; ring Pz = N1, C1, C2, $N1^i$, $C1^i$, $C2^i$; ring Py2 =$N2^i$, $C4^i$ - $C8^i$; plane A=O1, O2, C3; plane B=$O1^i$, $O2^i$, $C3^i$; (L^{2*}). plane C' = N3, C9, C10; plane C" = $N3^{ii}$, $C9^{ii}$, $C10^{ii}$; ring Py1 = N4, C12 - C16; ring Pz = N3, C9, C10, $N3^{ii}$, $C9^{ii}$, $C10^{ii}$; ring Py2 = N4ii, $C12^{ii}$- $C16^{ii}$; plane A=O3, O4, C11; plane B=$O3^{ii}$, $O4^{ii}$, $C11^{ii}$;

symmetry code: (i) = -x + 2, -y + 1; -z; (ii)=-x + 2, -y + 1, -z + 1

The stronger hydrogen bonds are given in Table 2-18. Like complex **36**, the parallel polymer chains are linked by a three dimensional hydrogen bonding network involving the water molecules of crystallization, the coordinated water molecule and the O-atoms of the carboxylate groups.

Table 2-18. Hydrogen bonding in **37**

Hydrogen bond	D...A (Å)	D--H (Å)	H...A (Å)	D-H..A(°)
Ow1--H11...$Ow5^i$	2.712	0.82	1.90	172
Ow1--H12...Ow3	2.749	0.84	1.92	168
Ow2--H21...$O3^{ii}$	2.775	1.30	1.56	153
Ow2--H22...$O1^{iii}$	2.819	0.75	2.16	147
Ow3--H31...$O4^{iii}$	2.829	0.85	1.98	176
Ow3--H32...Ow4	2.684	0.91	1.84	153
Ow4--H42...$Ow2^{iv}$	2.778	0.60	2.24	149
Ow5--H52...$O3^v$	2.713	1.11	1.72	145
average e. s. ds.	0.012	0.16	0.16	14

Symmetry code: (i). -x + 1, -y + 1, z; (ii). -x + 5/2, y - 1/2, -z + 1/2

(iii). -x + 3/2, y - 1/2, -z + 1/2; (iv). -x + 2, -y, -z; (v). x - 1, y, z

The molar χT product *vs* T of **37** is given in Figure 2-48. The $\chi_m T$ value decreases when the temperature is lowered. Below 25 K $\chi_m T$ decreases abruptly reaching a value of 2.39 x 10^{-2} cm^3 K mol^{-1} at 4 K.

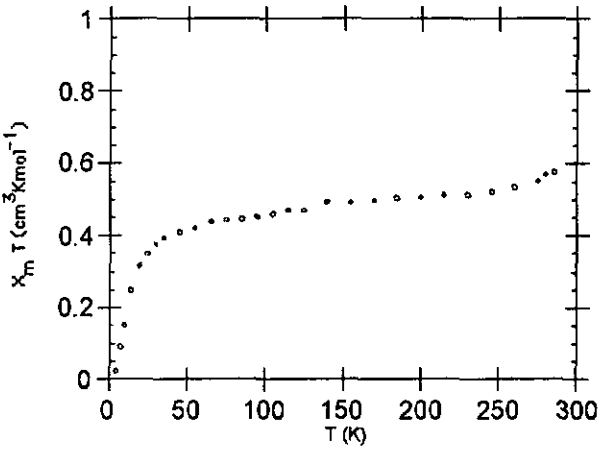

Fig. 2-48. The molar susceptibility (χ_mT/T) for

$\{[Cu_2(L^2)(L^{2*})(H_2O)_2](H_2O)_8\}_n$ (**37**)

The χ_m value increases when the temperature decreases, reaching a maxima at ca 15 K with χ_m value of 1.74 x 10^{-2} cm^3 mol^{-1}, Fig. 2-49. Below this temperature the curve decreases abruptly. The position of the maxima indicates moderate antiferromagnetic coupling between the copper (II) ions through the pyrazine bridges L^2. The experimental susceptibility data for **37** were fitted to the theoretical expression for a copper (II) dinuclear complex in the range 4 K to room temperature, also see Fig. 2-49. The expression used was again formula (4). The best fitting parameters obtained are J = -14.9 cm^{-1}, g = 2.25.

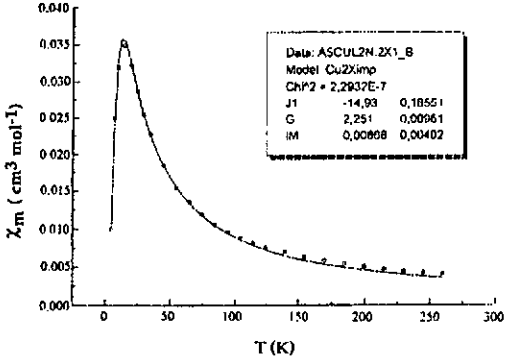

Fig. 2-49. Temperature dependence of χ_m for $\{[Cu_2(L^2)(L^{2*})(H_2O)_2](H_2O)_8\}_n$ (37), experimental (°) and theoretical (—)

The polycrystalline ESR spectra of complex 37 was recorded at room temperature, see Fig. 2-50, there is only a broad signal with an average g = 2.10 as expected for a chain structure.

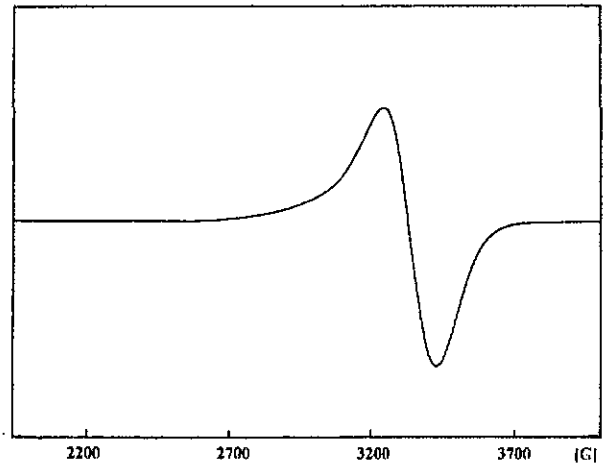

Fig. 2-50. ESR powder spectra (X-band at 298 K) for

$\{[Cu_2(L^2)(L^{2*})(H_2O)_2](H_2O)_8\}_n$ (37)

c). $\{[Cu_2(L^2)(H_2O)_5](SO_4)(H_2O)_3\}_n$ (38)

The crystal structure of complex **38** and the crystal packing are shown in Figs 2-51 and 2-52. Selected bond distances and angles are given in Table 2-19.

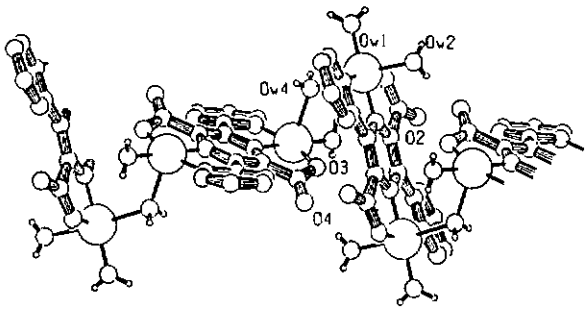

Fig. 2-51. Crystal structure of $\{[Cu_2(L^2)(H_2O)_5](SO_4)(H_2O)_3\}_n$ (38), showing the atom-numbering scheme.

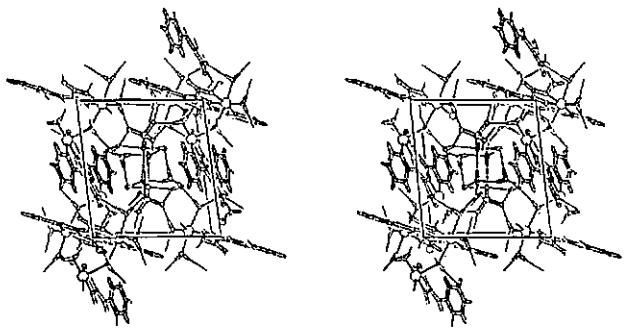

Fig. 2-52. A stereo crystal packing diagram of complex **38**.

Table 2-19. Selected Bond distances and angles in **38**

Bond	Distance (Å)	Bond	Distance (Å)
Cu1---Ow1	1.922(2)	Cu2---Ow3	1.944(2)
Cu1---N1	1.949(2)	Cu2---N3	1.954(2)
Cu1---O1	1.970(2)	Cu2---O3	1.968(2)
Cu1---N2	1.991(2)	Cu2---N4	2.011(2)
Cu1---Ow2^{i}	2,325(2)	Cu2---Ow4	2.352(2)
Cu1---Ow4^{ii}	2.560(2)	Cu2---Ow7	2.643(3)
Bond	**Angle (°)**	**Bond**	**Angle (°)**
Ow1--Cu1--N1	178.84(9)	Ow3--Cu2--N3	176.30(9)
Ow1--Cu1--O1	97.73(9)	Ow3--Cu2--O3	95.95(8)
N1--Cu1--O1	81.68(8)	N3--Cu2--O3	81.49(8)
Ow1--Cu1--N2	99.70(9)	Ow3--Cu2--N4	102.63(9)
N1--Cu1--N2	80.90(9)	N3--Cu2--N4	79.60(9)
O1--Cu1--N2	162.57(8)	O3--Cu2--N4	160.13(8)
Ow1--Cu1--Ow2^{i}	94.77(10)	Ow3--Cu2--Ow4	88.04(9)
N1--Cu1--Ow2^{i}	84.24(9)	N3--Cu2--Ow4	94.58(9)
O1--Cu1--Ow2^{i}	90.19(8)	O3--Cu2--Ow4	89.44(8)
N2--Cu1--Ow2^{i}	88.42(8)	N4--Cu2--Ow4	98.08(8)
Ow1--Cu1-Ow4^{ii}	88.77(9)	Ow7--Cu2--Ow4	169.38(8)
Ow2i-Cu1-Ow4^{ii}	172.37(8)	Ow3--Cu2--Ow7	87.19(10)
O1--Cu1--Ow4^{ii}	82.62(8)	O3--Cu2--Ow7	81.64(9)
N1--Cu1--Ow4^{ii}	92.14(8)	N3--Cu2--Ow7	89.79(9)
N2--Cu1--Ow4^{ii}	97.66(8)	N4--Cu2--Ow7	92.21(9)

Symmetry code: (i). 1 - x, 2 - y, 1 - z; (ii). x, y, -1 + z

In this polymer there are two forms of the binuclear units, α and β coordinating with Cu1 and Cu2 respectively, which are very similar in coordination geometry. The binuclear units α and β are alternately linked by a water molecule, Ow4, coordinating in an asymmetric manner with the Cu1---Ow4^{ii} distance of 2.560(2) Å and the Cu2---Ow4 distance of 2.352(2) Å, so forming an alternating polymer chain. The copper atoms in the forms α and β have a pseudo-octahedral coordination with a long Cu2---Ow7

distance of 2.643(3) Å. The average Cu---Npz distance of 1.952(2) Å is slightly longer the same distances in **31**, while the Cu---Npy distances are comparable, the average distance is 2.001(2) Å in **38** compared to 1.993(9) Å in **31**. The Cu1---Cu2 bridging distance is 4.461(2)Å. The Cu1---Cu1a and Cu2---Cu2b cross-linking distance are 6.516 and 6.515 Å, respectively.

The ligand is slightly twisted in both the α and β forms and the pyrazine-pyridine and pyrazine-carboxylate dihedral angles are given in Table 2-20.

Table 2-20. Dihedral angles (°) between the pyrazine ring (Pz) and the pyridine rings Py1 and Py2, carboxylates planes A and B in **38**

L	C' ^ C"	Py1 ^ Pz	Py2 ^ Pz	Py1 ^ Py2	A ^ Pz	B ^ Pz
α	0(0.4)	12.6(0.1)	12.6(0.1)	25.2(0.1)	8.2(0.3)	8.2(0.2)
β	0(0.5)	22.7(0.2)	22.7(0.2)	45.4(0.2)	20.1(0.5)	20.1(0.5)

(α). plane C' = N1, C1, C2; plane C" = $N1^{i}$, $C1^{i}$, $C2^{i}$; ring Py1 = N2, C4 - C8;
ring Pz = *N1*, C1, C2, $N1^{i}$, $C1^{i}$, $C2^{i}$; *ring Py2* = $N2^{i}$, $C4^{i}$ - $C8^{i}$; *plane A=O1*, O2, C3;
plane B=$O1^{i}$, $O2^{i}$, $C3^{i}$ (β). plane C' = N3, $C9^{ii}$, C10; plane C" = $N3^{ii}$, C9, $C10^{ii}$;
ring Py1 = N4, C12 - C16; ring Pz = N3, C9, C10, $N3^{ii}$, $C9^{ii}$, $C10^{ii}$;
ring Py1 = N4ii, $C12^{ii}$- $C16^{ii}$; plane A=O3, O4, C11; plane B=$O3^{ii}$, $O4^{ii}$, $C11^{ii}$;
symmetry code: (i) = -x + 1, -y + 2; -z; (ii)=-x + 1, -y + 2, -z + 1

The stronger hydrogen bonds are given in Table 2-21. The parallel polymer chains are linked by a three dimensional hydrogen bonding network involving the water molecules of crystallization, the coordinated water molecule, the O-atoms of the sulfate anions, and the carbonyl O-atoms of the carboxylate groups.

Table 2-21. Hydrogen bonding in **38**

Hydrogen bond	D...A (Å)	D--H (Å)	H...A (Å)	D-H..A(°)
Ow1--H11...O12^{i}	2.641	0.75	1.90	172
Ow1–H12...O13^{ii}	2.592	0.88	1.72	171
Ow2--H21..O11^{iii}	2.709	0.76	1.95	178
Ow2--H22...O4	2.884	0.76	2.15	166
Ow3--H31...O1^{iv}	2.725	0.79	1.95	167
Ow3--H32...O12	2.681	0.80	1.90	167
Ow4--H41...O2^{iv}	2.855	0.78	2.09	168
Ow4--H42...Ow5^{v}	2.697	0.69	2.02	171
Ow5–H51...Ow8	2.688	0.83	1.87	172
Ow5–H52...O13^{ii}	2.987	0.90	2.18	149
Ow5--H52...O14^{ii}	2.982	0.90	2.21	145
Ow6--H61...O11^{vi}	2.819	0.75	2.08	170
Ow6--H62...O14	2.777	0.76	2.02	172
Ow7--H71...Ow6^{ii}	2.896	0.85	2.05	176
Ow7–H72...O14	2.783	0.68	2.11	177
Ow8--H81...Ow7	2.773	0.92	1.86	174
Ow8--H82...Ow6	2.882	0.89	2.02	162
average e. s. ds.	0.003	0.05	0.05	4

Symmetry code: (i). x -1, y, z -1; (ii). -x + 1, -y + 1, -z + 1

(iii). x -1, y, z; (iv). x + 1, y, z +1; (v). -x + 1, -y + 2, -z + 1

(vi). -x 1 2, -y + 1, -z + 1

The molar Magnetism $\chi_m T$ product *vs* T of **38** is given in Figure 2-53. The $\chi_m T$ value decreases when the temperature is lowered. Below 25K $\chi_m T$ decreases abruptly reaching a value of 3.04 x 10^{-3} cm^3 K mol^{-1} at 4 K.

The χ_m value increases when the temperature decreases, reaching a maxima at ca 18 K with χ_m value of 2.78 x 10^{-2} cm^3 mol^{-1}, Fig. 2-54. Below this temperature the curve decreases abruptly. The position of the maxima indicates moderate antiferromagnetic coupling between the copper (II) ions through the pyrazine bridges. The experimental susceptibility data for **38** were fitted to the theoretical expression as a copper (II)

dinuclear complex in the rang 4 to 120 K, also see Fig. 2-54. The expression used was again formula (4). The best fitting parameters obtained are J = -19.16 cm^{-1}, g = 2.25.

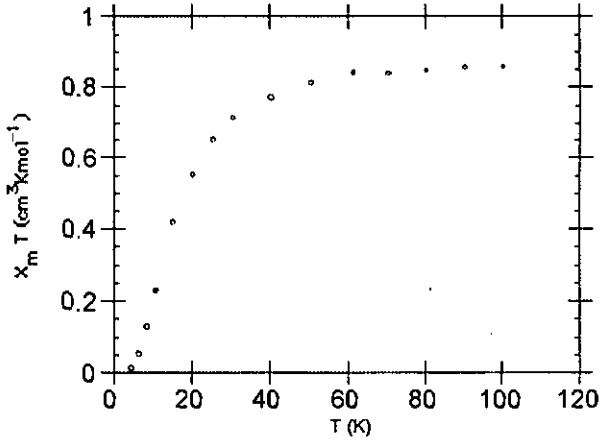

Fig. 2-53. The molar susceptibility ($\chi_m T/T$) for $\{[Cu_2(L^2)(H_2O)_5](SO_4)(H_2O)_3\}_n$ (**38**)

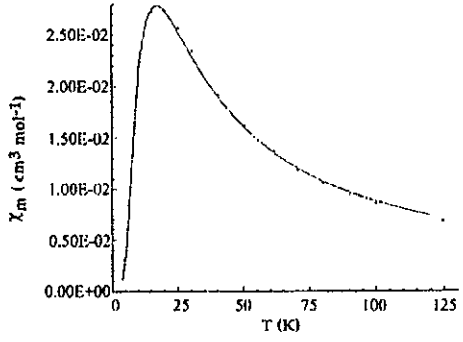

Fig. 2-54. Temperature dependence of χ_m for $\{[Cu_2(L^2)(H_2O)_5](SO_4)(H_2O)_3\}_n$ (**38**), experimental (+) and theoretical (—)

The polycrystalline ESR spectra of complex **38** was recorded at room temperature, see Fig. 2-55, it is axially distorted with $g_{\parallel} = 2.24$; $g_{\perp} = 2.10$. No resolved hyperfine structure for copper ions was observed.

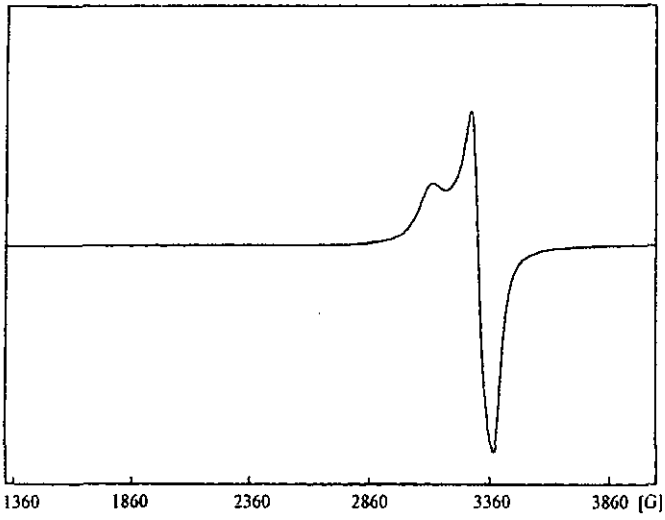

Fig. 2-55. ESR powder spectra (X-band at 298 K) for $\{[Cu_2(L^2)(H_2O)_5](SO_4)(H_2O)_3\}_n$ (**38**)

d). $\{[Cu_2(L^2)Cl_2(H_2O)](H_2O)\}_n$ (39)

Complex **39** was obtained as an olive green powder by reacting an aqueous solution of $CuCl_2.2H_2O$ with ligand 2 in Cu(II)/L^2 molar ratio of 2:1. The elemental analysis indicates that there are two Cl^- ions in this complex and it may be an alternating chain with a unit molecular formula $[Cu_2(L^2)Cl_2(H_2O)](H_2O)$. The magnetic measurement also shows an antiferromagnetic coupling between copper(II) ions. A proposed structure is given in Fig. 2-56.

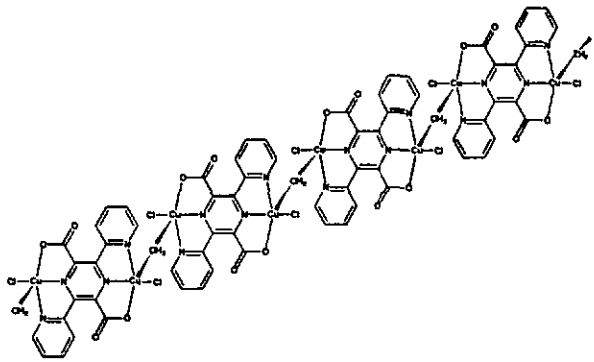

Fig. 2-56. A proposed structure for $\{[Cu_2(L^2)Cl_2(H_2O)](H_2O)\}_n$ (**39**)

The molar χT product *vs* T of **39** is given in Figure 2-57. The $\chi_m T$ value decreases when the temperature is lowered. Below 25 K $\chi_m T$ decreases abruptly reaching a value of 1.46×10^{-2} cm^3 K mol^{-1} at 4 K.

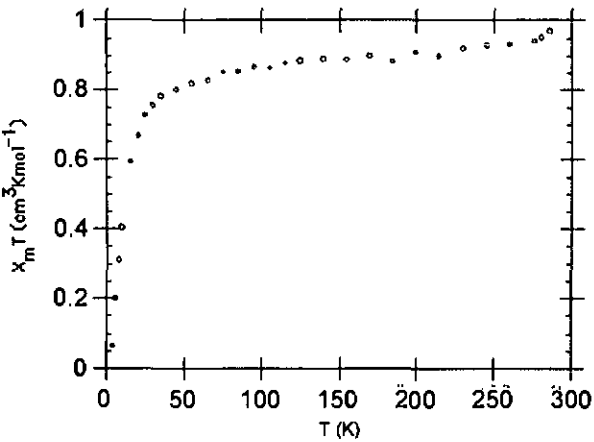

Fig. 2-57. The molar susceptibility ($\chi_m T/T$) for $\{[Cu_2(L^2)Cl_2(H_2O)](H_2O)\}_n$ (**39**)

The χ_m value increases when the temperature decreases, reaching a maxima at ca 10 K with χ_m value of 3.78 x 10^{-2} cm^3 mol^{-1}, Fig. 2-58. Below this temperature the curve decreases abruptly. The position of the maxima indicates moderate antiferromagnetic coupling between the copper (II) ions through the pyrazine bridges. The experimental susceptibility data for **39** were fitted to the theoretical expression as a copper (II) dinuclear complex in the rang 4 K to room temperature, also see Fig. 2-58. The expression used was formula (4). The best fitting parameters obtained are J = -12.51 cm^{-1}, g = 2.20.

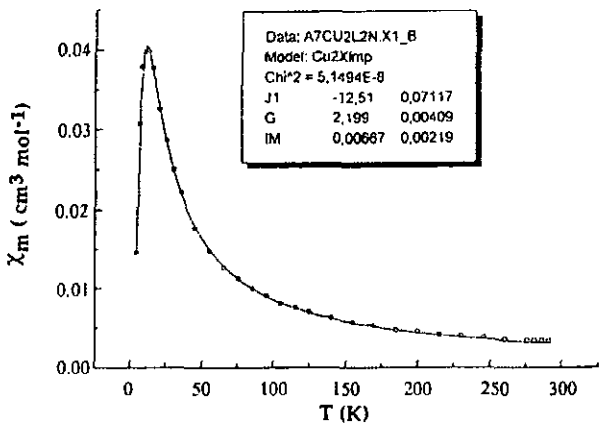

Fig. 2-58. Temperature dependence of χ_m for $\{[Cu_2(L^2)Cl_2(H_2O)](H_2O)\}_n$ (**39**), experimental (°) and theoretical (—)

The polycrystalline ESR spectra of complex **39** was recorded at room temperature, see Fig. 2-59, it is axially distorted with $g_{\parallel} = 2.25$; $g_{\perp} = 2.06$ as expected for a square-pyramidal coordination. No resolved hyperfine structure for copper ions was observed.

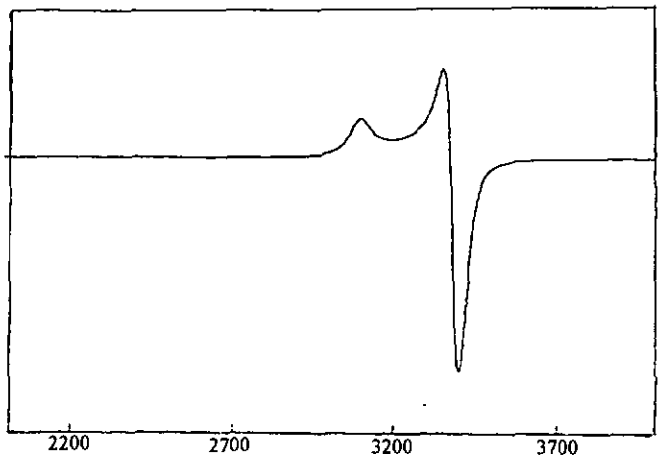

Fig. 2-59. ESR powder spectra (X-band at 298 K) for $\{[Cu_2(L^2)Cl_2(H_2O)](H_2O)\}_n$ (39)

e). $[Cu_2(L^2)(C_4O_4)(H_2O)_2](H_2O)_{1.5}$ (40)

Complex **40** was obtained as a very small brown crystal by reacting a solution of $Cu(ClO_4)_2.6H_2O$ and squaric acid ($C_4H_2O_4$) in water and ethanol with ligand 2 in a molar ratio 2:1:1 (Cu(II)/L^2/Sqa). The elemental analysis indicates that there is a squarate anion ion in this complex. The colour of this complex is different from complex **34**, which probably means that the squarate takes part in the coordination with copper. So it may be a alternating chain with a unit molecular formula $[Cu_2(L^2)(C_4O_4)(H_2O)_2](H_2O)_{1.5}$. The magnetic measurement shows an antiferromagnetic interaction between copper(II) ions. A proposed structure is given in Fig. 2-60.

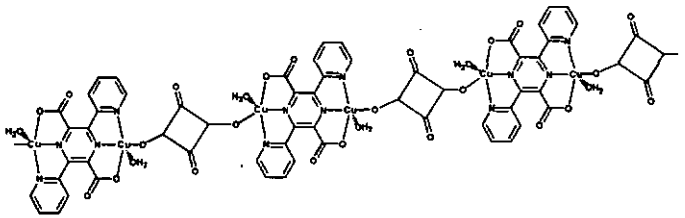

Fig. 2-60. A proposed structure for $\{[Cu_2(L^2)(C_4O_4)(H_2O)_2](H_2O)_{1.5}\}_n$ **(40)**

The molar $\chi_m T$ product *vs* T of **40** is given in Figure 2-61. The $\chi_m T$ value decreases when the temperature is lowered. Below 25 K $\chi_m T$ decreases abruptly reaching a value of 2.08×10^{-2} cm^3 K mol^{-1} at 4 K.

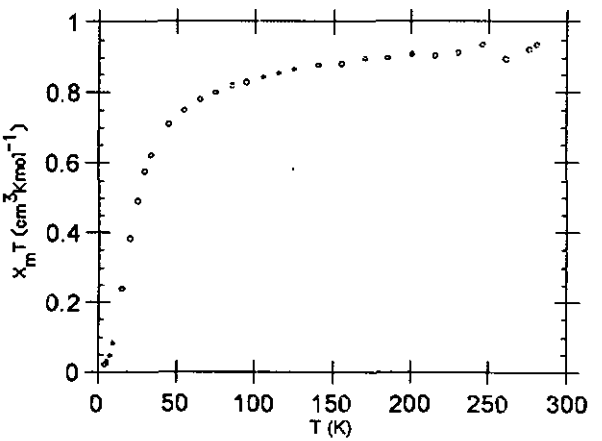

Fig. 2-61. The molar susceptibility ($\chi_m T/T$) for $\{[Cu_2(L^2)(C_4O_4)(H_2O)_2](H_2O)_{1.5}\}_n$ **(40)**

The χ_m value increases when the temperature decreases, reaching a maxima at ca 25 K with χ_m value of 1.96×10^{-2} cm^3 mol^{-1}, Fig. 2-62. Below this temperature the curve

decreases abruptly. The position of the maxima indicates moderate antiferromagnetic coupling between the copper (II) ions through the pyrazine bridges. The experimental susceptibility data for **40** were fitted to the theoretical expression as a copper (II) dinuclear complex in the range 4 K to room temperature, also see Fig. 2-62. The expression used was formula (**4**). The best fitting parameters obtained are J = -20.0 cm^{-1}, g = 2.24.

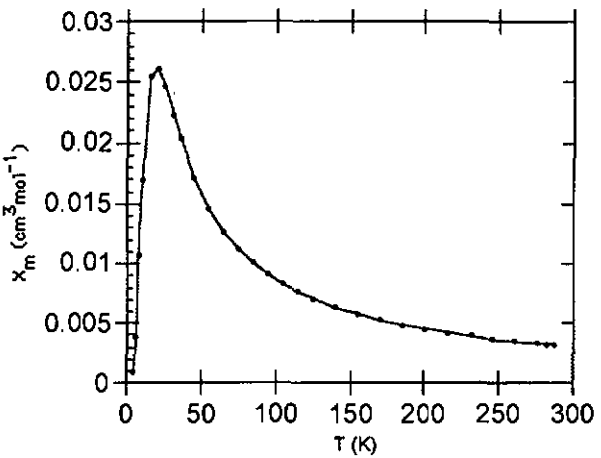

Fig. 2-62. Temperature dependence of χ_m for $\{[Cu_2(L^2)(C_4O_4)(H_2O)_2](H_2O)_{1.5}\}_n$ (**40**), experimental (·) and theoretical (—)

2.2.2.4. Two Dimensional Uniform Polymer $\{[Cu_2(L^2)(H_2O)_2](NO_3)_2\}_n$ (41)

Complex $\{[Cu_2(L^2)(H_2O)_2](NO_3)_2\}_n$ (**41**) was prepared by the reaction $Cu(NO_3)_2$ with H_2L^2 in water with a Cu(II)/H_2L^2 ratio 2:1 and lead to the formation of dark green block-like crystals, but during the initial stages of the reaction complex **32** appears in the solution. This complex can be directly obtained by reacting an aqueous solution of $Cu(NO_3)_2$ with H_2L^2 in a Cu(II)/H_2L^2 ratio of 4:1. The crystal structure of complex **41**

and the crystal packing are shown in Figures 2-63 and 2-64. Selected bond distances and angles are given in Table 2-22.

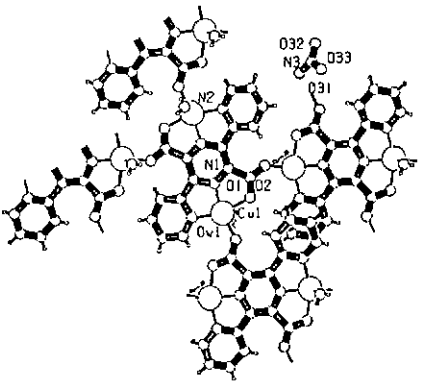

Fig. 2-63. Crystal structure of $\{[Cu_2(L^2)(H_2O)_2](NO_3)_2\}_n$ (**41**), showing the atom-numbering scheme.

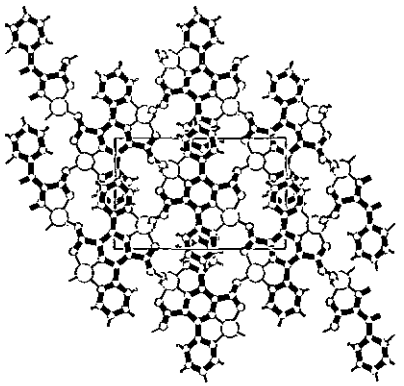

Fig. 2-64. A crystal packing diagram of complex **41**.

Table 2-22. Selected Bond distances and angles in **41**

Bond	Distance (Å)	Bond	Distance (Å)
Cu1---O2	1.939(3)	Cu1---N1	1.958(3)
Cu1---N2	2.021(3)	Cu1---O1	2.031(3)
Cu1---Ow1	2.208(5)		
Bond	**Angle (°)**	**Bond**	**Angle (°)**
O2--Cu1--N1	166.30(12)	O2--Cu1--N2	110.17(11)
N1--Cu1--N2	80.02(12)	O2--Cu1--O1	89.87(10)
N1--Cu1--O1	79.99(11)	N2--Cu1--O1	159.92(11)
O2--Cu1--Ow1	89.9(2)	N1--Cu1--Ow1	99.1(2)
N2--Cu1--Ow1	91.8(2)	O1--Cu1--Ow1	89.4(2)

The crystal has a symmetry center at the center of the pyrazine ring of the ligand. In **41** the ligand combines a bis-tridentate and bis-monodentate so all positions for coordination in the ligand are occupied. The structure of complex **41** consists of the trans-conformation binuclear units $[Cu_2(L^2)]$ linked by the two carbonyl groups of the carboxylates of the ligand to form a uniform two-dimensional polymer. As a matter of fact, the carboxylates of the ligand are coordinated in the syn-anti mode. The Cu---Npz distance of 1.958(3) Å and the Cu---Npy distances of 2.021(3) Å in **41** are slightly longer than the same distances in **31** (molecule B: 1.936(8) Å and 1.993(9) Å, respectively). In **41** the geometry of the copper atom is described as slightly distorted square pyramidal coordination with a τ value 0.11. A coordinated water molecule occupies the axial position of the square pyramid. The Cu1---Cu1d distance, bridged by a carboxylate, is 5.386(8)Å. The Cu1---Cu1b distance, across-pyrazine, is 6.514 (8) Å. The ligand is twisted and the pyrazine-pyridine and pyrazine-carboxylate dihedral angles are given in Table 2-23.

Table 2-23. Dihedral angles (°) between the pyrazine ring (Pz) and the pyridine rings Py1 and Py2, carboxylates planes A and B in **41**

C' ^ C"	Py1 ^ Pz	Py2 ^ Pz	Py1 ^ Py2	A ^ Pz	B ^ Pz
0(0.02)	17.4(0.2)	17.4(0.2)	34.8(0.2)	18.1(0.3)	18.1(0.3)

plane C' = N1, C1, C2; plane C" = $N1^{i}$, $C1^{i}$, $C2^{i}$; ring Py1 = N2, C4 - C8;
ring Pz = N1, C1, C2, $N1^{i}$, $C1^{i}$, $C2^{i}$; ring Py2 = $N2^{i}$, $C4^{i}$ - $C8^{i}$; plane A = O1, O2, C3;
plane B = $O1^{i}$, $O2^{i}$, $C3^{i}$; symmetry code (i) -x, -y, -z

There are only two strong hydrogen bonds involving the coordinated water molecule and the nitrate anion. The later is suspended on the 2D polymer sheet bridging the axially coordinated water molecules, Table 2-24. No strong hydrogen bond is found between the polymer layers.

Table 2-24. Hydrogen bonding in **41**

Hydrogen bond	D...A (Å)	D--H (Å)	H...A (Å)	D-H..A(°)
Ow1–H1A...$O33^{i}$	2.774	0.60	2.31	137
Ow1–H1B...O33	2.679	0.74	2.03	147
average e.s.ds.	0.008	0.10	0.10	13

symmetry code: (i). x, -y + 1/2, z + 1/2.

The molar $\chi_m T$ product *vs* T of **41** is given in Figure 2-65. The $\chi_m T$ value decreases when the temperature is lowered. Below 25 K $\chi_m T$ decrease abruptly reaching a value of 2.69×10^{-2} cm^3 K mol^{-1} at 4 K.

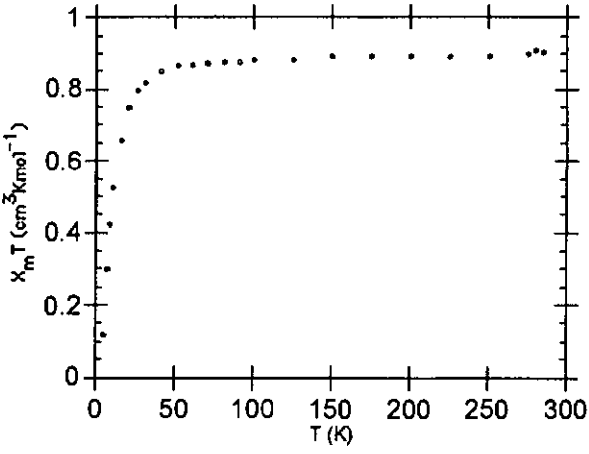

Fig. 2-65. The molar susceptibility ($\chi_m T/T$) for $\{[Cu_2(L^2)(H_2O)_2](NO_3)_2\}_n$ (41)

The χ_m value increases when the temperature decreases, reaching a maxima at ca 10 K with χ_m value of 4.91 x 10^{-2} cm^3 mol^{-1}, Fig. 2-66. Below this temperature the curve decreases abruptly. Since the interaction provided by syn-anti carboxylate bridge is generally very weak and the equation for a plane with two J parameters is not available, the position of the maxima indicates moderate antiferromagnetic coupling between the copper (II) ions through the pyrazine bridges. The experimental susceptibility data for **41** were fitted to the theoretical expression as a copper (II) dinuclear complex in the range 4 K to room temperature, also see Fig. 2-66. The expression used was formula (4). The best fitting parameters obtained are J = -10.3 cm^{-1}, g = 2.22.

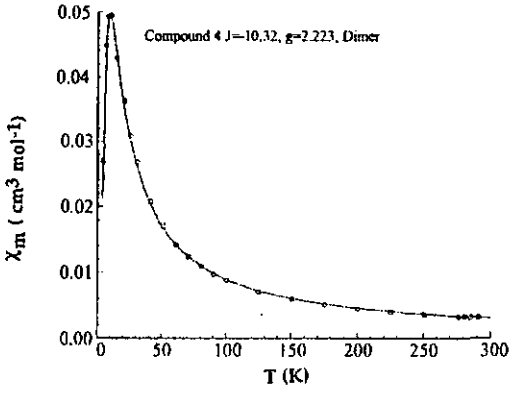

Fig. 2-66. Temperature dependence of χ_m for $\{[Cu_2(L^2)(H_2O)_2](NO_3)_2\}_n$ **(41)**, experimental (°) and theoretical (—)

The polycrystalline ESR spectra of complex **41** was recorded at 77 K, see Fig. 2-67, it is axially distorted with $g_{\parallel} = 2.21$; $g_{\perp} = 2.10$. No resolved hyperfine structure for copper ions was observed.

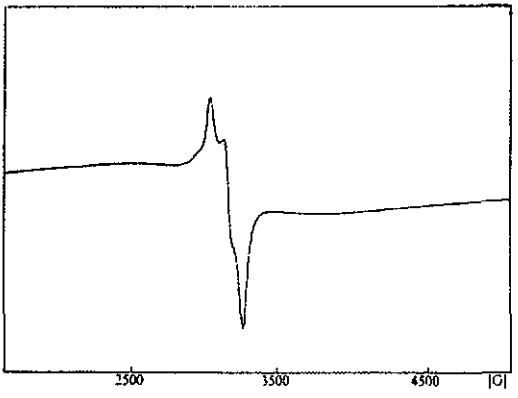

Fig. 2-67. ESR powder spectra (X-band at 77 K) for $\{[Cu_2(L^2)(H_2O)_2](NO_3)_2\}_n$ **(41)**

2.2.3. Synthesis, Structure and Magnetic Properties of Cu(II) Complexes of Ligand 3

So far we have only obtained two copper(II) complexes with ligand 3 by reacting an aqueous solution of copper salts with H_2L^3. Both are one dimensional polymer chain structures.

2.2.3.1 Uniform Chain $\{[Cu(L^3)(H_2O)](H_2O)_5\}_n$ (42)

Complex **42** was usually obtained by reacting an aqueous solution of the normal copper salts ($CuCl_2$, $Cu(ClO_4)2$, $CuSO_4$, $Cu(NO_3)_2$)with H_2L^3, irrespective of a wide variation of the Cu(II)/H_2L^3 ratio 1:1 to 4:1.The crystal structure of complex **42** is given in Figures 2-68 A and B and a stereo view of the crystal packing is shown in Figures 2-69. Selected bond distances and angles are given in Table 2-22.

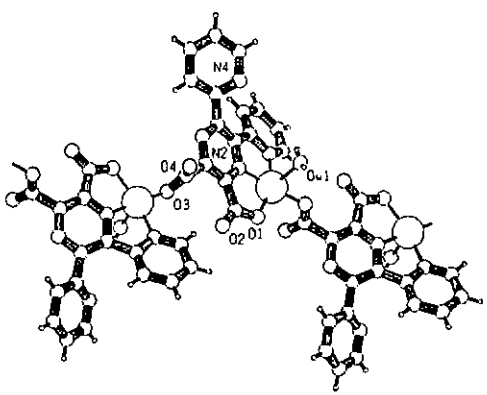

Fig. 2-68A. Crystal structure of $\{[Cu(L^3)(H_2O)](H_2O)_5\}_n$ (**42**), showing the atom-numbering scheme.

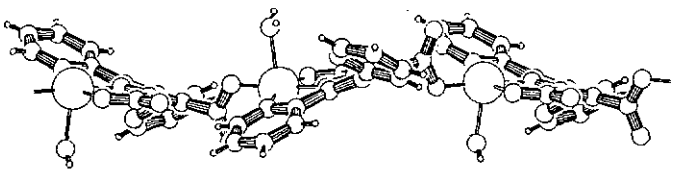

Fig. 2-68B. A side view of complex **42**

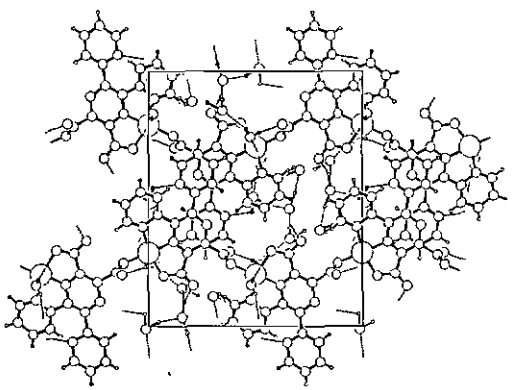

Fig. 2-69. A crystal packing diagram of complex **42**.

As seen from the figures the structural feature of this polymer is very similar to complex **33** and the polymer chain is composed of the same conformational (all *R* or all *S*) subunits related by a 2-fold screw axis, which leads to a helical chain. The ligand is coordinated in an asymmetric manner, combining a tridentate and a monodentate coordination.

Table 2-25. Selected Bond distances and angles in **42**

Bond	Distance (Å)	Bond	Distance (Å)
Cu1---O3	1.923(3)	Cu1---N1	1.932(4)
Cu1---N3	2.028(5)	Cu1---O1	2.012(4)
Cu1---Ow1	2.326(7)		
Bond	**Angle (°)**	**Bond**	**Angle (°)**
O3–Cu1–N1	176.7(3)	O3--Cu1--O1	99.4(2)
N1–Cu1–O1	80.5(2)	O3--Cu1--N3	101.4(2)
N1–Cu1–N3	79.2(2)	N3--Cu1--O1	157.1(2)
O3–Cu1–Ow1	85.1(2)	N1--Cu1--Ow1	91.6(2)
N3–Cu1–Ow1	93.6(3)	O1--Cu1--Ow1	97.6(2)

The copper atom has a highly distorted square pyramidal coordination with a τ value 0.33. A coordinated water molecule occupies the axial position of the square pyramid. The distance Cu---Npz of 1.932(4) Å is slightly shorter than the same distance (1.949 (3) Å) in **33** and the Cu---Npy distance of 2.028(5) Å is slightly longer than the same distance (2.000(4) Å) in **33**. The intramolecular Cu to Cu distance is 7.755 (5) Å.

Table 2-26. Dihedral angles (°) between the pyrazine ring (Pz) and the pyridine rings Py1 and Py2, carboxylates planes A and B in **42**

C' ^ C"	Py1 ^ Pz	Py2 ^ Pz	Py1 ^ Py2	A ^ Pz	B ^ Pz
5.2(0.7)	21.4(0.3)	39.8(0.2)	54.9(0.2)	12.6(0.4)	84.6(0.4)
plane C' = N1, C1, C4; plane C" = N2, C2, C3; ring Pz = N1, N2, C1-C4; ring Py1 = N3, C7 - C11; ring Py2 = N4, C12 - C16; plane A = O1, O2, C5; plane B = O3, O4, C6					

In Table 2-26 the dihedral angles between the pyrazine ring and the pyridine rings and the carboxylate groups are given. The ligand is extremely twisted in **42** with a dihedral angle of 54.9(2) ° between the pyridine rings. The central pyrazine ring is also slightly twisted with a dihedral angle of 5.2(7) ° between the planes C' and C". The carboxylate in the monodentate coordination position is almost perpendicular to the pyrazine plane.

The presence of the water molecules of crystallization plays an important role in crystal cohesion. The stronger hydrogen bonds are given in Table 2-27. In **42** the parallel polymer chains are linked by a three dimensional hydrogen network involving all of water molecules of crystallization the coordinated water molecule, and the carbonyl O atoms of the carboxylate groups.

Table 2-27. Hydrogen bonding in **42**

Hydrogen bond	D...A (Å)	D--H (Å)	H...A (Å)	D-H..A(°)
Ow1--H1w1..Ow5^{i}	2.767	0.71	2.06	176
Ow1--H2w1..Ow2^{ii}	2.752	0.66	2.12	163
Ow2--H21..Ow4^{iii}	2.735	1.09	1.69	158
Ow3--H31..Ow1^{iv}	2.881	0.50	2.41	160
Ow4--H41..O2^{v}	2.740	1.14	1.75	142
Ow4--H42..Ow3	2.800	1.17	1.64	171
Ow5--H51..O4^{vi}	2.700	0.77	1.93	174
Ow5--H52..Ow6	2.743	0.76	2.12	139
Ow6--H61..Ow4^{vii}	2.875	0.98	1.89	177
Ow6--H62..Ow3^{vi}	2.800	1.27	1.65	147
average e. s. ds.	0.009	0.02	0.02	2

Symmetry code: (i). 5/2 - x, 1 - y, -1/2 + z; (ii). 1/2 + x, 3/2 - y, 1- z
(iii). 3/2 - x, 2 - y, 1/2 + z; (iv). 2 -x, 1/2 + y, 1/2 -z; (v). -1/2 + x, 3/2 -y, 1 -z
(vi). 3/2 - x, 1 - y, 1/2 + z; (vii). 2 - x, -1/2 + y, 3/2 - z.

The molar $\chi_m T$ product *vs* T of **42** is given in Figure 2-70. No coupling, however, has been observed in the magnetic measurement of complex **42** and the $\chi_m T$ value at room temperature is approximately 0.54 much more than the normal value of 0.39 cm^3 $Kmol^{-1}$ for a single copper atom.

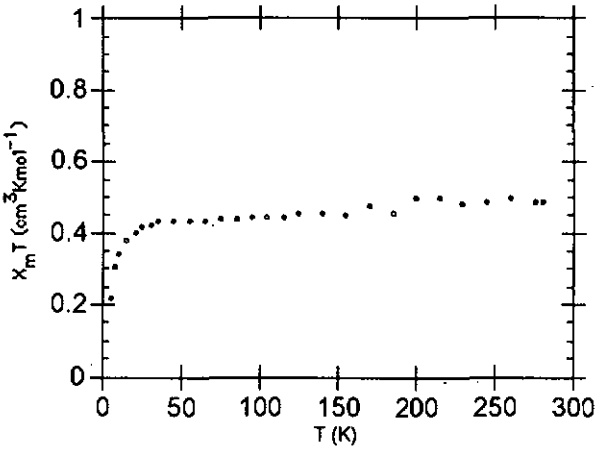

Fig. 2-70. The molar susceptibility ($\chi_m T/T$) for $\{[Cu(L^3)(H_2O)](H_2O)_5\}_n$ (**42**)

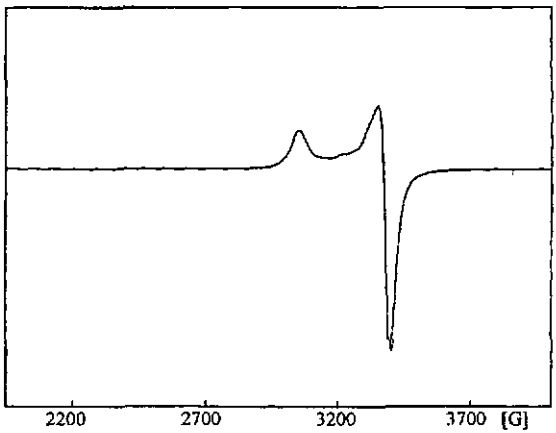

Fig. 2-71. ESR powder spectra (X-band at 298 K) for $\{[Cu(L^3)(H_2O)](H_2O)_5\}_n$ (**42**)

The polycrystalline ESR spectra of complex **42** were recorded at room temperature, see Fig. 2-71, which is axially distorted $g_{\parallel} = 2.29$, $g_{\perp} = 2.07$ as expected for a square-pyramidal coordination. No resolved hyperfine structure for copper ions was observed.

2.2.3.2. Alternating Polymer Chain $\{[Cu_2(L^3)Cl_2(H_2O)](H_2O)_2\}_n$ (43)

The reaction of H_2L^3 with a large excess $CuCl_2.2H_2O$ in water gave dark green block-like crystals. The elemental analysis of this crystal indicates that the unit formula is $[Cu_2(L^3)Cl_2(H_2O)](H_2O)_2$. The initial crystallographic investigation shows this complex to be an alternating polymer, Figures 2-72 and 2-73. The structure of complex **43** consists of $[Cu_2(L^3)]$ binuclear units linked by a water molecule to form a one-dimensional polymer chain.

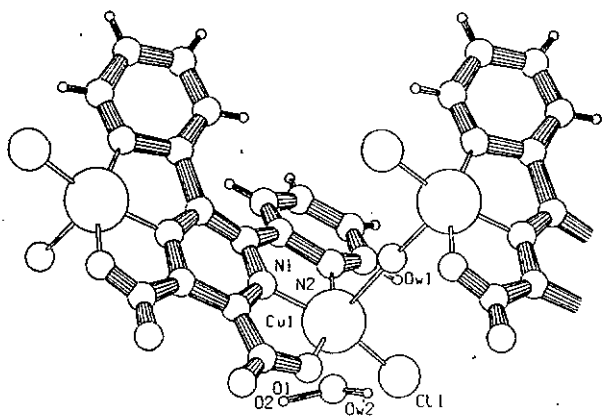

Fig. 2-72. Crystal structure of $\{[Cu_2(L^3)Cl_2(H_2O)](H_2O)_2\}_n$ (**43**), showing the atom-numbering scheme.

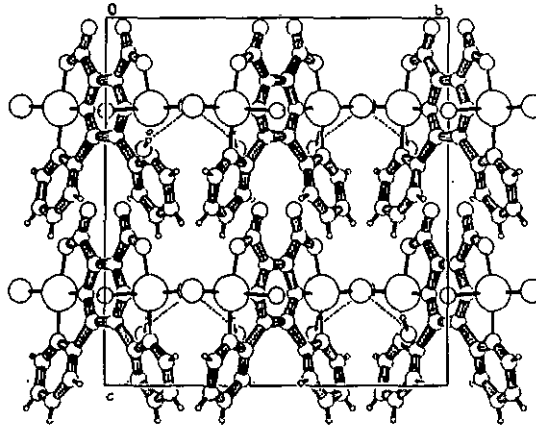

Fig. 2-73. A crystal packing diagram of complex **43**.

The molar $\chi_m T$ product *vs* T of **43** is given in Figure 2-74. The $\chi_m T$ value decreases when the temperature is lowered. Below 40 K $\chi_m T$ decreases abruptly reaching a value of 8.86 x 10^{-3} cm^3 K mol^{-1} at 4 K.

The χ_m value increases when the temperature decreases, reaching a maxima at ca 25 K with χ_m value of 2.17 x 10^{-2} cm^3 mol^{-1}, Fig. 2-75. Below this temperature the curve decreases abruptly. The position of the maxima indicates moderate antiferromagnetic coupling between the copper (II) ions through the pyrazine bridges. The experimental susceptibility data for **43** were fitted to the theoretical expression as a copper (II) dinuclear complex in the rang 4 K to room temperature, also see Fig. 2-75. The expression used still was formula (4). The best fitting parameters obtained are J = -24.87 cm^{-1}, g = 2.26.

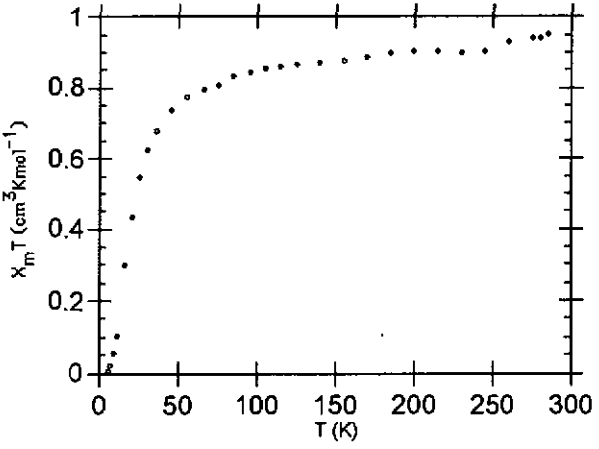

Fig. 2-74. The molar susceptibility ($\chi_m T/T$) for $\{[Cu_2(L^3)Cl_2(H_2O)](H_2O)_2\}_n$ **(43)**

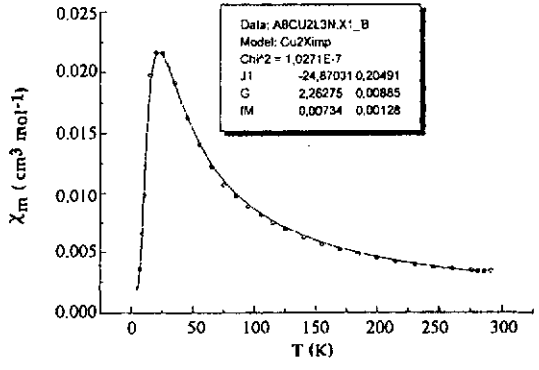

Fig. 2-75. Temperature dependence of χ_m for $\{[Cu_2(L^3)Cl_2(H_2O)](H_2O)_2\}_n$ **(43)**, experimental (°) and theoretical (—)

The polycrystalline ESR spectra of complex **43** was recorded at room temperature, see Fig. 2-76. There is a high rhombic distortion with three signals: $g_1 = 2.19$, $g_2 = 2.12$, and $g_3 = 2.05$. No resolved hyperfine structure for copper ions was observed.

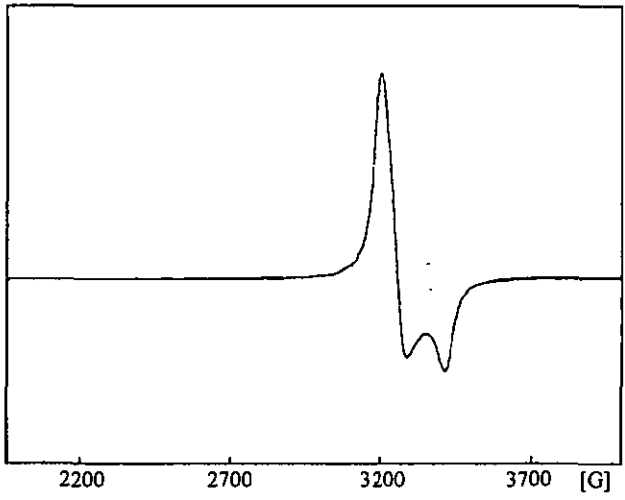

Fig. 2-76. ESR powder spectra (X-band at 298 K) for
$\{[Cu_2(L^3)Cl_2(H_2O)](H_2O)_2\}_n$ (**43**)

References.

[1] Katritzky A. R.; Boulton, A. J., "*Advances in Heterocyclic Chemistry*" *vol.* **14**, Academic Press Inc., New York, (1980.).

[2] Adkins, H; Reeve, E. W., *J. Am. Chem. Soc.*, **60**, 1328-1331(1938).

[3] Iida, H.; Hayashida, K.; Yamada, M.; Takahashi, K.; Yamada, K. *Synthetic Communications*, **3**, 225-230 (1973).

[4] Bramwell, A. F.; Wells, R. D., *Tetrahedron*, **28**, 4155-4170 (1972).

[5] Bramwell, A. F.; Wells, R. D., *Tetrahedron*, **29**, 3939-3942 (1973).

[6] Cambridge Structural Database (1992), Version 4.6. Cambridge Crystallographic Data Centre, 12 Union Road, Cambridge, England.

[7] Woznial, K.; Krygowski, T. M.; Grech, E.; Kolodziejski, W.; Klinowski, J.; *J. Phys. Chem.* **97**, 1862-1867(1993).

[8] Nishiyama, H.; Kondo, M.; Nakamura, T.; Itoh, K., *Organometallics* **10**, 500-508 (1991).

[9] Corey, E. J.; Imai, N.; Zhang, H.-Y., *J. Am. Chem. Soc.* **113**, 728-729(1991).

[10] Graf, M.; Stoeckli-Evans, H.; Whitaker, C.; Marioni, P.-A.; Marty, W. *Chimia*, **47**, 202-205 (1993).

[11] Stoeckli-Evans, H.; Wang, Y., to be published.

[12] Addison, A. W.; Rao, T. N.; Reedijk, J.; van Rijn, J.; Verschoor, G. C., *J. Chem. Soc., Dalton Trans.*, 1349-1356 (1984).

[13] *International Tables for X-Ray Crystallography*, Volume C, Ed. Wilson, Kluwer Academic Publishers, Dordrecht, 1995.

[14] Neels, A.; Stoeckli-Evans, H., *Chimia*, **41**, 198-202 (1993).

[15] Graf, M.; Greaves, B.; Stoeckli-Evans, H., *Inorg. Chim. Acta*, **204**, 239-246 (1994).

[16] Kahn, O., *Molecular Magnetism*, VCH Publishers, Inc., New York, 1993, p. 252.

[17] Hathaway, B. J., *Struct. Banding (Berlin)*, **57**, 55(1984)

[18] See ref. [16], p. 107.

DISCUSSION-CONCLUSION

3.1. The Use of a One-pot Reaction in the Synthesis of the Symmetrically Tetra-substituted Pyrazine Derivatives

In the synthesis of the precursors of ligands 1 and 2, the 3,6-disubstituted pyrazine-2,5-dicarboxylic esters, a new strategy was employed. The pyrazine ring was formed directly by a one-pot reaction, combining catalytic hydrogenation, self-condensation and oxidation, instead of carrying out separately each reaction, step by step. The advantage of this stratgy is obvious. It not only simplifies the reaction route, but also makes possible the synthesis of compound 17, the precursor of ligand 2.

Using a supported Rh catalyst to reduce the oximes at low pressure is an important modification in the synthesis of ligand 1 and we have obtained a moderate yield compared to the method of Iida et al. [1]. An overall yield of 55-56 % was obtained in our one-pot reaction compared to 66-69 % for the two separate steps of Iida et al. Although their yield is a little bit higher, HCl-containing ethanol was involved in the catalytic reduction step with Pd/C at a higher pressure (ca. 18 atm), which is less convenient.

Perhaps the most interesting feature is the solvent effect in the one-pot reaction. In the synthesis of the precursor of ligand 1, ethanol was used as solvent for the catalytic hydrogenation, the condensation and oxidation steps. Compared with ligand 1, the synthesis of ligand 2, which has two 2-pyridyl groups in the 3,6-positions, is more complicated. Two kinds of solvents were employed. At first ethyl acetate was used as solvent in the catalytic reduction step of the precursor

chloroform immediately after hydrogenation, otherwise the desired product can not be obtained. In the case when ethyl acetate was used for the entire one-pot reaction an attempt to isolate the final products was performed but the composition of the products was so complicated that only one main product could be identified:

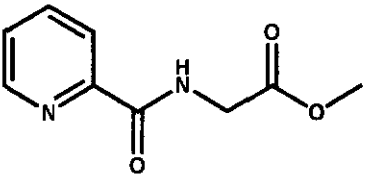

For this compound, a proposed mechanism is given in scheme 15.

Scheme 15

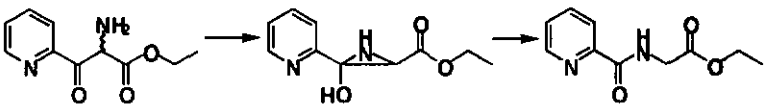

A rearrangement is probably involved in the reaction, which leads to the formation of the unexpected product. In the presence of chloroform the results of the one-pot reaction are completely different. Figure 3-1 shows the results of an *in situ* NMR study during the formation of the desired compound **17**.

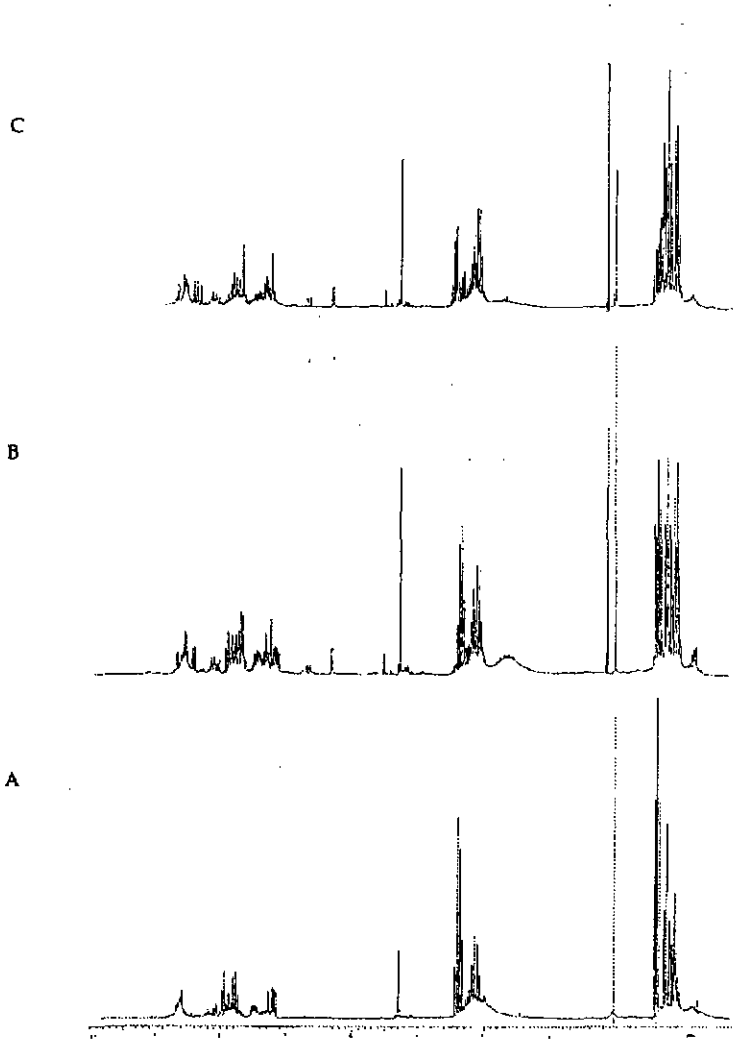

Fig. 3-1. An *in situ* ^1H NMR ($CDCl_3$, 200 MHz, room temperature) study in the formation of compound **17**. A). The ^1H NMR spectrum after the hydrogenation; B). the measurement on day + 2; C). the measurement on day + 4.

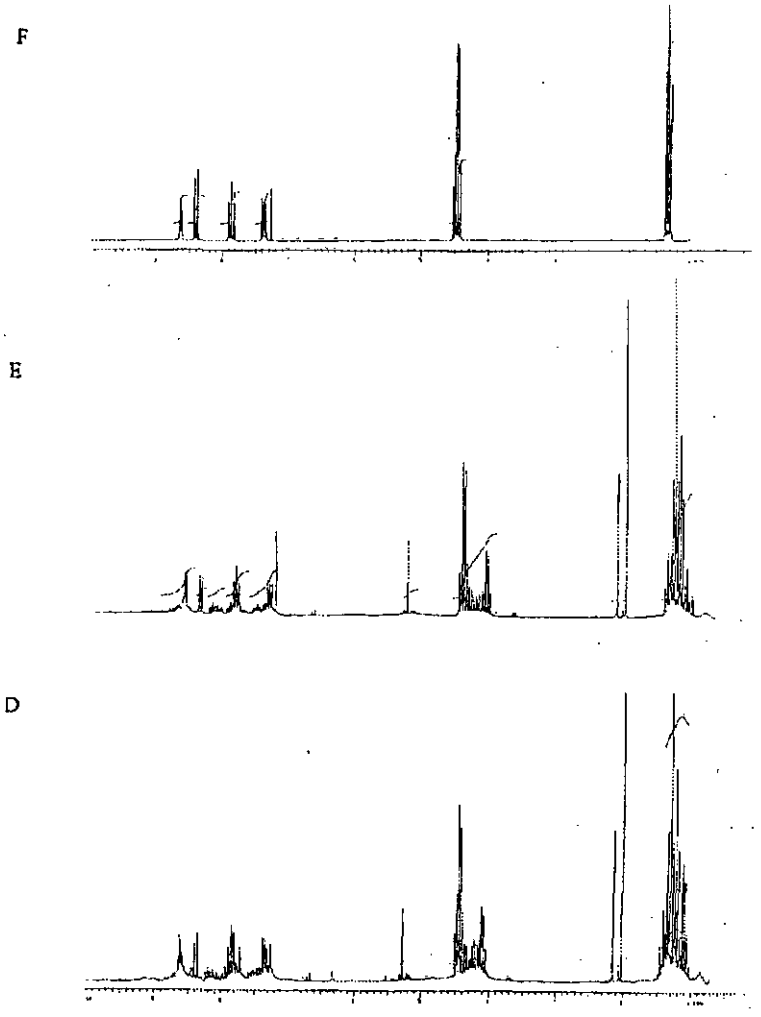

Fig. 3-1. (continued) D). the measurement on day + 6; E). the measurement on day + 8; F). ^{1}H NMR spectrum of the pure compound 17 as reference.

As seen in these spectra, after undergoing a series of intermediate, the reaction stopped at a stable state with the desired compound as the main product. Although the mechanism of the reaction remains unclear, the solvent certainly plays a key role in this one-pot reaction. An attempt to synthesize the two following compounds has also been tested but was unsuccessful, so far. Here again it is thought that the choice of the solvent(s) will be extremely important for success.

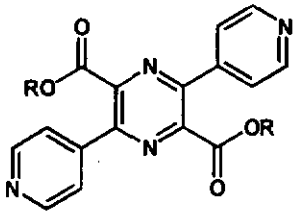

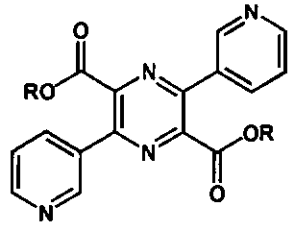

3.2. The Diversity of Ligand 2 and the Molecular Self-assembly Reactions in the Formation of Coordination Polymers

The ligand 2, 3,6-bis(2'-pyridyl)pyrazine-2,5-dicarboxylic acid, combines a bis-bidentate 2,5-bis(2'-pyridyl)pyrazine (BPPZ) unit with two harder carboxylate sites. This presents a diversity for chelate formation in the coordination chemistry with transition metals.

A prominent characteristic of this ligand is its amphoteric character. A study of the crystal structures of ligand 2 has shown that the molecule can exist in various forms, depending on the solvent and the pH value of the solvent. An inner salt zwitterion like amino acid (**19a**), a HCl salt (**19b**) and a normal organic carboxylic acid (**19c**) have been observed. **19a** forms a double-strand molecular ribbon, in which every molecule partakes in four hydrogen-bonds with symmetry related molecules. The hydrogen bonding has a great influence upon the solubility. We suppose there is an acid-base equilibria equation

as shown in scheme 16. Certainly it is this equilibrium that is the important factor in determining the coordination diversity of ligand 2.

Scheme 16

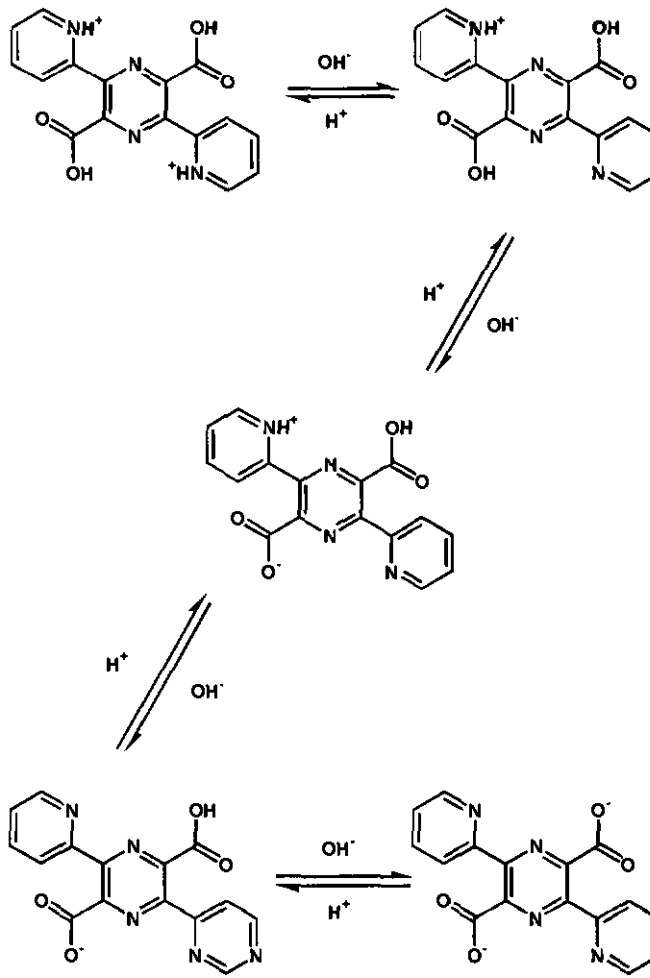

The coordination chemistry of this ligand with copper (II) in water is extremely rich. We have already obtained 11 copper(II) complexes by reacting an aqueous solution of different copper(II) salts with ligand 2. This reaction is a molecular self-assembly reaction. The complexes present different structural features, in which the ligand also shows a number of different coordination modes. Many of the complexes in the present work can be obtained by different synthetic routes or different initial Cu/H_2L^2 ratios. Moreover, there are some transformations between the complexes. In order to determine the relationship between the complexes a systematic study has been performed, as shown in Fig. 3-2.

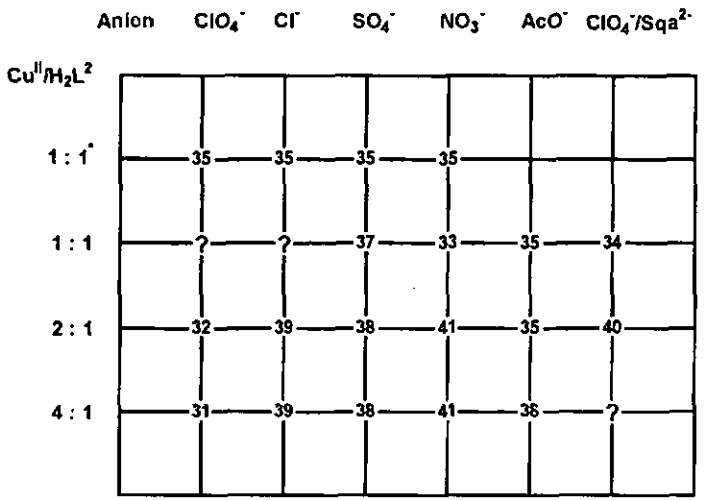

Figure 3-2. A network of the parallel test in which different copper(II) salts and Cu/H_2L^2 ratios were varied. The arrow represents a transformation between two complexes. * is a transition state.

The Cu/L^2 ratio was varied along the y axis from 4:1 to 1:1 and in the x direction different copper salts were set up. The results of this study are very interesting. All of the 11 complexes in the present work were identified in this network and they were the principal products at the relative crossing points of intersection. In addition some unknown complexes were also formed, represented with a ?. However further separation was difficult. Here we only show a simple system with two variables. If a third variable, for example a second bridging ligand, was introduced, this method would probably lead to discovery of many new complexes. Recently Schultz et al. [2] reported a combination of thin film deposition and physical techniques which were used for parallel synthesis of spatially addressable libraries of solid-state material. Arrays containing different combinations, stoichiometries, and deposition sequences of $BaCO_3$, Bi_2O_3, CaO, CuO, PbO, $SrCO_3$, and Y_2O_3 were used to generate a series of binary masks. The arrays were sintered and BiSrCaCuO and YBaCuO superconducting films were identified. They consider that the methodology, even in its current form, has already shown its effectiveness as a tool for discovering new materials.

Figure 3-3 shows six types of coordination mode of ligand 2 found in the 11 copper complexes and the two mononuclear complexes with Ni(II) and Co(II) [3]. In the figure, the arrows represent the coordination bonds and the numbers in parentheses indicate the related complexes corresponding to this coordination mode.

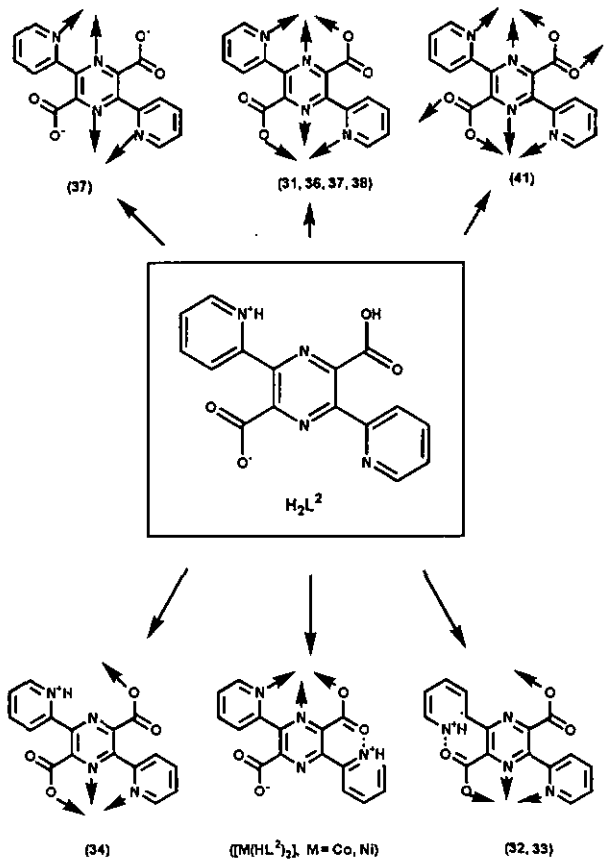

Fig. 3-3 The Diversity of Ligand 2 in Coordination with Copper(II)

3.3. The Relationship Between the Magnetic Properties and the Structures of the Coordination Polymers

Table 3-1 gives an overall comparison of magnetic and structural data related to the exchange coupling in the present work and some pyrazine-bridged copper(II) complexes from the literature.

Table 3-I. Magnetic and structural data related with the exchange coupling in some pyrazine-bridged copper(II) complexes

Complex [Reference] or (Compd. No.) in this work	Bridge Ligand	Cu—Npz Distance(Å)	Cu—Py Distance(Å)	Cu—O Distance(Å)	Cu—Cu Distance(Å)	τ Value	g Value	J (cm-1)
$[Cu_2(TPPZ)Cl_4](H_2O)_5$ [4]	TPPZ	av. 1.976(4)	av. 2.023(4)		6.565(2)	0.09, 0.20	2.05	- 17.1
$[Cu_2(TPPZ)(H_2O)_4](ClO_4)_4(H_2O)_2$ [4,5]	TPPZ	1.962(3)	av. 2.003(4)		6.497(2)	0.27	2.13	- 30.6
$[Cu_2(TAMP)Cl_2]Cl_2((H_2O)_{2.25}$ [6,7]	TAMP	1.945(4)	2.036(3)[a]		6.557(1)	0.28	2.23	- 20.0
$[Cu_2(NO_3)_2(BPPZ)(H_2O)_4](NO_3)_2$ [8]	BPPZ	2.021(3)	2.012(3)		6.760(1)	0.06	2.23	< 0.5
$[Cu_2L^bCl_2](ClO_4)_2 \cdot 2MeOH$ [9]	L^b	2.169(5)	2.028(5)[a]			0.72		< 0.5
$[Cu_2(DAPZ^c)(dien^d)_2](ClO_4)_4$ [10]	DAPZ	2.052(5)	2.243(3)[a]		6.775(2)	0.64	2.106	- 1.7
$\{Cu(pz)(NO_3)_2\}_n$ [11,12]	Pyrazine	1.984(4)			6.712(1)		2.22	- 6.0
$\{Cu(pz)_2(ClO_4)_2\}_n$ [13]	Pyrazine	2.062(3)					2.107	- 5.3
$[Cu_2(pz)(L^e)_2(H_2O)_2]$ [14]	Pyrazine	2.000(4)				0.10	2.14	- 3.7
$\{[Cu_2(L^2)(AcO)_2](H_2O)_3\}_n$ (36)	L^2	1.944 (5)	1.988(5)	1.966 (4)	6.490(4)	0.29, 0.27	2.14	- 20.3
		1.944 (5)	1.996 (5)	1.952(5)				
$\{[Cu_2(L^2)(L^{2a})(H_2O)_2](H_2O)_8\}_n$ (37)	L^2	1.973 (6)	1.977 (6)	1.971 (6)	6.555(3)		2.25	- 14.9
$\{[Cu_2(L^2)(H_2O)_5](SO_4)(H_2O)_3\}_n$ (38)	L^2	1.949(2)	1.991(2)	1.970(2)	6.516(2)		2.25	- 19.2
		1.954(2)	2.011(2)	1,968(2)	6.515(2)			
$\{[Cu_2(L^2)Cl_2(H_2O)](H_2O)\}_n$ (39)	L^2						2.20	- 12.5
$\{[Cu_2(L^2)(C_4O_4)(H_2O)_2](H_2O)_{1.5}\}_n$ (40)	L^2						2.24	- 20.0
$\{[Cu_2(L^2)(H_2O)_2](NO_3)_2\}_n$ (41)	L^2	1.958(3)	2.021(3)	2.031(3)	6.514(2)	0.11	2.22	- 10.3
$\{[Cu_2(L^3)Cl_2(H_2O)](H_2O)_2\}_n$ (43)	L^3	1.974	2.055	1.979	6.567	0.09	2.26	- 24.9
$\{[Cu(HL^2)(H_2O)](NO_3)\}_n$ (33)	HL^2	1.949(3)	2.000(4)	1.958(3)	7.495(4)	0.15	2.32	- 6.5

Abbreviations: (a). Here the bond distances are Cu---N(amino groups); (b). L = 2,5-bis[(N. N-(2-pyridylmethyl)aminomethyl]pyrazine; (c). DAPZ = 2,5-bis[(dimethylamino)methyl]pyrazine; (d). dien = diethylenetriamine; (e). L = 2,6-xylylaminodiacetato dianion;
av. = average value when more than two values for same distance exist.

It can be seen in Table 3-1, that an important relationship between the magnetic properties and structure exists. That is, the shorter Cu---Cu distance the stronger the coupling. The stronger exchange, in the present work and that reported in literature, takes place when the Cu---Cu separation is below 6.6 Å. In fact, the pyrazine bridged Cu---Cu separation depends on the Cu---Npz distance. How to make this distance shorter is probably an important condition to generate a strong interaction. A multidentate chelate may be profitable in the formation of short coordination bonds. For example, the copper complexes with TPPZ have Cu---Npz distances of 1.962-1.976 Å, much shorter than the same distance found in the copper complex with BPPZ (2.012 Å). In the present work, all of Cu---Npz distances are below 1.975 Å and the average distance is shorter than the same bond lengths in the unsubstituted pyrazine bridged copper complexes reported so far. Based on Table 3-1, Figure 3-4 shows the relationship between the J values and Cu---Npz distances.

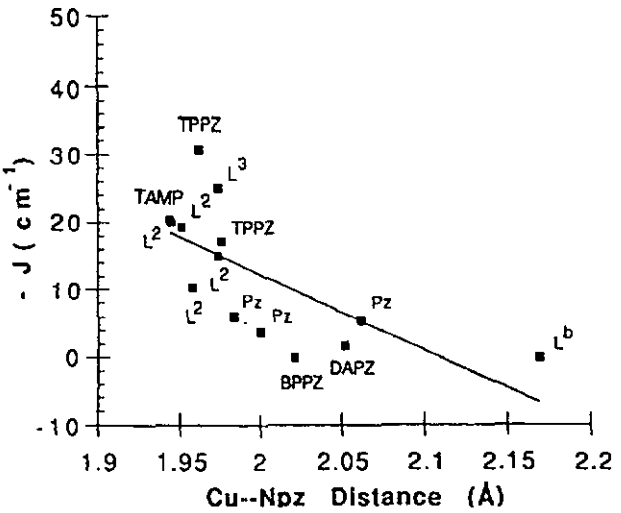

Figure 3-4. The relationship between the J values and Cu--Npz distances

In all coordination polymers with structural data in the present work, the magnetic orbitals ($d_{x^2-y^2}$), which lie in the basal coordination plane of the copper atoms, are almost coplanar with the pyrazine rings. Hence, according to Hatfield's model [15,16] the coupling between the copper atoms bridged by pyrazine should be weak. However, the magnetic measurements in the present work show a significant exchange interaction (J values from -10.3 to -24.9 cm^{-1}), which does not support the weak interaction predicted by the π pathway. In contrast, these results provide solid proof to support the σ pathway proposed by Hendrickson[17, 18]. In addition, a very rare exchange interaction (J = 6.5 cm^{-1}) was obtained in the uniform polymer **33** with a Cu---Cu separation of 7.495(4) Å. Recently, Chaudhuri[19] has reported a dinuclear complex bridged by a terephthalato group, with as a substantial antiferromagnetic interaction (J = - 70 cm^{-1}) in spite of a Cu---Cu intramolecular distance of 11.252 Å. Hence we assume that the superexchange is propagated through the σ pathway.

Finally, it must be pointed out that the rational design of the ligand is extremely important in order to obtain both a polymeric structure and a strong magnetic interaction.

References.

[1] Iida, H.; Hayashida, K.; Yamada, M.; Takahashi, K.; Yamada, K., *Synthetic Communications* **3**, 225-230 (1973).

[2] Xiang, X.-D.; Sun, X.-D.; Briceno, G.; Lou, Y.-L.; Wang, K.-A.; Chang, H.; Wallace-Freedman, W. G.; Chen, S.-W.; Schultz, P. G., *Science*, **268**, 1738-1740 (1995).

[3] Stoeckli-Evans, H.; Wang, Y., to be published.

[4] Graf, M.; Stoeckli-Evans, H.; Escuer, A.; Vicente, R. *Inorg. Chim Acta.*, in press.

[5] Graf, M.; Greaves, B.; Stoeckli-Evans, H., *Inorg. Chim. Acta* , **204**, 239-246 (1993).

[6] Ferigo, M.; Marty, W., Stoeckli-Evans, H., Escuer, A.; Vicente, R., to be published.

[7] Ferigo, M.; Bonhôte, P.; Marty, W., Stoeckli-Evans, H., *J. Chem. Soc. Dalton Trans.*, 1549-1554 (1994).

[8] Neels, A.; Stoeckli-Evans, H., *Chimia* , 47, 198-202 (1993).

[9] Oshio, H.; Toriumi, K.; Hayashi, J., *J. Chem. Soc. Dalton Trans.*, 293- (1990).

[10] Oshio, H.; Nagashima, U., *Inorg. Chem.*, **29**, 3321-3325(1990).

[11] Villa, J. F.; Hatfield, W. E. *J. Am. Chem. Soc.*, **93**, 4081-4082 (1971).

[12] Santoro, A.; Mighell, A. D.; Reimann, C. W.; *Acta, Crystallagr. Section B*, **26**, 979-84 (1970).

[13] Darriet, J.; Haddad, M. S.; Dusler, E. N.; Hendrickson, D. N.; *Inorg. Chem.* **18**, 2679-(1979).

[14] Suarez-Varela, J.; Colacio, E.; Romerosa, A.; Avila-Roson, J. C.; Hidalgo, M. A.; Romero, J.; *Inorg. Chim. Acta* , **217**, 39-44 (1994).

[15] Richardson, H. W. ; Hatfield, W. E. *J. Am. Chem. Soc.*, **98**, 835-8359(1976).

[16] Richardson, H. W.; Wasson, J. R. Hatfield, J. R. *Inorg. Chem.*, **16**, 484-486(1977).

[17] Haddad, M. S.; Hendrickson, D. N.; Cannady, J. P.; Drago, R.; Bieksza, D. S. *J. Am. Chem. Soc.*, **101**, 898-906(1979).

[18] Felthouse, T. R.; Hendrickson, D. N., *Inorg. Chem.*, **17**, 2636(1978).

[19] Chaudhuri, P.; Oder, K.; Wieghardt, K.; Gehring, S.; Haase, W.; Nuber, B.; Weiss, J., *J. Am. Chem. Soc.*, **110**, 3657365-8 (1988).

SUMMARY

In this work, some new and novel tetra-substituted pyrazine derivatives were designed and synthesized with the idea of forming coordination polymers with transition metals. Among these compounds two new ligands, ligands 2 and 3, have been extensively investigated, in particularly H_2L^2. A number of copper(II) coordination polymers were obtained. The structures of the ligands and their related compounds and the coordination polymers were characterized crystallographically. A study of the magnetic properties of these polymers has also been carried out. They exhibit significant antiferromagnetic coupling for pyrazine bridged copper systems.

The precursors of ligands 1 and 2 were synthesized by a one-pot reaction. A supported Rh catalyst was employed in the reduction of the oximes, which can operate at more facile conditions. The crystal structures of the ligands and some ligand candidates were investigated by X-Ray crystal structure analysis. The ligands 2 and 3 form unique hydrogen bonded molecular ribbons in the solid state. They have amphoteric character, like amino acids, and can exist in different forms in the solid state.

11 copper complexes with ligand 2 were synthesized and most of them were characterized crystallographically. They present different structural features, including: uniform polymer chains, alternating polymer chains, a two dimensional uniform polymer, and dinuclear complexes. The ligand also shows a number of different coordination modes. In addition, two copper coordination polymers with ligand 3 were obtained.

Magnetic measurements of the alternating polymer chains and the two dimensional polymer, both having dinuclear units, show significant antiferromagnetic coupling for pyrazine bridged copper complexes with J values from - 24.9 to - 10.3 cm^{-1}. Based on these data, a relationship between the magnetic properties and structures was established. A rare magnetic exchange interaction propagated through the pyrazine ring with a large Cu---Cu separation was also observed. These results provide solid proof to support the σ pathway.

EXPERIMENTAL

Materials

All chemicals were reagent grade and used as received unless stated otherwise. TLC was carried out on silica gel (Alugram Sil G/UV_{254}).

Instruments

Melting points were obtained on an electrothermal digital melting point apparatus and are uncorrected. The ^{1}H- and ^{13}C-NMR spectra of all compounds were recorded on a Varian Gemini-200 (200 MHz) and a Bruker-Spectrospin AMX-400 (400 MHz) spectrometers in $CDCl_3$, D_2O, CD_3OD, and DMSO-d_6. Chemical shift with respect to TMS as internal standard or DSS while D_2O was used as solvent. Infrared spectra were recorded on a Perkin-Elmer FT-IR 1720X spectrometer with KBr pellet. The mass spectra were obtained on a NERMAG R 30-10 MS-MS system, EI at 70 eV for EI and DCI. FAB-MS, HR(EI)-MS and CI-MS were measured on a VG 7070E sector mass spectrometer and HP 5988A quadrupole mass spectrometer, Institut für Organische Chemie, Universität Freiburg. The C, H, N,and Cl microanalysis were carried out by the "Organischchemisches Mikrolabor" of the Swiss Federal Institute of Technology (ETH), Zürich and "Forschungszentrum" of Ciba-Geigy AG, Marly.

X-ray Crystallography

All crystal data were collected on a Stoe AED2 four-circle diffractometer equipped with graphite-monochromatized Mo Kα radiation (λ = 0.71073 Å). The data collections

were mostly carried at room temperature (293 ±2 K), for some crystals at 193 and 211 ±2 K. The structures were solved by direct methods using *SHELXS-86* [1].

The *SHELXL-93* [2] was used for all further calculations. Hydrogen atoms were located from difference maps and refined isotropically or included in calculated positions. The non-hydrogen atoms were refined anisotropically using weighted full-matrix least-squares. The structural diagrams were drawn using the programme *PLUTON* [3].

Magnetic Measurements

Variable-temperature magnetic measurements were carried out by Departament de Quimica Inorganica, Universitat de Barcelona, Barcelona, Spain, on polycrystalline samples using a Faraday type magnetometer (Manics DSM8) equipped an oxford helium continuous-flow cryostat working in the 4-300 K range and a Drusch EAF 16UE electromagnet or a Quantum Design SQUID susceptometer. The magnetic field was approximately 1.5 Tesla. The diamagnetic corrections were estimated from the Pascal tables. ESR spectra were recorded on powder sample at X-band frequencies with a Bruker ESP-300E spectrometer in the temperature range 4-298 K.

5.1. Synthesis of Ligands

5.1.1 Syntbesis of Ligand 1

5.1.1.1. Methyl 2-oximinoacetoacetate (1)

$C_5H_7NO_4$ F.W. 145.11

Following the same procedure as for **2**, methyl acetoacetate (133.54 g, 1.15 mol) and sodium nitrite (90 g, 1.28 mol) afforded compound **1** (108.47 g, 65%) as colorless crystals, m.p. 35-36 °C (lit. 35-36 °C),

^{1}H NMR ($CDCl_3$, 200 MHz) δ: 9.40(br s, 1H, N-OH), 3.91(s, 3H, OCH_3), 2.42(s, 3H, CH_3) ppm,

^{13}C NMR ($CDCl_3$, 50 MHz) δ: 194.5, 162.4, 150.9, 53.0, 25.4 ppm.

EI-MS m/z, 145(M^+, 3.2), 128(2.2), 113(9.8), 102(3.9), 86(10.0), 70(3.8), 43(base).

5.1.1.2. Ethyl 2-oximinoacetoacetate (2)

$C_6H_9NO_4$ F.W. 159.14

Ethyl 2-oximinoacetoacetate was prepared by the method of Iida et al. [4]. To a mechanically stirred solution of ethyl acetoacetate (146 g, 1.15 mol) and glacial acetic acid (148 ml) was added 200 ml aqueous solution of sodium nitrite (90 g, 1.28 mol) during two hours adjusting so as to maintain the temperature of the solution at 5°C. After the solution was stirred for an additional hour, a solution of KCl (80 g) in water (400 ml) was added. The aqueous layer was extracted three times with isopropyl ether (50 ml). The extracts were combined with the oil layer, and the mixture was washed, dried over anhydride $CaCl_2$, and concentrated on a rotovapor to yield crude product. Recrystallization of the crude product from toluene (80 ml) at -15°C afforded 135.43 g (74 %) of 1 as colorless crystals, m.p. 55-56°C (lit. 56 °C).

^{1}H NMR ($CDCl_3$, 200MHz) δ: 9.57(br s, 1H, N-OH), 4.38(q, 2H, J=7.1 Hz, CH_2), 2.41(s, 3H, CH_3), 1.35(t, 3H, J=7.1 Hz, CH_3) ppm.

^{13}C NMR ($CDCl_3$, 50 MHz) δ: 194.5, 162.2, 151.1, 62.3, 25.2, 14.0 ppm.

EI-MS m/z, 159(M^+, 6.4), 131(79.2), 113(58.3), 86(18.0), 70(6.0), 54(5.9), 43(base).

5.1.1.3. Dimethyl-3,6-dimethylpyrazine-2,5-dicarboxylate (3)

$C_{10}H_{12}N_2O_4$ F.W. 224.21

Compound 2 (29.22 g, 0.2 mol) was dissolved 120 ml of absolute ethanol and Rh/C (1 g, 5%) was added to the solution. The reaction mixture was hydrogenated in an

autoclave until 2 had been consumed (TLC) at room temperature, normally which took 5-8 hours. The initial pressure of hydrogen was 3.2 bar. After stopping the reaction, the solution was filtered to remove the catalyst and then allowed to stand without a stopper until the crude product crystallized(ca. a week). Recrystallization from methanol afforded **3** (12.47 g, 55.6 %) as colorless crystals, m.p. 137-138 °C (lit. 137-138 °C).

IR, 3423(m), 3046(w), 3005(w), 2962(m), 2929(w), 2860(w), 1723(s), 1454(s), 1418(s), 1381(s), 1361(m), 1289(m), 1263(s), 1191(s) 1127(s), 1035(m), 990(m), 844(m),790(m), 764(m) cm^{-1};

^1H NMR ($CDCl_3$, 200 MHz) δ: 4.02(s, 6H, OCH_3), 2.82(s, 6H, CH_3) ppm,

^{13}C NMR (CDCl3, 50 MHz) δ: 165.3, 151.3, 143.6, 53.3, 22.4 ppm;

EI-MS m/z, 224(M^+, 48.5), 209(3.6), 194(32.0), 166(base), 149(2.4), 134(17.4).

5.1.1.4. Diethyl-3,6-dimethylpyrazine-2,5-dicarboxylate (4)

$C_{12}H_{16}N_2O_4$ F.W. 252.26

Following the same procedure as for **3**, Ethyl 2-oximinoacetoacetate (31.83 g, 0.2 mol) in absolute ethanol(120 ml) and Rh/C (0.6 g, 5%) afforded compound 4 (14.13 g, yield: 56 %)as colorless crystals, m.p. 88-89 °C (lit. 88 °C). Selected IR bands (KBr pellet): 3410(w), 3006(w), 2975(m), 2935(w), 1708(s), 1463(m), 1452(m), 1418(s), 1399(s), 1385(s), 1371(m), 1362(m), 1304(m), 1259(s), 1176(s), 1127(s), 1096(s), 1042(m), 1008(m), 866(m), 789(m), 758(m) cm^{-1};

^1H NMR($CDCl_3$, 200 MHz) δ: 4.48(q, 4H, J=7.0 Hz, CH_2), 2.79(s, 6H, CH_3), 1.44(t, 6H, J=7.0 Hz, CH_3) ppm,

^{13}C NMR ($CDCl_3$, 50 MHz) δ: 165.1, 150.8, 144.1, 62.1, 22.3, 14.2 ppm;

EI-MS, m/z , 253 (MH^+, 15.6), 223(1.5), 208(12.3), 180(base), 151(9.0), 135(7.5).

5.1.1.5. 3,6-Dimethylpyrazine-2,5-dicarboxylic acid (5)

$C_8H_8N_2O_4$ F.W. 196.13

This compound was prepared by the method of Iida, *et al.* [4], A mixture of **3** (2.0 g , 8.9 mmol) and KOH (3.2 g) in water (8 ml) was refluxed for 4 hours, cooled and acidified the solution with concentrated HCl (4N) afforded crude product. Recrystallization from ethanol gave 5 (1.66 g, 80%) as colorless crystals. Single crystals were obtained from an aqueous solution. Thermal analysis and crystal structure analysis indicate that there are two water molecules of crystallization. m.p. 201-202 °C (lit. 201 °C) dec.,

IR (KBr pellet): 3464(s), 3329(m), 3208(w), 2981(w), 2854(w), 2499(m), 1959(m), 1699(s), 1632(m), 1469(w), 1441(m), 1418(m), 1381(m), 1368(w), 1283(s), 1158(s), 1020(m), 832(m), 779(m), 750(m) cm^{-1},

^1H NMR (DMSO-d_6, 200MHz) δ: 2.67 (s, 6H, CH_3) ppm.

^{13}C NMR (DMSO-d_6, 50 MHz) δ: 166.4, 149.3, 144.4, 21.6 ppm;

EI-MS m/z: 196(M+, 37.1), 178(70.7), 152(51.5), 150(41.9), 134(3.5), 122(5.1).

5.1.1.6. 3,6-Dimethylpyrazine-2,5-dicarboxamide (6)

$C_8H_{10}N_4O_2$ F.W. 194.19

Compound 6 was prepared by a method analogous to that for pyrazine-2,3,5-tricarboxamide [5]. Compound 4 (3.20 g, 12.6 mmol) was dissolved in 100 ml of methanol containing sodium methylate (from 0.1 g sodium) which had been previously saturated with anhydrous ammonia in the cold for 30 min.. The stoppered solution was allowed to stand in a refrigerator for 24 hours. The white solid which formed was filtered off, washed with water and dried under vacuum to afford 6 (2.15 g, 88%) , m.p. >300 °C dec;

IR (KBr pellet): 3410(S), 3368(m), 3287(w), 3251(w), 3190(m), 1699(s), 1666(s), 1615(s), 1436(m), 1412(m), 1360(m), 1329(m), 1190(w), 1169(s), 1110(m), 1081(m), 1036(w), 982(w), 822(w), 772(w), 704(s) cm^{-1},

^1H NMR (DMSO-d_6, 200 MHz), δ: 8.13(br s, 2H, NH), 7.72(br s, 2H, NH), 2.71(s, 6H, CH_3) ppm,

^{13}C NMR (DMSO-d_6, 50 MHz) δ: 166.9, 148.5, 145.0, 21.7 ppm.

5.1.1.7. 2,5-Dimethylpyrazine-3,6-dithiocarboxamide (7)

$C_8H_{10}N_4S_2$ F.W. 226.32

Compound 6 (1.0 g, 5 mmol) and Lawesson reagent [6] (2.02 g, 5 mmol) in 10 ml of hexamethylphosphoramide (HMPA) were heated, with magnetic stirring at 80 °C until 6 had been consumed (TLC). The reaction mixture was allowed to cool to room temperature, and then poured into water. A pale yellow precipitate was formed and filtered off, yield 0.63 g (56 %), subliming point: >256 °C,

Selected IR bands (KBr pellet): 3448(m), 3267(s), 3106(s), 1672(m), 1646(s), 1440(m), 1407(m) 1359(m), 1286(w), 1147(m), 991(w), 917(m), 754(w) cm^{-1};

^1H NMR (DMSO-d_6, 200MHz), δ: 2.69 (s, 6H, CH_3) ppm;

^{13}C NMR (DMSO-d_6, 50 MHz), δ: 198.9, 150.6, 144.3, 20.6 ppm;

EI-MS, m/z: 226(M^+, base), 209(85.0), 192(83.8), 176(21.3), 166(16.8), 159(18.3), 148(7.8).

5.1.1.8. 5-Cyano-3,6-dimethylpyrazine-2-carboxylic acid (8)

$C_8H_7N_3O_2$, F.W. 177.16

To an aqueous solution (20 ml) of cadmium nitrate tetrahydrate (155 mg, 0.5 mmol) was added a solution of compound 7 (58 mg, 0.25 mmol) in DMF (5ml) with magnetic stirring. The mixture was stirred for 12 hours at 70 °C and a light yellow solution was

obtained. This solution was allowed to stand for a week without stopper at room temperature, gave light brown needle-like crystals in yield 39 % and a small amount of colorless crystal. The latter is 2,5-dicyano-3,6-dimethylpyrazine. m.p. 195-196 °C.

Selected IR bands (KBr pellet): 3412(vs), 3285(m), 3182(s, br), 2238(m), 1708(vs), 1600(m), 1552(m), 1437(w), 1412(s), 1365(w), 1335(m), 1180(s), 1097(w), 1035(w), 983(w), 816(w), 796(m), 712(m) cm^{-1},

^1H NMR(CD_3OD, 200MHz), δ: 2.84(q, 3H, $J = 0.7$ Hz, CH_3), 2.76(q, 3H, $J = 0.7$ Hz, CH_3) ppm;

^{13}C NMR (CD_3OD, 50 MHz), δ: 169.08, 155.12, 153.61, 147.24, 131.60, 116.74, 22.93, 21.31 ppm;

DCI-MS(NH_3, +): m/e 177(M^+, base), 148, 91.

5.1.1.9. 3,6-Dimethyl-2,5-pyrazinedicarbonyl dichloride (9)

$C_8H_6Cl_2N_2O_2$, F.W. 233.04

3,6-Dimethyl-2,5-pyrazine-dicarboxylic acid (0.93 g, 4 mmol) was treated with distilled thionyl chloride (10 ml) at reflux temperature for 10 h. Excess SOCl2 was then removed under reduced pressure to afford the acid chloride(0.91 g, yield 98 %) as a white solid, m.p. 109-110 °C,

Selected IR bands (KBr pellet), 2978(w), 1749(vs), 1681(b), 1436(w), 1415(s), 1358(m), 1218(m), 1175(m), 1038(m), 991(m), 851(s), 779(s) cm^{-1},

^1H NMR ($CDCl_3$, 200 MHz) δ: 2.88 (s, 6H, CH_3) ppm,

EI-MS, *m/z:* 234(MH^+, 3.3), 197(88.9), 169(base), 141(32.0), 134(4.5).

5.1.1.10. N,N'-Bis[2-(4-imidazolyl)-ethyl]-3,6-dimethylpyrazine-2,5-dicarboxamide (10a)

$C_{18}H_{22}N_8O_2$, F.W. 382.42

This compound was prepared by a method analogous to that for N-(2-(4-imidazolyl)ethyl)pyridine-2-carboxamide[7]. 1.26 g (5 mmol) amount of Diethyl-3,6-dimethylpyrazine-2,5-dicarboxylate (4) was mixed with histamine (1.12 g, 10 mmol) in 20 ml of benzene, and the mixture was refluxed for 18 h. After removal of solvent, the crude product was recrystallized from hot water to yield 1.30 g (68%). m.p. 260 °C dec.

Selected IR bands (KBr pellet): 3240(br s), 2950(m), 1666(vs), 1524(vs), 1448(s), 1417(m), 1357(m), 1290(m), 1258(s), 1227(m), 1198(s), 1160(m), 1089(s), 1030(m), 981(m), 800(m), 768(s) cm^{-1},

^1H NMR (DMSO-d_6, 200 MHz) δ: 11.87(br s, 2H, NH, Im), 8.90(t, 2H, J = 5.6 Hz, CONH), 7.57(d, 2H, J = 1.1 Hz, Im), 6.87(s, 2H, Im), 3.56(m, 4H, CH_2), 2.79(t, 4H, J = 7.3 Hz, CH_2), 2.72(s, 6H, CH_3) ppm,

^{13}C NMR (DMSO-d_6, 50 MHz) δ: 164.4, 148.5, 144.7, 135.0, 134.8, , 116.9, 39.1, 26.8, 21.8 ppm,

EI-MS m/z: 382(M^+, base), 354(17.6), 326(70.6), 301(38.2), 289(61.8), 233(36.5), 207(17.1).

N,N'-Bis[2-(4-imidazolyl)ethyl]-3,6-dimethylpyrazine- 2,5-dicarboxamide dihydrochloride (10b)

$C_{18}H_{22}N_8O_2.(HCl)_2(H_2O)_2$

This compound was prepared for crystal structure analysis. X-ray quality crystal were obtained from a 1M HCl aqueous solution, m.p. >300 °C dec, Anal. calcd for

$C_{18}H_{28}Cl_2N_8O_4$, 491.38 : calc C 44.00, H 5.74, N 22.80. Found: C 43.87, H 5.69, N 22.93;

IR (KBr pellet): 3317(vs, br), 3113(vs), 2933(s, br), 2835(s, br), 1754(w), 1667(vs), 1621(s), 1516(vs), 1445(m), 1433(m), 1411(s), 1359(m), 1333(m), 1294(m), 1262(m), 1198(s), 1177(m), 1158(s), 1014(m), 980(m), 914(m), 849(s), 814(m) cm^{-1}.

5.1.2. Synthesis of Ligand 2

5.1.2.1. 3-Oxo-3-(2-pyridyl)-propanoic acid ethyl ester (11)

$C_{10}H_{11}NO_3$, F.W. 193.20

This compound was prepared by the method of Helbling and Viscontini [8]. To a suspension of 5 g (0.12 mol) of NaH in 250 ml benzene was added a 13.5 ml (0.1 mol) of distilled ethyl picolinate with mechanical stirring at 60 °C, then a 15 ml (0.15 mol) of ethyl acetate was added slowly dropwise, after 20 min. the temperature rose to 70 °C. The mixture was stirred for 3 hous at 70 °C. After stopping the reaction the mixture was poured into water with stirring. The mixture was extracted with ether, the aqueous phase was added slowly 0.5 M solution of HCl to adjust the ph value to 1-2. This solution was then extracted again with ether. The ether phases were combined and dried over anhydrous Na_2SO_4. After removing solvent, the crude product was distilled under vacuum (115-120 °C/0.08 Torr, lit. 108-111 °C/0.07 Torr) to afford 11 as a colorless oil (16.61 g, 86%).

^1H NMR($CDCl_3$, 200MHz), keto-enol-mixture(ca. 6:1), δ : 12.39(br. s, HO-C(3)), 8.67-8.64(m, 1H, PyH3'), 8.08-8.03(m, 1H, PyH6'), 7.88-7.79(m, 1H, PyH4'), 7.50-7.28(m, 1H, PyH5'), 6.32(s, H-C(2) (Enolform)), 4.29-4.13(m, ca. 2H-CH_2 + H-C(2) (ketoform)), 1.34-1.18(2t, 3H, CH_3) ppm;

EI-MS, m/z: 193 (M^+, 12.8), 165(0.6), 146(51.5), 136(1.2), 121(77.9), 106(36.2), 93(15.7), 87(4.7), 78(base).

5.1.2.2. 3-Oxo-3-(4-pyridyl)-propanoic acid ethyl ester (12)

$C_{10}H_{11}NO_3$, F.W. 193.20

This compound was prepared by the method of Carabateas, et al [9]. A 1L, round-bottomed flask equipped with a reflux condenser was charged with 15.2 g (0.1 mol) of *ethyl isonicotinate*, ethyl acetate (17.6 g, 0.2 mol), and EtONa(95%, 11g, 0.153 mol). The reaction mixture was refluxed at 81 °C for 10 h. After stopping the reaction the mixture was diluted with water (200 ml), stirred to dissolve the sodium salt with acetic acid and the resulting upper layer of orange-red oil was separated. The lower layer was extracted twice with methylene dichloride and the extracts combined with the oil layer. After drying ($MgSO_4$) , the solvent was evaporated to a red oil that crystallized. The solid was slurried with cold cyclohexane to give crude product. Recrystallization from ethanol yielded 17.4 g (90 %) of **12** as a white solid, mp 55-56 °C (lit. 55-57 °C);

^{1}H NMR (200 MHz, $CDCl_3$), keto-enol-mixture(ca. 1.25 : 1), δ: 12.41(br. s, HO-C(3)), 8.68-8.84 (m, 2H, PyH), 7.63-7.75 (m, 2H, PyH), 5.77(s, ca. 1H from H-C(2) (enolform)), 4.15-4.34 (m, 2H, CH_2) , 3.98(s, ca 1H from H-C(2) (ketoform), 1.20-1.38 (2t, 3H, CH_3) ppm;

EI-MS m/z: 193(M^+, 29.4), 165(3.3), 148(19.2), 105(base), 78(28.2).

5.1.2.3. 2-Hydroxyimino-3-oxo-3-(2-pyridyl)-propanoic acid ethyl ester (13)

$C_{10}H_{10}N_2O_4$ F.W. 222.20

To a mechanically stirred solution of compound **11** (6.4 g, 0,033 mol) and glacial acetic acid (4.7 g) was added 6.5 ml aqueous. solution of sodium nitrite (2.5 g) during a period of one hour, maintaining the temperature of the solution at 5 °C. The solution was stirred for an additional two hours until a large quantity of a white solid had been formed. The temperature of the solution was raised to room temperature on leaving the solution to stand in ambient temperature. The mixture was filtered, well-washed with

water, and dried to give a white solid, yield 7.1 g (96 %), m.p. 138-139 °C. Anal. calcd for $C_{10}H_{10}N_2O_4$ (222.20) : C 54.05, H 4.54; N, 12.61. Found: C, 53.90; H, 4.58; N, 12.81.

Selected IR bands (KBr pellet) 3123(br. w), 2998(br. m), 2754(br. m), 1729(vs), 1691(s), 1631(w), 1589(m), 1471(m), 1442(w), 1374(m), 1328(s), 1299(m), 1272(w), 1140(s), 1094(m), 1024(s), 1004(m), 941(s), 839(w), 789(m) cm^{-1};

^1H NMR (CD_3OD, 200 MHz) 8.69-8.65(m, 1H, PyH), 8.10-7.98(m, 2H, PyH), 7.68-7.61(m, 1H, PyH), 4.27(q, J = 7.1 Hz, 2H, CH_2), 1.23(t, J = 7.1 Hz, CH_3) ppm; ^{13}C NMR (CD_3OD, 50 MHz,) 192.2, 162.8, 153.0, 151.1, 150.8, 139.0, 129.6, 123.2, 62.9, 14.3 ppm;

EI-MS, m/z: 222 (M^+, 9.6), 205(3.0), 177(6.0), 165(3.0), 149(7.5), 133(5.4), 121(2.4), 106(39.5), 95(9.3), 78(base).

5.1.2.4. 2-Hydroxyimino-3-oxo-3-(3-pyridyl)-propanoic acid methyl ester (14)

$C_9H_8N_2O_4$, F.W. 208.17

To a mechanically stirred solution of methyl nicotinoylacetate (1.35 g, 7.5 mmol) and glacial acetic acid (1.06 g) was added a 1.5 ml aqueous solution of sodium nitrite (0.58 g, 8.4 mmol) during a period of one hour, maintaining the temperature of the solution at 5 °C. The solution was stirred for an additional two hours until a large quantity of a white solid had been formed. The temperature of the solution was raised to room temperature on leaving the solution to stand in ambient temperature. The mixture was filtered, well-washed with water, and dried to give crude product. Recrystallization from ethanol afforded 14 (1.3g, 83%) as colorless crystals, m.p. 167-168 °C dec.; Anal. calcd for $C_9H_8N_2O_4$ (208.17): C 51.93, H 3.87, N 13.46 %, Found: C 51.66, H 3.84, N 13.43 %;

Selected IR bands (KBr pellet): 3110(m), 3005(m), 2497(br s), 1916(br m), 1727(vs), 1687(vs), 1597(vs), 1494(s), 1474(s), 1438(s), 1421(m), 1334(m), 1302(s), 1260(vs), 1194(s), 1139(m), 1030(vs), 964(s), 917(s), 833(s), 796(s), 756(m)cm^{-1};

^1H NMR ($CDCl_3$, 400 MHz) δ: 15.94(br s, 1H, NOH), 9.63-9.62(m, 1H, PyH), 8.71-8.70(m, 1H, PyH), 8.42-8.40(m, 1H, PyH), 7.65-7.58(m, 1H, PyH), 3.99(s, 3H, CH_3) ppm;

^{13}C NMR($CDCl_3$, 100 MHz,) δ: 185.1, 162.8, 151.4, 151.3, 140.1, 133.2, 125.6, 53.5 ppm;

EI-MS, m/z: 208 (M^+ , 24.6), 191(1.8), 176(2.7), 163(1.5), 149(3.6), 132(1.8), 106(base).

5.1.2.5. 2-Hydroxyimino-3-oxo-3-(4-pyridyl)-propanoic acid ethyl ester (15)

$C_{10}H_{10}N_2O_4$, F.W. 222.20

To a mechanically stirred solution of ethyl isonicotinoylacetate (19.3 g, 0,1 mol) and glacial acetic acid (14.1 g) was added 20 ml aqueous solution of sodium nitrite (7.7 g, 0.11 mol) during a period of one hour, maintaining the temperature of the solution at 5 °C. The solution was stirred for an additional two hours until a large quantity of a white solid had been formed. The temperature of the solution was raised to room temperature on leaving the solution to stand in ambient temperature. The mixture was filtered, well-washed with water, and dried to give crude product. Recrystallization from ethanol to yield product as a white solid (17.6 g, 80 %), m.p. 171-172 °C. Anal. calcd for $C_{10}H_{10}N_2O_4$ (222.20) : C, 54.05; H, 4.54; N, 12.61. Found: C, 53.88; H, 4.52; N, 12.32.

Selected IR bands (KBr pellet): 3079(w), 2990(w), 1732(w), 1651(s), 1625(s), 1597(s), 1555(m), 1501(w), 1475(w), 1445(w), 1425(m), 1382(m), 1339(m), 1203(vs), 1087(s), 1028(s), 995(m), 827(s), 808(s), 746(w) cm^{-1};

^{1}H NMR (CD_3OD, 200 MHz) 8.84-8.81(m, 2H, PyH), 7.79-7.76(m, 2H, PyH), 4.30(q, J = 7.2 Hz, 2H, CH_2), 1.27(t, J = 7.2 Hz, 3H, CH_3) ppm ,

^{13}C NMR (CD_3OD, 50 MHz) 192.3, 162.3, 152.0, 149.3, 142,3, 123.1, 63.4, 14.3 ppm; El-MS, m/z: 222 (M^+).

5.1.2.6. 2-Amino-3-oxo-3-(2-pyridyl)-propanoic acid ethyl ester (16)

$C_{10}H_{12}N_2O_3$, F.W. 208.21

Compound **13** (2.23 g, 0.01 mol) in dry ethyl acetate (150 ml) was hydrogenated using 5 % Rh/Al_2O_3 catalyst (0.3 g) in an autoclave for 24 hr. at room temperature. The initial pressure of hydrogen was 3.5 bars. After stopping the reaction, the solution was filtered to remove the catalyst, then the solution was concentrated under reduced pressure as quickly as possible to afford compound **16** (2.02 g, 97%) as a white solid. m.p. 128-131 _C dec;

Selected IR bands (KBr pellet) 3296(m), 2988(w), 1738(vs), 1676(m), 1594(m), 1572(w), 1524(m), 1465(w), 1439(m), 1370(m), 1341(w), 1312(s), 1201(m), 1165(m), 1130(m), 1057(m), 1023(m), 882(m), 810(w), 777(m), 755(m) cm^{-1} ; El-MS, *m/z*:: 208 (M^+, 27.2), 162(23.8), 149(2.4), 135(33.2), 107(30), 79(base).

NOTE: This compound is not stable in solution.

5.1.2.7. Diethyl-3,6-bis(2-pyridyl)-pyrazine-2,5-dicarboxylate (17)

$C_{20}H_{18}N_4O_4$ F.W. 378.39

The crude product of **16** (4.16 g , 20 mmol) was dissolved in chloroform (200 ml). The solution was stirred with a condenser at room temperature until the starting material had been consumed, then the solvent was removed under reduced pressure to yield the crude product. Recrystallization of the crude product from ethanol afforded **17** (1.40 g, 37% for the hydrogenation and condensation) as colorless crystals, m.p. 187-189 °C. X-

ray quality crystals were grown from a diluted solution of mixed cyclohexane and ethyl acetate (1:1) by slow evaporation. Anal. calcd for $C_{20}H_{18}N_4O_4$ (378.39): C, 63.49; H, 4.79; N, 14.81. Found C, 63.24; H, 4.80; N, 14.79.

Selected IR bands (KBr pellet), 2989(m), 1747(vs), 1587(m), 1478(m), 1447(m), 1395(s), 1296(s), 1199(s), 1163(vs), 1109(m), 1087(m), 1069(s), 1042(m), 1016(m), 999(m), 854(m), 798(m), 759(s), 742(m) cm^{-1}.

^1H NMR ($CDCl_3$, 200 MHz), δ: 1.34(t, J = 7.2 Hz, 6H, CH_3), 4.48(q, J = 7.2 Hz, 4H, OCH_2), 7.33-7.40(m, 2H, PyH5), 7.86(dt, J = 7.8, 1.77 Hz, 2H, PyH4), 8.41(dt, J = 7.8, 1.0 Hz, 2H, PyH6) , 8.61-8.65(m, 2H, PyH3) ppm;

^{13}C (50 MHz, $CDCl_3$), δ: 13.92, 62.0, 123.1, 124.7, 136.94, 145.3, 147.2, 148.6, 152.8, 166.6 ppm;

EI-MS: *m/z*, 378(M^+, 15.3), 349(23.7), 334(34.1), 305(13.5), 288(59.3), 277(12.6), 260(24.0), 249(14.4), 234(35.9), 206(8.4), 130(15.0), 106(31.7), 78(base).

5.1.2.8. Dimethyl-3,6-bis(2-pyridyl)-pyrazine-2,5-dicarboxylate (18)

$C_{18}H_{14}N_4O_4$, F.W. 350.32

To a stirred solution of methanol (20 ml) containing concentrated H_2SO_4 (98%, 1 ml) Compound **17** (100 mg, 0.26 mmol) was added, then the mixture was refluxed overnight at 75 °C. After stopping the reaction, the temperature of the solution was allowed to cool to room temperature and then poured into an aqueous solution of sodium acetate (6 g in 150 ml water). A white precipitate formed. Filtrating and drying under vacuum gave compound **18** (89 mg, 96 %) as a white solid. The crystal suitable for X-ray was obtained from ethanol, colorless crystal, m.p. 233-235 °C, Anal. for $C_{18}H_{14}N_4O_4$ (350.33): C 61.71, H 4.03, N 15.99; found C 61.62, H 3.97, N 16.08;

Selected IR bands (KBr pellet) 1752(vs), 1586(m), 1571(m), 1450(m), 1409(s), 1387(s), 1295(m), 1240(s), 1207(s), 1159(vs), 1088(w), 1070(s), 1042(w), 998(w), 963(m), 831(m), 798(m), 758(s), 743(m) cm^{-1};

^{1}H NMR ($CDCl_3$, 200 MHz), δ: 3.99(s, 6H, OCH_3), 7.33-7.40(m, 2H, PyH5'), 7.86(dt, J = 7.8, 1.8 Hz, 2H, PyH4'), 8.41(dt, J = 7.8, 1.0 Hz, 2H, PyH6'), 8.62-8.66(m, 2H, PyH3') ppm ;

^{13}C(, $CDCl_3$, 50 MHz), δ:: 52.9, 123.2, 124.9, 137.1, 145.2, 147.3, 148.8, 152.6, 167.2 ppm.

El-MS, *m/z*: 350(M^+, 10.8), 335(25.8), 319(19.8), 303(4.2), 291(16.2), 263(6.6), 247(9.0), 232(13.2), 149(7.2), 130(16.2), 106(15.6) 78(base).

5.1.2.9. 3,6-Bis(2-pyridyl)-pyrazine-2,5-dicarboxylic acid (19)

$C_{16}H_{10}N_4O_4$ F.W. 322.26 (19a)

To an aqueous solution of KOH (5g, 13ml H_2O) was added compound **17** (775 mg, 2.05 mmol). The mixture was refluxed at 102 °C for three hours. Then the temperature of the solution was allowed to cool to room temperature and the solution was acidified with 4N HCl until a white solid was formed (ca. pH = 2). The white solid was filtered off , washed with water and chloroform and dried under vacuum to yield 640 mg of **19a** (92 %) as a white solid. m.p. 242-243 °C dec. Anal. calc. for $C_{16}H_{10}N_4O_4.H_2O$ (340.29) Calcd. C 56.47, H 3.55, N 16.47 %; found. C 56.14, H 3.05, N 16.39 %.

Selected IR bands (KBr pellet) 3093(m), 2585(b), 1926(b), 1707(s), 1617(m), 1590(m), 1536(s), 1409(s), 1321(m), 1296(m), 1259(vs), 1204(vs), 1176(vs), 1075(s), 1046(m), 996(s), 817(vs), 759(m), 743(s), 714(m) cm^{-1} .

^{1}H NMR (DMSO-d_6, 200 MHz), δ: 7.59-7.64(m, 2H, PyH), 8.07-8.15(m, 2H, PyH), 8.26-8.30(m, 2H, PyH), 8.72-8.74(m, 2H, PyH), 12.45(s, 2H, COOH)ppm; ^{13}C NMR (DMSO-d_6, 50 MHz), δ: 123.2, 125.4, 138.2, 145.8, 146.4, 148.7, 152.4, 166.9 ppm;

DCI-MS: *m/z*, 323 (MH^+), 312, 279, 263, 235.

$C_{16}H_{10}N_4O_4$. 2HCl (**19b**)

Compound **19b** was obtained by dissolving **19a** in a 1M HCl aqueous solution. Colorless crystal, m.p. 264 °C, dec.,

selected IR bands (KBr pellet): 3387(br. s), 3059(w), 2616(br. vs), 2040(w), 1979(w), 1918(w), 1867(w), 1712(vs), 1633(m), 1617(m), 1546(w), 1468(w), 1432(w), 1380(m), 1304(m), 1270(s), 1199(m), 1160(s), 1080(m), 1012(w), 955(br. w), 810(m), 795(m), 773(m) cm^{-1}.

$C_{16}H_{10}N_4O_4$ .2DMSO (**19c**)

Compound **19b** was obtained by dissolving **19a** in a solution of DMSO. Colorless crystal, m.p. 226-8 °C, dec.,

selected IR bands (KBr pellet): 3421(br. w), 3066(w), 2473(br. m), 1867(br. w), 1701(vs), 1587(m), 1462(s), 1402(s), 1300(s), 1267(m), 1243(m), 1204(s), 1163(s), 1094(m), 1074(m), 979(br. vs), 813(m), 806(m), 761(s) cm^{-1}.

5.1.2.10. 3,6-Bis(2-pyridyl)-2,5-pyrazinedicarbonyl dichloride (20)

$C_{16}H_8Cl_2N_4O_2$ F.W. 359.15,

3,6-Bis(2-pyridyl)pyrazine-2,5-dicarboxylic acid (645 mg, 2 mmol) was treated with $SOCl_2$ (8 ml) at reflux temperature (79-80 °C) for 6 hours. Excess $SOCl_2$ was then removed under reduced pressure to give the acid chloride (704 mg, 98%) as an orange solid. m.p. >300 °C dec.

Selected IR bands(KBr pellet), 3059(m), 2706(br s), 1841(m), 1718(vs), 1629(s), 1616(s), 1541(m), 1476(m), 1467(m), 1434(m), 1380(m), 1302(s), 1269(s), 1168(s), 1078(m), 1041(w), 1008(w), 948(w), 903(m), 808(m), 794(s), 725(m) cm^{-1}.

5.1.3. Synthesis of Ligand 3

5.1.3.1. 2,3-Bis(2-pyridyl)-quinoxaline (21)

$C_{18}H_{12}N_4$ F.W. 284.32

This compound was prepared according to the procedure indicated by Goodwin and Lions [10]. To a solution of 2,2'-pyridil (21.2g, 0.1 mol) in ethanol (120 ml) was added a solution (80 ml) of o-phenylenediamine (11 g, 0.1 mol) in ethanol at 50 °C with stirring, then the mixture was refluxed for an hour. After stopping reaction, the mixture was immediately filtered to remove the black impuries. On cooling, light brown crude product was obtained. Recrystallization from ethanol with a slurry charcoal to yield 17 g (60 %) of 2,3-bis(2-pyridyl)-quinoxaline as colorless crystals, m.p. 185-186 °C (lit. 180 °C). Selected IR bands (KBr pellet): 3057(m), 1589(s), 1567(m), 1557(m), 1480(s), 1471(m), 1455(w), 1432(m), 1394(w), 1351(s), 1328(w), 1282(m), 1261(w), 1141(m), 1130(m), 1091(m), 1076(s), 1050(w), 997(s), 985(m), 897(w), 823(w),808(w), 791(s), 757(s), 745(s), 707(m) cm^{-1}.

^1H NMR($CDCl_3$, 200 MHz), δ : 7.20-7.27 (m, 2H, Aryl-H), 7.77-7.85(m, 4H, Aryl-H), 7.94-8.00 (m, 2H, Aryl-H), 8.18-8.28 (m, 2H, Aryl-H), 8.36-8.40 (m, 2H, Aryl-H) ppm;

^{13}C NMR($CDCl_3$, 50 MHz) δ: 123.0, 124.3, 129.4, 130.5, 136.7, 141.2, 148.6, 152.5, 157,5 ppm.

EI-MS m/z: 284(M^+, 35), 283 (base), 256(9), 179(6), 153(1), 142(4), 129(1.6), 102(0.5), 78(6).

5.1.3.2. 5,6-Bis(2-pyridyl)-pyrazine-2,3-dicarboxylic acid (22)

$C_{16}H_{10}N_4O_4$ F.W. 322.26

A 1 L, round-bottomed flask equipped with a reflux condenser was charged with 2,3-Bis(2-pyridyl)-quinoxaline (5.7 g, 20mmol) and 450 ml of water. The reaction mixture was mechanically stirred at 95 °C and 25 g (0.16 mol) of $KMnO_4$. was added in small portion during two hours. The reaction mixture was stirred at same temperature for an additional hour and the temperature then was decreased down 75 °C. A 10 ml of ethanol was added to remove excess $KMnO_4$. The reaction mixture was filtered to give a colorless filtrate. The filtrate was concentrated to 20 ml and acidified with 4 N HCl until a lot of white precipitate forming. The crude product was dissolved in 15 ml of water and the solution was acidified again with concentrate hydrochloric acid to yield white solid. The product was filtered off, washed with ethanol. Recrystallization from water and dried under vacuum afforded **22** (3.9 g , 60.5 %) as a white solid. mp 260-261 °C dec. Anal. calcd for $C_{16}H_{10}N_4O_4$ (322.28): C 59.63, H 3.13, N 17.39 %; found. C 59.51, H 3.02, N 17.30 %.

Selected IR bands (KBr pellet): 3426(br. m), 3083(w), 3026(w), 2922(w), 2854(w), 1706(m), 1653(m), 1602(vs), 1488(s), 1433(m), 1337(m), 1268(s), 1148(s), 1115(s), 1083(s), 1040(m), 943(m), 865(m), 820(w), 793(vs), 743(s) cm^{-1};

^1H NMR (D_2O, 200 MHz) δ: 8.84-8.82(m, 2H, PyH), 8.46-8.37(m, 2H, PyH), 8.08-7.99(m, 4H, PyH) ppm;

^{13}C-NMR (D_2O, 50 MHz) δ: 170.2, 150.2, 148.3, 148.1, 147.8, 147.4, 130.6, 130.3 ppm;

DCI-MS m/z: 323(MH^+, 4), 322(M^+, 2),

5.1.3.3. 5,6-Bis(2-pyridyl)-2,3-pyrazinedicarboxylic anhydride (23)

$C_{16}H_8N_4O_3$, F.W. 304.26

5,6-Bis(2-pyridinyl)pyrazine-2,3-dicarboxylic acid (640 mg, 2 mmol) was treated with $SOCl_2$ (8 ml) at reflux temperature (79-80 °C) for 6 hours. Excess $SOCl_2$ was then removed under reduced pressure to give the acid anhydride as a pale yellow solid, yield: 95 %, mp 239-240 °C dec.

Selected IR bands (KBr pellet): 3455(br. w), 3105(m), 2540(br. m), 2459(br. m), 2400(br, m), 1742(vs), 1722(w), 1606(s), 1530(m), 1463(m), 1427(m), 1377(w), 1353(s), 1281(m), 1215(vs), 1176(s), 1163(s), 1092(m), 1043(w), 1003(m), 940(w), 806(s), 785(s), 772(s) cm^{-1};

CI-MS(CH_4) m/z: 305(MH^+, base), 291(1.4).

5.1.3.4. 1,1'-(Methylene-di-4,1-phenylene)-bis[N-2-carboxyl-5,6-bis(2'-pyridyl)-pyrazine-3-carboxamide] (24)

$C_{45}H_{30}N_{10}O_6$ F.W. 806.79

This compound was synthesized by reacting compound **23** with 4,4'-methylenedianiline in dry DMF. To a solution of 4,4'-methylenedianiline (0.4g, 2 mmol) in dry DMF (20 ml)was added the fresh preparation **23** (calculating amount based on compound 22, 1.3 g, 4 mmol) with magnetic stirring. The mixture was stirred for 4 hours at 80 °C. After stopping the reaction the reaction mixture was allowed to cool to room temperature and poured into water. A yellow solid was formed and filtered off. The crude product was washed with water and ethanol and dried under vacuum, yield 0.88 g (55 %) m.p. 205-209 °C (dec).

Selected IR bands (KBr pellet): 3334(s), 3057(m), 2924(w), 1724(m), 1681(vs), 1596(vs), 1537(vs), 1414(m), 1391(m), 1316(m), 1249(s), 1163(s), 1089(s), 995(w), 957(m), 865(m), 782(s), 767(m), cm^{-1};

^1H NMR(200 MHz, $CDCl_3$), δ: 10.86(s, 2H, NH), 8.46-8.40(m, 4H, PyH), 8.20-7.97(m, 8H, PyH), 7.76(d, J = 8.5 Hz, 4H, PhH), 7.58-7.49(m, 4H, PyH), 7.29(d, J = 8.5 Hz, 4H, PhH), 3.97(s, 2H, CH_2) ppm ;

^{13}C NMR (50 MHz, $CDCl_3$), δ : 165.8, 162.0, 154.4, 153.9, 150.9, 149.5, 147.9, .147.4, 143.9, 143.8, 138.6, 138.2, 137.4, 136.4, 129.1, 125.3, 124.7, 124.6, 120.4, 40.8 ppm.

FAB-MS (NBA) m/z: 807(M^+, 22.6), 719(60.5), 485(14.5), 457(21.0), 366(20.2), 273(68.6), 233(base).

5.1.3.5. 2,3-Dicyano-5,6-bis(2-pyridyl)-pyrazine (25)

$C_{16}H_8N_6$ F.W. 284.28

To a solution of 2,2'-pyridil (3.2g, 15 mmol) in ethanol (18 ml) was added a solution of diaminomaleonitrile (1.67g, 15 mmol) in ethanol (45 ml) at 50 °C with stirring, then the mixture was refluxed for two hours. After stopping reaction, the mixture was immediately filtered to remove the brown impuries. On cooling, light brown crude product was obtained. Recrystallization from ethanol with a slurry charcoal gave 2,3-dicyano-5,6-bis(2-pyridyl)-pyrazine as pale yellow crystals, 1.49 g (yield 35 %), m.p. 181-182 °C. Anal. for $C_{16}H_8N_6$ (284.28) Calcd. C 67.60, H 2.84, N 29.56 %, Found C 67.35, H 2.91, N 29.50 %;

Selected IR bands(KBr pellet): 3433(br. w), 3067(w), 2403(w), 2308(w), 2242(w), 1994(w), 1969(w), 1588(s), 1571(m), 1523(m), 1473(m), 1438(m), 1386(vs), 1299(w), 1283(m), 1247(m), 1234(m), 1200(m), 1153(m), 1131(m), 1097(s), 1049(m), 996(s), 975(w), 961(w), 895(w), 824(w), 793(s), 741(s), 711(w) cm^{-1},

^{1}H NMR ($CDCl_3$, 200 MHz) δ: 7.29-7.36 (m, 2H, PyH), 7.85-7.94 (m, 2H, PyH), 8.04-8.09 (m, 2H, PyH), 8.30-8.33(m, 2H, PyH) ppm;

^{13}C NMR ($CDCL_3$, 50 MHz) δ: 113.0, 124.7, 124.8, 130.2, 137.2, 148.9, 153.9, 154.9 ppm;

EI-MS (m/e): 284(M^+, 43), 283(base), 256(9), 204(3), 180(5), 152(3), 128(2), 104(10), 78(13), 51(11).

5.1.4. Synthesis of the Oxazolines

General Comments

All compounds were prepared by an analogous method [11]. All reactions were carried out under an atmosphere of nitrogen. Chloroform was dried by distillation under nitrogen with $CaCl_2$. All optically active amino alcohols were used as received. Triethylamine was dried with CaH_2, then distilled under nitrogen.

5.1.4.1. 2,5-Bis[4'-(*R*)-ethyloxazolin-2'-yl]-3,6-dimethylpyrazine (26)

$C_{16}H_{22}N_4O_2$, F.W. 302.38

3,6-Dimethylpyrazine-2,5-dicarboxylic acid (700 mg 3 mmol) was treated with $SOCl_2$ (6 ml) at reflux temperature (78-79 °c) for 10h. Excess $SOCl_2$ was then removed under reduced pressure to give the acid chloride as a white solid. To a solution of (*R*)-2-amino-butanol(600 mg, 6.7 mmol) and triethylamine (1.82g, 18 mmol) in chloroform (12 ml), was slowly added a solution of the acid chloride in chloroform (8 ml) at 0 °C. The mixture was stirred for 1 day at room temperature. Then $SOCl_2$ (2.5 ml) was added, and the mixture was headed at reflux temperature for 3h and was slowly poured into ice water. The organic layer was collected, washed with brine (10 ml) and an aqueous solution of K_2CO_3 (0.1 M, 10 ml), and dried over anhydrous Na_2SO_4. After concentration a pale yellow solid was obtained, which was recrystallized in an ethanol

solution to give mainly the 2HCl salt of **26** (890 mg, 2.37 mmol, 79%) as a white solid. The 2HCl salt was treated with an aqueous solution of NaOH(5%, 5 ml in 15 ml methanol) at room temperature for 4 days. The mixture was extracted with CH_2Cl_2 (100 ml). The extract was washed with brine and concentrated to give the white solid in 56% total yield (500 mg, 1.56 mmol), m. p. 97-98 °C. $[\alpha]^{20}_D$ = + 113.5° (c = 1.08, $CHCl_3$).

Selected IR bands (KBr pellet), 2963(s), 2932(m), 2875(m), 1660(w), 1635(s), 1514(w), 1480(m), 1463(m), 1430(s), 1401(m), 1362(m), 1317(m), 1247(m), 1193(m), 1128(m), 1087(vs), 1063(s), 1004(m), 986(s), 947(m), 911(m) cm^{-1};

^{1}H NMR ($CDCl_3$, 200 MHz), δ: 1.04(t, J = 7.4 Hz, 6H, CH_3), 1.61-1.85(m, 4H, CH_2), 2.89(s, 6H, CH_3), 4.1(t, J = 7.7 (x2) Hz, 2H, OCH), 4.37(m, 2H, N-CH), 4.55 (dd, J = 7.7 (x2) Hz, 2H, O-CH) ppm;

^{13}C-NMR ($CDCl_3$, 50 MHz) δ : 10.2, 23.3, 28.7, 69.1, 72.2, 114.1, 151.2, 161.1 ppm;

EI-MS *m/z*: 302(M+, base), 273, 245, 173, 146. HR-MS *m/z*, calc. for $[C_{16}H_{22}N_4O_2]^+$ 302.1743, found 302.1743.

5.1.4.2. 2,5-Bis(4', 4'-dimethyloxazolin-2'-yl)-3,6-dimethyl-pyrazine (27)

$C_{16}H_{22}N_4O_2$, F.W. 302.36

This compound was prepared by the same method as for **26**, 3,6-dimethylpyrazine-2,5-dicarboxylic acid (1.02 g, 4 mmol), $SOCl_2$ (6 ml), 2,2-dimethyl-amino ethanol (2.3 g, 25 mmol), triethylamine (7.5 g, 74 mmol), and $SOCl_2$ (3 ml) gave **27** as a white solid in 46 % overall yield (560 mg, 1.85 mmol); m.p. 168-169 °C,

Selected IR bands (KBr pellet), 3286(w), 2962(s), 2933(m), 2903(m), 2868(m), 1656(s), 1465(s), 1428(s), 1383(m), 1366(m), 1348(m), 1278(m), 1248(w), 1192(m), 1174(s), 1084(vs), 1017(m), 980(s), 958(m), 934(m), 915(m), 878(m), 821(m), 774(w), 728(w) cm^{-1};

^{1}H NMR ($CDCl_3$, 200 MHz) δ: 1.43(s, 12H, CH_3), 2.88(s, 6H, CH_3), 4.17(s, 4H, CH_2) ppm;

^{13}C NMR($CDCL_3$, 50 MHz), δ: 23.2, 28.4, 68.9, 79.1, 141.3, 151.2, 159.6 ppm;

EI-MS: *m/z*: 302(M^+, base), 287, 259, 247, 230. HR-MS *m/z*, calc. for $[C_{16}H_{22}N_4O_2]^+$ 302.1743, found 302.1748.

5.1.4.3. 2,5-Bis(4'-(*R*)-phenyloxazolin-2'-yl)-3,6-dimethylpyrazine (28)

$C_{24}H_{22}N_4O_2$, F.W. 398.45

This Compound was also prepared by the method described above. The acid (580 mg, 2.5 mmol), $SOCl_2$ (4 ml), (*R*)-phenylglycinol (1.1 g, 8 mmol) triethylamine (2.43 g, 24 mmol), and $SOCl_2$ (1.5 ml) gave the intermediate salt (700 mg, 1.49 mmol) in 59 % yield. The salt (650 mg, 1.38 mmol) was treated with an aqueous solution of NaOH (5 % 7 ml) in 20 ml methanol at room temperature for six days to give 28 as a white solid in 80 % yield (44o mg, 1.1 mmol). m.p. 136-138 °C; $[\alpha]^{20}_D$ = + 174.8° (c = 1.11, $CHCl_3$).

Selected IR bands (KBr pellet) 3027(w), 2927(w), 1734(m), 1641(vs), 1603(w), 1495(m), 1449(m), 1423(s), 1352(m), 1295(w), 1273(m), 1193(m), 1096(vs), 1052(w), 1024(m), 985(s), 955(m), 906(m), 754(s), 700(s), 629(m), 536(w) cm^{-1};

^1H NMR ($CDCl_3$, 200 MHz) δ: 2.99(s, 6H, CH_3), 4.36(t, J = 8.7 (x2) Hz, 2H), 4.90(dd, J = 8.6 , 10.4 Hz, 2H), 5.56(dd, J = 8.7, 10.4 Hz, 2H), 7.26-7.40(m 10H, PhH);

^{13}C NMR ($CDCl_3$, 50 MHz) δ: 23.6, 71.0, 74.7, 126.7, 127.9, 128.9, 141.0, 141.6, 151.6, 162.4 ppm;

EI-MS, *m/z*: 399(M+), 308, 284, 221, 104, 91(base).

5.2. Synthesis of Complexes

General Comments

Most of the complexes were prepared according to the following procedure unless stated otherwise. To an aqueous solution of a copper(II) salt was added the ligand in solid form at room temperature. The reaction vessel was placed in an "ultrasonic cleaner" until a clear solution was obtained. The solution was then allowed to stand with or without stopper until crystals or a solid was formed.

Caution ! Perchlorate salts with organic ligands are potentially explosive and should be handled with the necessary precautions [12].

5.2.1. Synthesis of Complexes with Ligand 1

5.2.1.1. $[Cu(MeL^1)_2(H_2O)_2]$ (29)

$C_{18}H_{22}N_4O_{10}Cu$ F.W. 517.94

To an aqueous solution of $Cu(ClO_4)_2 \cdot 6H_2O$ (371 mg, 1 mmol) in 10 ml of water a suspension of Me_2L^1 (3) (116 mg, 0.5 mmol) in 10 ml of water was added with magnetic stirring at 70 °C. The green precipitates were formed over a variable period. The precipitates were filtered off, washed with water and ethanol, and dried in air to afford 29 as a pale green powder (87 mg, 67%). The single crystals for X-ray analysis were found on the wall of glassware. m.p. >300 °C dec.;

selected IR bands (KBr pellet): 3441(m), 3006(w), 2956(w), 1737(s), 1651(s), 1413(s), 1357(w), 1324(w), 1291(m), 1243(w), 1194(m), 1161(s), 1066(m), 1035(w), 995(w), 862(s), 825(w), 794(m), 778(m) cm^{-1}.

5.2.1.2. $\{[Cu(L^1)(H_2O)_2](H_2O)_{0.8}\}_n$ (30)

$C_8H_{11}N_2O_{6.5}Cu$ F.W. 302.73

To an aqueous solution of $CuCl_2.2H_2O$ or $Cu(NO_3)_2.3H_2O$ (1 mmol) in 10 ml of water a suspension of H_2L^1, compound 5, (116 mg, 0.5 mmol) in 10 ml of water was added with magnetic stirring at 70 °C. The green precipitates were formed over a variable period. The precipitates were filtered off, washed with water and ethanol, and dried in air to afford **30** as a pale green powder (118 mg, 78%), m.p. >268 °C dec., Anal., calc. for $C_8H_{11}N_2O_{6.5}Cu$ (302.73), C 31.74, H 3.66, N 9.25; found C 32.06, H 3.52, N 9.28;

Selected IR bands (KBr pellet) 3427(s), 3072(br m), 1625(vs), 1415(s), 1402(s), 1376(m), 1329(m), 1177(s), 1028(w), 985(w), 880(m), 828(w), 801(w), 781(w) cm^{-1}.

5.2.2. Complexes with Ligand 2

5.2.2.1. $[Cu_2(L^2)(H_2O)_4](ClO_4)_2(H_2O)_{3.75}$ (31)

$C_{16}H_{23.5}Cl_2Cu_2N_4O_{19.75}$ F.W. 785.87

$Cu(ClO_4)_2.6H_2O$ (75 mg, 0.2 mmol) in 10 ml water was treated with H_2L^2 (16 mg, 0.05 mmol) according to the general procedure. The resulting green solution was allowed to stand for two weeks. Deep green prismatic crystals were collected and dried in air (23 mg, 59 %);

Selected IR bands (KBr pellet), 1671(vs), 1638(vs), 1601(m), 1477(m), 1452(s), 1407(s), 1371(m), 1338(w), 1322(m), 1301(w), 1263(m), 1213(m), 1187(s), 1144(vs), 1116(vs), 1083(vs), 1030(m), 1019(w), 844(s), 776(s) cm^{-1}.

5.2.2.2. $\{[Cu(HL^2)(H_2O)](ClO_4)(H_2O)\}_n$ (32)

$C_{16}H_{13}ClCuN_4O_{10}$ F.W. 520.30

$Cu(ClO_4)_2 \cdot 6H_2O$ (37 mg, 0.1 mmol) in 5 ml water was treated with H_2L^2 (16 mg, 0.05 mmol) according to the general procedure. The resulting green solution was allowed to stand

for two weeks and greenish blue sheet-like crystals (**32**) were collected and dried in air (13 mg, 50 %);

Selected IR bands (KBr pellet), 3503(m), 3114(w), 1996(w), 1669(m), 1618(vs), 1601(w), 1495(m), 1430(m), 1391(s), 1338(s), 1288(m), 1254(m), 1196(m), 1163(w), 1103(vs), 969(m), 847(m), 808(w), 791(m), 768(w) cm^{-1}.

5.2.2.3. $\{[Cu(HL^2)(H_2O)](NO_3)\}_n$ (33)

$C_{16}H_{11}CuN_5O_8$ F.W. 464.84

$Cu(NO_3)_2 \cdot 3H_2O$ (24 mg, 0.1 mmol) in water (10 ml) was treated with H_2L^2 (32 mg, 0.1 mmol). The resulting green solution was allowed to stand for two weeks. The blue crystals were collected and dried in air (31 mg, 67%),

m.p. > 300°C dec. Anal. Calcd for $C_{16}H_{11}CuN_5O_8$ (464.84): C, 41.34; H, 2.39; N, 15.07. Found: C, 41.51; H, 2.54; N, 15.29.

Selected IR bands (KBr pellet): 3397(br. m), 1620(vs), 1601(m), 1514(m), 1388(s), 1337(s), 1319(s), 1301(w), 1261(m), 1214(w), 1186(s), 1091(w), 1046(w), 1022(w), 974(w), 951(w), 848(m), 820(w), 805(w), 782(m), 760(m), 738(w) cm^{-1}.

5.2.2.4. $\{[Cu(HL^2)(H_2O)](C_4HO_4)(H_2O)_2\}_n$ (34)

$C_{20}H_{16}CuN_4O_{11}$ F.W. 551.91

To a solution of squaric acid (29 mg, 0.25 mmol) in water and ethanol (v/v, 1: 1, 5 ml) was added 87 mg of $Cu(ClO_4)_2 \cdot 6H_2O$ (0.25 mmol) with a magnetic stirring. The resulting yellow solution was treated with H_2L^2 (80 mg, 0.25 mmol) according the general procedure. The color of the solution changed to green and the solution was allowed to stand for 2-3 days. The green cubes suitable for X-ray analysis were collected and dried in air. (78 mg, 57 %).

m.p. > 30 °C dec., Anal. for $C_{20}H_{16}CuN_4O_{11}$ (551.91): Calcd. C, 43.53; H, 2.92; N, 10.15. Found C, 43.72; H, 3.08; C, 10.07.

Selected IR bands (KBr pellet), 3277(b), 3116(w), 3079(w), 2586(w), 2465(b), 1801(m), 1700(s), 1672(s), 1644(s), 1607(w), 1561(vs), 1505(w), 1457(m), 1428(s), 1404(m), 1353(m), 1281(m), 1261(m), 12178m), 1186(s), 1120(m), 1040(w), 1026(m), 973(m), 870(m), 838(m), 828(m), 808(m), 784(m), 769(w), 746(w), 718(m) cm^{-1}.

5.2.2.5. $\{\{Cu(L^2)(H_2O)_2](H_2O)_{4.5}\}_n$ (35)

$C_{16}H_{21}CuN_4O_{10.5}$ F.W. 500.90

$CuSO_4 \cdot 5H_2O$ (25 mg, 0.1 mmol) in 20 ml water was treated with H_2L^2 (32 mg, 0.1 mmol) according to the general procedure. The resulting pale green suspension was obtained. The pale green cottonwool-like solid was filtered off and dried in air (22 mg , 43%). m.p. > 300°C dec.; Anal. Calcd. for $C_{16}H_{21}N_4O_{10.5}Cu$ (500.90): C 38.37, H 4.23, N 11.19; Found: C 38.38, H 3.65; N 11.09;

Selected IR bands (KBr pellet), 2923(m), 2853(w), 1652(vs), 1605(m), 1490(m), 1455(m), 1414(m), 1397(s), 1366(m), 1312(s), 1286(w), 1250(w), 1218(m), 1192(m), 1128(w), 1081(m), 1061(w), 1020(m), 836(s), 786(w), 756(w) cm^{-1}.

5.2.2.6. $\{[Cu_2(L^2)(CH_3COO)_2](H_2O)_3\}_n$ (36)

$C_{20}H_{20}Cu_2N_4O_{11}$ F.W. 619.49

$Cu(ClO_4)_2{\cdot}6H_2O$ (185 mg, 0.5 mmol) in water (5 ml) and AcOH/AcOK buffer (2 M, 5 ml) was treated with H_2L^2 (80 mg, 0.25 mmol) according to the general procedure. The resulting dark green solution was allowed to stand for a week. The dark green crystals were collected and dried in air. (81 mg, 52%).

m.p. > 238°C dec. Anal. Calc. for $C_{20}H_{20}N_4O_{11}Cu_2$(619.49): C, 38.78; H, 3.25; N, 9.04. Found: C, 38.66; H, 3.46; N, 9.06.

Selected IR bands (KBr pellet) 3131(m), 3082(w), 1674(vs), 1623(s), 1603(s), 1481(w), 1457(m), 1416(s), 1378(s), 1326(s), 1317(s), 1264(w), 1221(m), 1196(m), 1128(m), 1083(w), 1024(m), 972(w), 835(m), 812(w), 781(m), 744(w) cm^{-1}.

5.2.2.7. $\{[Cu_2(L^2)(L^{2a})(H_2O)_2](H_2O)_8\}_n$ (37)

$C_{32}H_{36}Cu_2N_8O_{18}$ F.W. 947.78

Above suspension of **35** was allowed to stand in the mother liquor for a week . The resulting deep green cubes formed, the crystals were collected and dried in air (18 mg, 38%). m.p. > 300°C dec., Anal. Calcd. for $C_{32}H_{36}Cu_2N_8O_{18}$ (947.78): C, 40.55; H, 3.83; N, 11.82. Found: C, 40.77; H, 4.02; N, 12.05.

Selected IR bands (KBr pellet), 3354(br. m), 3238(br. s), 1684(vs), 1606(vs), 1574(w), 1479(m), 1463(m), 1452(m), 1429(w), 1406(s), 1397(s), 1374(m), 1338(s), 1316(s), 1262(m), 1215(s), 1181(s), 1170(s), 1123(m), 1086(m), 1055(m), 1023(m), 911(w), 839(s), 810(m), 790(m), 778(m), 742(m) cm^{-1}.

5.2.2.8. $\{[Cu_2(L^2)(H_2O)_5](SO_4)(H_2O)_3\}_n$ (38)

$C_{16}H_{24}Cu_2N_4O_{16}S$ F.W. 687.54

$CuSO_4 \cdot 5H_2O$ (25 mg, 0.1 mmol) in water (10 ml) was treated with 16 mg H_2L^2 (16 mg, 0.05 mmol). The resulting green solution was allowed to stand for two weeks. The block-like green crystals were collected and dried in air (21 mg, 61 %); m.p. > 300°C (dec). Anal. for $C_{16}H_{24}Cu_2N_4O_{16}S$ (687.54): Calcd. C, 27.95; H, 3.52; N, 8.15. Found C, 28.17; H, 3.70; N, 8.27.

Selected IR bands (KBr pellet) 3138(w), 1670(vs), 1637(vs), 1601(m), 1477(m), 1452(m), 1404(s), 1369(m), 1338(m), 1321(m), 1262(w), 1213(m), 1188(m), 1112(vs), 1055(w), 1029(m), 844(s), 775(s), 742(w) cm^{-1}.

5.2.2.9. $\{[Cu_2(L^2)Cl_2(H_2O)](H_2O)\}_n$ (39)

$C_{16}H_{12}Cl_2Cu_2N_4O_6$ F.W. 554.29

$CuCl_2.2H_2O$ (17mg, 0.1 mmol) in water (5 ml) was treated with H_2L^2 (16 g, 0.05 mmol). An olive green precipitate was immediately obtained. The solid was collected by filtration, washed with 5 ml of ethanol, and dried in air. (21 mg, 76 %); m.p. > 300 °C dec. Anal. Calcd. for $C_{16}H_{12}Cl_2Cu_2N_4O_6$ (554.29): C, 34.67; H, 2.18; N,10.11; Cl, 12.79. Found C. 34.78; H, 1.92; N, 10.24; Cl, 12.58. Selected IR bands (KBr pellet): 3371(br. m), 3111(m), 3093(w), 1685(vs), 1596(m), 1475(w), 1456(w), 1444(w), 1413(s), 1372(m), 1301(m), 1291(m), 1263(w), 1220(m), 1182(s), 1120(m), 1082(w), 1050(w), 1020(m), 829(s), 789(s) cm^{-1} .

5.2.2.10. $\{[Cu_2(L^2)(C_4O_4)(H_2O)_2](H_2O)_{1.5}\}_n$ (40)

$C_{20}H_{15}Cu_2N_4O_{14.5}$ (622.45)

To a solution of squaric acid (14.5 mg, 0.125 mmol) in water and ethanol (v/v 1:1, 5 ml) $Cu(ClO_4)_2 \cdot 6H_2O$ (93 mg, 0.25 mmol) was added with a magnetic stirring. The resulting yellow solution was treated with H_2L^2 (40 mg, 0.125 mmol) according the general procedure. An olive green precipitate formed immediately and was filtered off and dried in air (55 mg, 71%), m.p. > 300°C dec, Anal. Calc. for $C_{20}H_{15}Cu_2N_4O_{14.5}$ (622.45): C, 38.59; H, 2.43; N, 9.00. Found: C, 38.41; H, 2.39; N, 8.87;

Selected IR bands (KBr pellet): 3530(m), 3139(br. w), 1670(s), 1601(w), 1578(w), 1555(s), 1442(vs), 1410(m), 1315(m), 1213(m), 1193(m), 1121(w), 1053(w), 1030(w), 836(m), 773(m) cm^{-1}.

5.2.2.11. $\{[Cu_2(L^2)(H_2O)_2](NO_3)_2\}_n$ (41)

$C_{16}H_{12}Cu_2N_6O_{12}$ F.W. 607.39

$Cu(NO_3)_2 \cdot 3H_2O$ (24 mg, 0.1 mmol) in water (10 ml) was treated with H_2L^2 (16 mg, 0.05 mmol)according the general procedure. The resulting green solution was allowed to stand without a stopper for two weeks. Blue crystals appeared at first , which proved to be complex **33** by IR. After a week green block crystals were obtained, collected and dried in air (17mg, 56 %), m.p. > 300°C dec. Anal. calcd for $C_{16}H_{12}Cu_2N_6O_{12}$ (607.39): C, 31.64; H, 1.99; N, 13.84. Found: C, 31.28; H, 2.12; N, 13.85.

Selected IR bands (KBr pellet): 3374(br. m), 3135(w), 1618(s), 1458(m), 1435(m), 1385(s), 1355(s), 1234(w), 1209(s), 1124(w), 1084(w), 1055(w), 1020(m), 981(m), 907(w), 849(m), 827(w), 781(s), 746(w) cm^{-1}.

5.2.3. Complexes with Ligand 3

5.2.3.1. $\{[Cu(L^3)(H_2O)](H_2O)_5\}_n$ (42)

$C_{16}H_{20}CuN_4O_{10}$ F.W. 491.10

To an aqueous solution (10 ml) of 50 mg (0.2 mmol) of copper sulfate pentahydrate was slowly added a 33 mg (0,1 mmol) amount of H_2L3 with a magnetic stirring. A dark green solution was immediately obtained. During a few hours the color of solution became light green and the solution was allowed to stand at room temperature. The resulting green crystals appeared within 24 h. The crystals were collected by filtration, washed with ethanol, and dried in air: yield (80%); m.p. > 300°C dec. Anal. Calcd. for $C_{16}H_{20}CuN_4O_{10}$ (491.10): C, 39.07; H, 4.10; N, 11.39. Found C, 39.34; H, 4.23; N, 11.58.

Selected IR bands (KBr pellet): 3372(br. vs), 1636(br. vs), 1541(w), 1478(m), 1450(m), 1429(w), 1402(m), 1365(s), 1320(s), 1279(m), 1227(w), 1196(m), 1173(w), 1125(m), 1095(w), 1085(w), 1049(w), 1020(w), 1006(w), 852(m), 821(s), 796(s), 759(m) cm^{-1}.

5.2.3.2. $\{[Cu_2(L^3)Cl_2(H_2O)](H_2O)_2\}_n$ (43)

$C_{16}H_{14}Cl_2Cu_2N_4O_7$ F.W. 572.31

To an aqueous solution of copper chloride dihydrate (171 mg, 1mmol) in 20 ml water was added a 33 mg (0.1 mmol) of ligand 3 with magnetic stirring at room temperature. A green solution was immediately obtained and this solution was allowed to stand for a week. The dark green crystals appeared, they were collected by filtration, washed with ethanol and dried in air. (45 mg , 78 %). m.p. > 248°C dec. Anal. Calcd. for $C_{16}H_{14}Cl_2Cu_2N_4O_7$ (572.31): C, 33.58; H, 2.47; N, 9.79; Cl, 12.39. Found: C, 33.31; H, 2.44; N, 9.74; Cl, 12.47.

Selected IR bands(KBr pellet): 3416(br. s), 1693(vs), 1664(m), 1600(m), 1551(w), 1469(m), 1424(w), 1375(w), 1313(m), 1290(s), 1268(w), 1244(s), 1206(m), 1166(m), 1127(m), 1102(w), 1019(m), 852(m), 786(s) cm^{-1}.

References:

[1] Sheldrick, G. M., *SHELXS86, Acta Crystallogr.*, **A46**, 467-73 (1990).

[2] Sheldrick, G. M., *SHELXL93, Programme for the Refinement of Crystal Structures.* Univ. of Göttingen, Germany (1993).

[3] Spek, A. L., *PLUTON, Acta Crystallogr.*, **A46**, C34 (1990).

[4] Iida, H.; Hayashida, K.; Yamada, M.; Takahashi, K.; Yamada, K., *Synthetic Communications* **3**, 225-230 (1973).

[5] Rao, R. B.; Castle, R. N., *J. Heterocycl. Chem.* **6**, 255-258 (1969).

[6] Scheibye, S.; Pedersen, B. S.; Lawesson, S.-O., *Bull. Soc. Chim. Belg.* **87**, 229-238(1978).

[7] Brown, S. J.; Tao, X.-L.; Stephan, D. W.; Mascharak, P. K., *Inorg. Chem.* **25**, 3377-3384 (1986).

[8] Helbling, A. M.; Viscontini, M., *Helv. Chim. Acta* **59**, 938-940 (1976).

[9] Carabateas, P. M.; Brundage, R. P.; Gelotte, K. O.; Cruett, M. D.; Lorenz, R. R.; Opalka, Jr, C. J.; Singh, B.; Thielking, W. H.; Williams, G. L.; Lesher, G. Y., , *J. Heterocyclic Chem.* **21**, 1849-1856 (1984).

[10] Googwin, H. A.; Lions, F., *J. Am. Chem. Soc.* **81**, 6415- 6422 (1959).

[11] Nishiyama, H.; Konda, M.; Nakamura, T.; Itoh, K., *Organometallics* **10**, 500-508 (1991).

[12] Wolsey, W. C. *J. Chem. Educ. 50*, A335 (1973).